LATERAL GROUND MOVEMENT EFFECTS NEAR CONNECTION OF MEDIUM DENSITY POLYETHYLENE GAS DISTRIBUTION PIPES

by

© Tanmoy Sinha

A Thesis submitted to the

School of Graduate Studies

in partial fulfillment of the requirements for the degree of

Master of Engineering

Faculty of Engineering and Applied Science

Memorial University of Newfoundland

October 2021

St. John's Newfoundland

ABSTRACT

Buried medium-density polyethylene (MDPE) pipes are extensively used for gas distribution systems. These pipes are sometimes exposed to geotechnical hazards such as ground movement, which may cause significant damage to the pipes. Understanding the behaviour of the pipes subjected to the ground movement is critical for transporting natural gas safely and economically using these pipings. This thesis presents an investigation of MDPE gas distribution pipes subjected to lateral ground movements near a connection. Gas distribution systems include a number of connections and lateral branches to supply gas to communities. When a pipe is subjected to the load from the lateral ground movement, the branch pipes experience axial force, and the pipe itself experiences bending deformation. As a result, excessive strains can develop on the pipes, leading to leakage or breakage. In this study, the bending strain on the pipes and the axial force on branch pipes are investigated using full-scale testing. Tests were conducted using 42.2-mm and 60-mm diameter MDPE pipes buried in the ground in a full-scale test facility. Each type of pipe was tested at two different burial depths in dense sand and loose sand. Test results showed that the axial force on the lateral branch depends on the burial depth, the pipe diameter, and soil density. The pipe under lateral ground movement experienced significant bending strain near the connection. The measured responses of the pipes were reasonably estimated within the linear range of deformations using beam-on-elastic spring idealization. For large deformations, elastoplastic spring parameters were required to simulate the pipe behaviour. The bilinear elastoplastic spring parameters recommended in the pipe design guidelines for steel pipes were modified to simulate the measured responses for the MDPE pipes. Based on the validated spring parameters, a parametric study was conducted using a python script to investigate the effect of burial depth, soil density and landslide magnitude on the pulling force and the bending strain.

ACKNOWLEDGEMENTS

Throughout my time spent in the master's program in the Faculty of Engineering and Applied Science at the MUN, I have come across numerous individuals who contributed to this fantastic experience. First and foremost, I would like to take this opportunity to express my sincere gratitude to my supervisor, Dr. Ashutosh Dhar, for sharing his knowledge and expertise and for his continuous encouragement during the research program. His guidance has advanced my technical knowledge and critical thinking capability which helped me improve my overall confidence in this field.

I gratefully acknowledge the financial support for this research by the School of Graduate Studies at MUN, National Science and Engineering Research Council (NSERC) of Canada, and FortisBC Energy Inc. Canada. Thanks to the faculty members at the Faculty of Engineering and Applied Science who provided me the knowledge through formal courses or informal discussions. Special thanks to Mr. Jason Murphy, Mr. Matt Curtis and Mr. Jamal Tinkov for helping in the laboratory.

I would also like to sincerely thank my colleagues, Mr. Auchib Reza and Mr. Sudipta Chakraborty, for helping during the laboratory work and for their invaluable advice, suggestions, and time. Thanks to Mr. Riju Saha for helping with the geotechnical engineering testing and Mr. Suborno Debnath, Mr. Suprio Das, and Mr. Pritam Kundu for helping with numerical modeling.

I would not have been able to have this opportunity to study at MUN without the recommendations given by Dr. Md. Moinul Islam, Dr. G.M. Sadiqul Islam and Dr. Aftabur Rahman. I will be forever grateful to them for the support. I am also indebted to many friends in St. John's, Newfoundland, for their support, encouragement, and friendship. Finally, I would like to thank my parents and friends, living in Bangladesh, for providing unconditional support and constant encouragement during these past two years.

Table of Contents

List of Figures

List of Tables

List of Symbols

c	Cohesion of soil
D	External diameter of pipe
E_s	Elastic modulus of soil
E_b	Elastic modulus of pipe
f	Coating factor of pipe material
H	Depth of soil to springline of the pipe
I	Moment of inertia of pipe section
K_o	Coefficient of lateral earth pressure at rest
k	Winkler's modulus
k_i	Initial modulus of subgrade reaction
L	Length of the pipe
N_{ch}	Horizontal bearing capacity factor for clay
N_{qh}	Horizontal bearing capacity factor for sand
T-x, P-y, Q-z	Soil forces applied to unit length of pipe in axial, lateral and vertical direction
T_u, P_u	Ultimate soil forces applied to unit length of pipeline in axial, lateral direction
ϕ	Internal friction angle of soil
ϕ'	Effective internal friction angle of soil
δ	Interface friction factor of pipe and soil
γ	Unit weight of soil
γ_d	Dry unit weight of sand
γ_{d-min}	Minimum dry unit weight
ν	Poisson's ratio of soil
Δp	Peak displacement at P_u
ε	Bending strain

CHAPTER 1

Introduction

1.1 Background

Buried pipeline systems form a crucial part of the global lifeline infrastructure. Pipe networks are regularly being used to transport vast amounts of liquids between geographic areas at a lower cost per unit volume compared to other modes of transportations. Canada has the second largest pipeline network in the world (Katebi et al., 2019); there are approximately 840,000 km of gas and oil distribution pipelines across the country, including 119,000 km for oil and gas transmission (NRCAN, 2020). The total length of the oil and natural gas distribution pipelines is around 4.8 million km in the USA. Pipeline systems often exposed to various natural or man-made hazards might cause damage to the system. It is always necessary to consider potential loads from external hazards in addition to the operational loads that have a negative impact on the pipelines. Any damage or performance failure of the pipeline often causes unfortunate consequences to local business, the economy and living conditions of the people of that area. According to the database of the National Energy Board of Canada (NEB), more than 1426 pipeline accidents were reported from 2008 to 2020, including oil leakage, serious injury, death, and severe environmental impact (NEB, 2017). In 2019, a total of 48 reportable pipeline incidents were reported by the Transportation Safety Board of Canada (TSB, 2019). The reasons for those incidents were the release of hydrocarbon gas, release of HVP (High Vapour Pressure) hydrocarbons, release of LVP (Low Vapour Pressure) hydrocarbons, fire/ignition, explosion, rupture, pipeline contacted by an object, operation beyond the limit, geotechnical, hydrological and environmental activity, etc.

Among them, geotechnical factors have the most damaging and long-term effect on the pipeline. Between 2017—2019, on average, 27.3% of pipeline incidents were the result of geotechnical and environmental activities (TSB, 2019). In the US, on average, 6 pipeline incidents due to geotechnical hazards are observed each year (Porter et al., 2016).

The major events associated with buried pipelines resulting from geotechnical hazards are landslides, slope failure, land subsidence and earthquake. Of these events, landslides have a severe impact on the pipeline, sometimes causing unacceptable strains owing to the various directional movements. The landslide incidents near a joint can cause stresses and strains on the pipes connected to the joint (Figure 1.1) that depend on the interaction of the pipes with the surrounding soil.

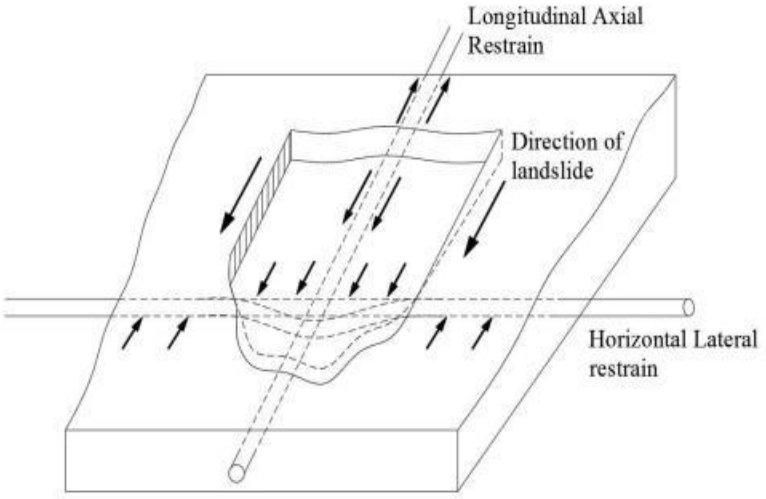

Figure 1.1: Buried pipes subjected to lateral and longitudinal ground loads (Karimian, 2006)

The impact of landslides on buried pipelines can be divided into four major categories based on the relative movement of soil against pipelines: axial movement, upward movement, lateral movement, and downward movement (Figure 1.2). These ground movement magnitudes can be

defined as stream slides (more than 5 m), lateral spreading stream slides (5 m to 0.3 m), and ground swaying (under 0.3 m) (Youd and Perkins, 1987). Youd and Perkins (1987) have defined "ground movement susceptibility" as the capacity of the soil to resist the movement both in the horizontal and vertical directions. The approach of Youd and Perkins (1987) provides a general method for mapping ground movement susceptibility based on the geological characteristics of a given area. While assessing a wide area of the pipeline system, it is also required to employ a regional approach to determine the ground displacement hazards. Ground settlement also is responsible for permanent ground deformation that should be considered for pipeline susceptibility (Wijewickreme and Sanin, 2010). Much larger vertical movements are expected at river crossings, in the vicinity of dikes, ditches, road embankments, etc., due to distortion of the soil mass. Estimation of such vertical deformations would require rigorous site-specific analyses.

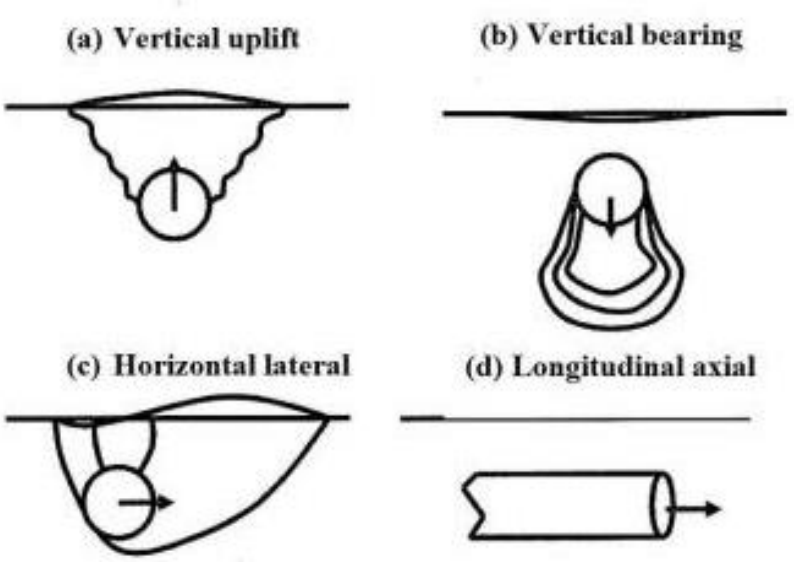

Figure 1.2: Anticipated modes of relative movement of pipe (Karimian, 2006)

Polyethylene (PE) pipes are becoming more popular due to their low cost, high corrosion resistance, high fatigue resistance, ease of replacement, and other advantageous properties. Two

types of polyethylene pipes are widely used: (1) Medium Density Polyethylene (MDPE) and (2) High-Density Polyethylene (HDPE). The basic and key difference between HDPE and MDPE pipe is that HDPE is highly sensitive to stress cracking, whereas MDPE has better stress cracking resistance. More than 60% of MDPE pipe is used in natural gas distribution sectors, due to its high flexural strength, ductility and high strain susceptibility (Stewart et al., 1999).

The behaviour of MDPE pipe subjected to lateral ground deformation is governed by the complex interaction of pipe and the surrounding soil. A better understanding of the complex relationship between the pipeline and the surrounding soil is required to develop rational design methods for the pipes.

1.2 Problem statement

Pipelines under lateral soil loads are expected to undergo flexural deformations which are influenced by interaction with the surrounding soil. The effects of ground deformation on pipelines subjected to permanent ground deformation (PGD) are difficult to predict due to differences in the stiffness of the pipe and the surrounding soil. Distribution MDPE pipelines are often connected with the lateral connection to supply liquids or gas at different locations. Pipelines connected with lateral branches can be exposed to ground deformation, which can cause cracking near the connection. Ground deformation can also generate bending deformation of the distribution main, along with axial deformation of the lateral branches, which may lead to failure by leakage or joint failure. Though MDPE pipe offers high resistance to deformation due to its ductile behaviour, with very large deformation, mechanical failure of the pipe can be observed. Thus, it is important to assess the bending strain on a pipe subjected to lateral ground deformation and the axial force on branch pipes.

Current design guidelines (ALA, 2005; ASCE, 1984) adopted design equations for estimating the lateral load on buried pipelines, which were developed considering plane strain conditions of rigid pipes. The flexural behaviour of the pipes under lateral soil loads is not considered in the design equations. Researchers conducted physical model tests to develop an improved understanding of the soil-pipe interactions subjected to relative ground movements in the lateral direction using rigid pipe (Almahakeri et al., 2014; Anderson, 2004; Hsu, 1993; Konuk et al., 1999; Paulin et al., 1998; Trautmann, 1983). Finite element modeling was also employed to understand the mechanisms of pipe-soil interaction for rigid pipelines (Almahakeri et al., 2016; C-CORE and Honegger, 2003; Daiyan et al., 2011; Guo and Stolle, 2005; Yimsiri et al., 2004; Yimsiri and Soga, 2006). However, very limited information is available in the published literature on the flexural behaviour of MDPE gas distribution pipelines. Therefore, there is a need to understand the behaviour of MDPE pipes using physical experiments and develop predicting tools through validation with the experimental results.

1.3 Objectives

The goal of the current study is to develop an understanding of the pipe-soil interaction behaviour of buried MDPE pipes subjected to lateral ground movement near a connection. The main objectives of the study are to:

- Develop an experimental database on the behaviour of MDPE gas distribution pipes buried in loose and dense sand under different burial conditions. Burial depth, soil density, and pipe diameter are varied to examine the effects.

- ❖ Evaluate the applicability of existing pipe design guidelines for steel pipes for assessing MDPE pipe behaviour.
- ❖ Develop methods to account for the soil-pipe interaction for MDPE gas distribution pipes.
- ❖ Perform a parametric study to identify the effects of MDPE pipe installation parameters on the performance of the pipes.

These objectives were achieved through a laboratory test program conducted using the facility at Memorial University of Newfoundland and developing numerical modeling techniques using the finite element method. Pipe commonly used in gas distribution systems, i.e., 60-mm and 42.2-mm diameter pipes, were considered in the investigation. The finite element modeling techniques were validated with the experimental measurements of pipe deformation and pipe wall strains. Then, an extensive parametric study was conducted to evaluate the effects of pipe diameter, burial depth, soil density, soil internal friction angle, landslide magnitude on the maximum pullout force, and the maximum strain distribution on the pipe.

1.4 Framework of thesis

The thesis is organized into five chapters. The following presents the outlines of the chapters.

- **Chapter 1:** highlights the background, scope, significance, and objectives of the current study.
- **Chapter 2:** presents the existing design guidelines for lateral pipe-soil interaction, the numerical modeling technique and a comprehensive literature review on experimental and numerical studies on lateral pipe-soil interaction.

- **Chapter 3:** contains the experimental studies on the effect of lateral ground movements near the connection of MDPE pipes. Ten lateral pullout tests were conducted using a laboratory test facility. Preliminary analyses of the results using finite element and analytical methods are presented.
- **Chapter 4:** presents the numerical investigation of lateral ground deformations effect on MDPE pipe. The finite element model was developed and validated with the experimental results. A parametric study was conducted to study the effects of burial depth, landslide magnitude, soil density and soil internal friction angle.
- **Chapter 5:** summarizes the overall outcomes of the study with recommendations and suggestions for future works.

CHAPTER 2

Literature Review

2.1 Introduction

Permanent ground deformation (PGD) can be caused by natural or man-made factors such as landslides, earthquakes, land subsidence, rock falling, infrastructure development or wheel pressure. Pipelines subjected to lateral PGD experience increased loading as the pipelines resist the movement created by these geohazards. It is crucial to evaluate the pipeline's ability to withstand the load and strain generated, as well as the behaviour of the soil surrounding the pipe. A number of laboratory full-scale and field-scale tests, along with numerical and analytical modeling, have been conducted in the past to investigate the interaction between pipe and soil when exposed to permanent ground movements. Based on these studies, design guidelines have been developed to assess the performance of the pipelines subjected to ground movements.

This chapter presents existing design, and the previous studies conducted in this area, including physical modeling and computational modeling. It provides an overall review of the studies conducted on pipelines subjected to lateral ground movements. Chapter 3 and Chapter 4 include literature reviews more specific to the problems discussed in this thesis. Since the focus of the current study is the pipelines in cohesionless soil, the design guidelines related to cohesionless soil are only discussed.

2.2. Existing design guideline

Many geotechnical problems involve the interaction of soil and structures buried in the soil. Physical modeling of soil-structure interaction for those problems, such as piles, caissons, and pipes, would be very complex and time-consuming. The design guidelines and modeling techniques commonly used aim to balance the precision of the theoretical experiment and the simplicity expected for implementation by design engineers. To this end, the current engineering design practice for modeling pipe-soil interaction employs the idealization of the pipelines as a beam supported by the soil springs. Soil is often represented by three discrete nonlinear, stress-dependent load-deformation characteristic spring elements derived from the sub-grade reaction concept proposed by Winkler (Winkler, 1867). Three discrete nonlinear springs are indicated by *T-x, P-y, Q-z* curves that represent the soil behaviour in axial, horizontal, and vertical directions, respectively, as shown in Figure 2.1 (ALA, 2005; ASCE, 1984; Honegger et al., 2002).

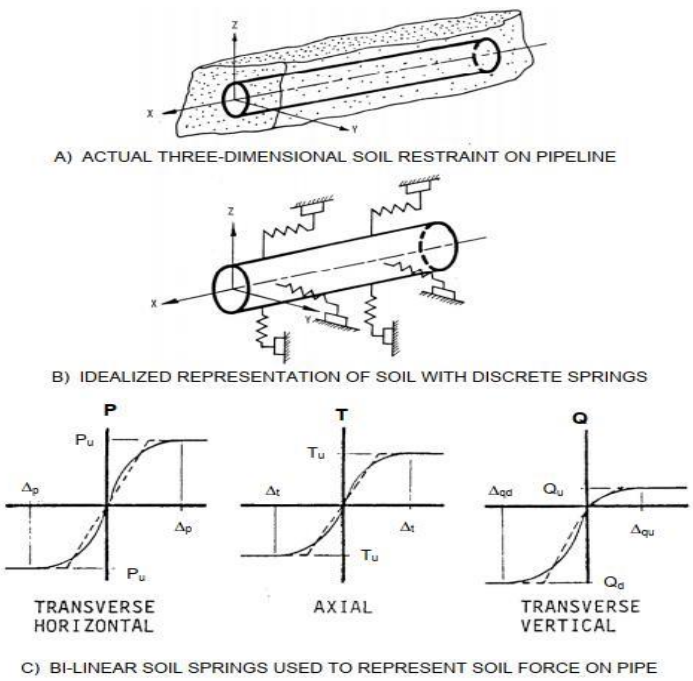

Figure 2.1: Representation of soil spring (ALA, 2005)

The three springs are classified as distinct and are located perpendicular to each other to illustrate the resistance of the soil to the beam or pipeline. In this model, the load-displacement relationships for springs are expressed as follows:

$$T = f(x), P = g(y), Q = h(z) \quad [2.1]$$

where *T, P,* and *Q* indicate the forces applied along the length of the pipe (N/m). The relative displacements between the pipe and soil are indicated by *x, y,* and *z* in the axial, lateral, and vertical directions, respectively. Based on previous studies on piles and other structures (e.g., plates, anchors, pipes), the force-displacement relationship between the soil springs and the pipeline is considered to be nonlinear. However, the design guidelines (e.g., ALA, 2005) recommend using bilinear models or hyperbolic functions, which are easier to use in the analysis.

The conventional Winkler model (Winkler, 1867) considers each spring as a distinct entity, which means that any loading in one direction does not translate to loading in the other two directions. This type of assumption prevents the replication of all shearing modes within the soil and can result in an oversimplified model, particularly if the loading occurs in multiple planes. Several multi-parameter models have been suggested to further address this shortcoming, including Reisner's simplified continuum model and the modified Reisner's model (Horvath, 2002 and Horvath et al., 2011). In those models, the spring does not work independently as it allows coupling. Thus, the effect of loading in a single direction translates into different planes. This spring coupling enables more effective soil shears around the pipeline more effectively, but usually, the applications are concentrated only on two axes being coupled for ease of use and convenience.

2.3 Defining pipe-soil interaction

The pipe-soil interaction is generally defined in the design guidelines (e.g., ALA, 2005) using Winkler springs in the direction of loading. The springs in three independent directions (i.e., axial, lateral, or vertical) are defined for the pipeline independently of the loading type, based on the force-displacement relationship for each direction, depending on the pipe size and burial conditions. The friction between the pipe and the surrounding soil contributes to the force-displacement relations, which is accounted for as the interface friction angle δ obtained from the angle of internal friction of the soil, ϕ. The interface friction angle for pipe and soil depends on the coating factor of pipe material and the internal soil friction angle, as described below:

$$\delta = f\phi \qquad [2.2]$$

where f represents the coating factor and ϕ represents the internal friction angle of soil. The coating factor normally varies between 0.5 to 1, depending upon the type of external coating and smoothness of the pipe surface (Table 2.1).

Table 2.1: Friction factors for different pipe coatings (ALA, 2005)

Pipe Coating	f
Concrete	1.0
Coal tar	0.9
Rough steel	0.8
Smooth steel	0.7
Fusion bonded epoxy	0.6
Polyethylene	0.6

2.3.1 Axial pipe-soil interaction

The maximum axial soil force acting per unit length of the pipe can be described as below (ALA, 2005; ASCE, 1984):

$$T_u = \pi D H \gamma \frac{1+K_0}{2} \tan(\delta) \quad [2.3]$$

Here, T_u is the ultimate soil load on the pipe per unit length, D is the external diameter of the pipe, H is the depth of pipe up to the springline from the soil surface, K_0 is the coefficient of earth pressure at rest, and δ is the interface friction angle for pipe and soil.

The peak displacement required to obtain the ultimate axial soil force per unit length of the pipe varies between 3 to 5 mm in dense sand and 5 to 8 mm in loose sand, depending on the soil density and internal friction angle. This equation implies the pipeline at rest and does not allow for any lateral or longitudinal loads that might exist on the pipeline. The value of the interface angle of friction (δ) can be obtained from the soil internal friction angle and the coating factor provided in Table 2.1.

Various approaches can be used to calculate the coefficient of earth pressure at rest (K_0). According to the continuum mechanics theory, K_0 solely depends on the Poisson's ratio ν and is given by Equation (2.4) (Tschebotarioff, 1973).

$$K_0 = \frac{\nu}{1-\nu} \quad [2.4]$$

Jacky (1944) suggested a relationship that can be used for loose sands and normally consolidated clay as described below:

$$K_0 = 1 - \sin(\phi') \quad [2.5]$$

where ϕ' stands for the effective internal friction angle of the soil.

Sherif et al. (1984) provided an equation to calculate the coefficient of earth pressure at rest (K_0) for dense over consolidated sands, as in Equation (2.6).

$$K_0 = (1 - \sin \phi') + 5.5 \left(\frac{\gamma_d}{\gamma_{d-min}} - 1\right) \quad [2.6]$$

where ϕ' is the effective internal friction angle of the soil, γ_d is the dry unit weight of sand, γ_{d-min} is the minimum dry unit weight.

2.3.2 Lateral pipe/soil interaction

The maximum lateral spring force suggested in the design guidelines (ALA, 2005; ASCE, 1984) is given as below:

$$P_u = N_{ch} cD + N_{qh} \bar{\gamma} HD \quad [2.7]$$

where

N_{ch} = Horizontal bearing capacity factor for clay (0 when c = 0)

$$= a + bx + \frac{c}{(x+1)^2} + \frac{d}{(x+1)^3} \leq 9 \quad [2.8]$$

N_{qh} = Horizontal bearing capacity factor for sand (0 when $\emptyset = 0^{\circ}$)

$$= a + bx + c(x)^2 + d(x)^3 + e(x)^4 \quad [2.9]$$

P_u is the peak load per unit length of the pipe, H is the depth to pipe centerline, $\bar{\gamma}$ is the effective unit weight of soil, D is the pipe outside diameter, and c represents the soil cohesion. N_{ch} and N_{qh}

are two dimensionless parameters that depend on the internal friction angle and burial depth to diameter ratio. Other parameters for Equations (2.8) and (2.9) are provided in Table 2.2.

Equation (2.10) provides the peak displacement at the ultimate lateral spring force, according to the design guidelines.

$\Delta p =$ displacement at P_u

$$= 0.04\left(H + \frac{D}{2}\right) \leq 0.10D \; to \; 0.15D \qquad [2.10]$$

ALA (2005) and ASCE (1984) guidelines provide parameters to calculate N_{ch} and N_{qh} in Table 2.2, based on Hansen (1961). PRCI (2017) design guidelines recommend a different chart for the N_{ch} and N_{qh}. Figure 2.2 presents the charts for N_{ch} and N_{qh} based on Hansen (1961) and PRCI (2017) recommendations.

Table 2.2: Horizontal bearing capacity factor

Factor	∅	*x*	*a*	*b*	*c*	*d*	*e*
N_{ch}	0°	*H/D*	6.752	0.065	-11.063	7.119	--
N_{qh}	20°	*H/D*	2.399	0.439	-0.03	$1.059(10)^{-3}$	$-1.754(10)^{-5}$
N_{qh}	25°	*H/D*	3.332	0.839	-0.090	$5.606(10)^{-3}$	$-1.319(10)^{-4}$
N_{qh}	30°	*H/D*	4.565	1.234	-0.089	$4.275(10)^{-3}$	$-9.159(10)^{-5}$
N_{qh}	35°	*H/D*	6.816	2.019	-0.146	$7.651(10)^{-3}$	$-1.683(10)^{-4}$
N_{qh}	40°	*H/D*	10.959	1.783	0.045	$-5.425(10)^{-3}$	$-1.153(10)^{-4}$
N_{qh}	45°	*H/D*	17.658	3.309	0.048	$-6.443(10)^{-3}$	$-1.299(10)^{-4}$

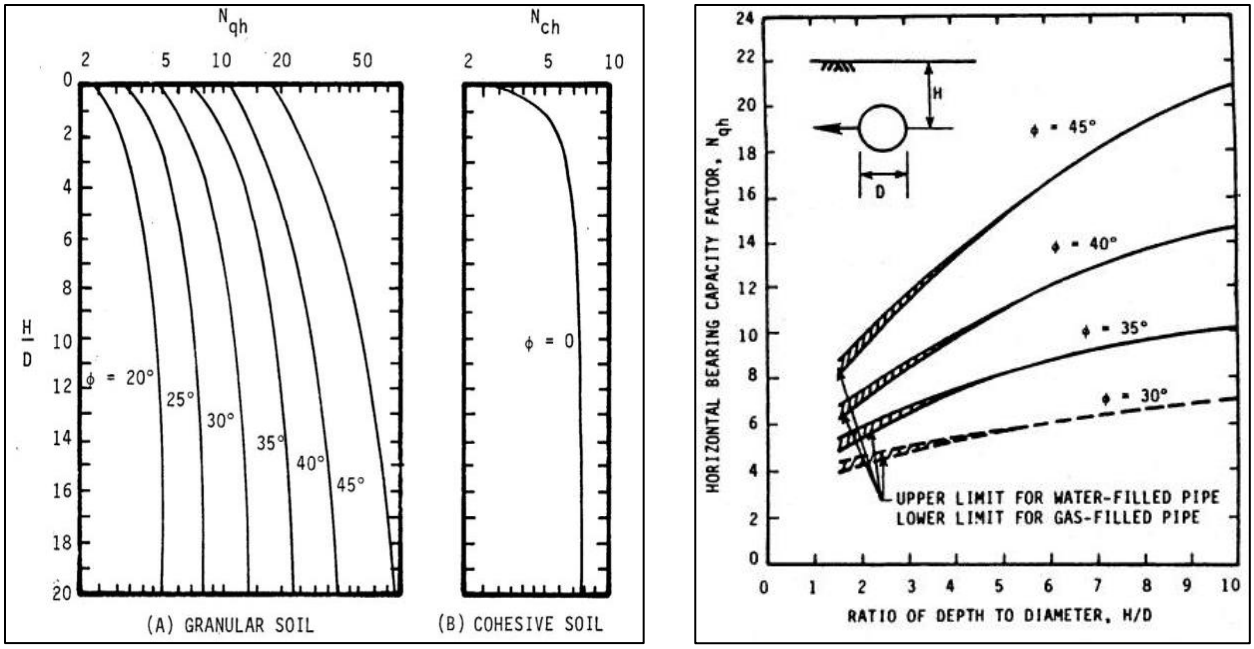

(a) (b)

Figure 2.2: Horizontal bearing capacity factor: (a) Hansen (1961), and (b) PRCI (2017)

2.3.3 Vertical spring

2.3.3.1 Uplift soil springs

The equation suggested by (ALA, 2005; ASCE, 1984) to calculate the maximum vertical uplift spring force per unit length is described below (Equation 2.11). The applicability of the equation (Equation 2.11) is limited to lower embedment ratio (*H/D*), and for the greater *H/D* ratio, case-specific geotechnical guidances are required to obtain the magnitude of soil spring force.

$$Q_u = N_{cv} c D + N_{qv} \bar{\gamma} H D \quad [2.11]$$

where

N_{cv} = vertical uplift factor for clay

N_{qv} = vertical uplift factor for sand

Q_u is the ultimate load per unit length of the pipe, *H* is the depth to pipe centerline, $\bar{\gamma}$ is the effective unit weight of soil, *D* is the pipe's outside diameter, and *c* represents the soil cohesion. The peak displacement required to obtain the ultimate force per unit length of the pipe varies between *0.01H* to *0.02H* mm for dense to loose sand, depending on the pipe diameter.

2.3.3.2 Bearing soil spring

The maximum bearing soil spring force suggested in the design guidelines (ALA, 2005; ASCE, 1984) is given below:

$$Q_d = N_c cD + N_q \bar{\gamma} HD + N_\gamma \gamma \frac{D^2}{2} \quad [2.12]$$

Here, N_c, N_q and N_γ are the bearing capacity factors which can be obtained from Figure 2.3. Q_d is the ultimate load per unit length of the pipe, *H* is the depth to pipe centerline, $\bar{\gamma}$ is the effective unit weight of soil, γ is the total unit weight of soil, *D* is the pipe outside diameter, and *c* represents the soil cohesion. The peak displacement at ultimate force per unit length is *0.1D* for granular soils and *0.2D* for cohesive soils.

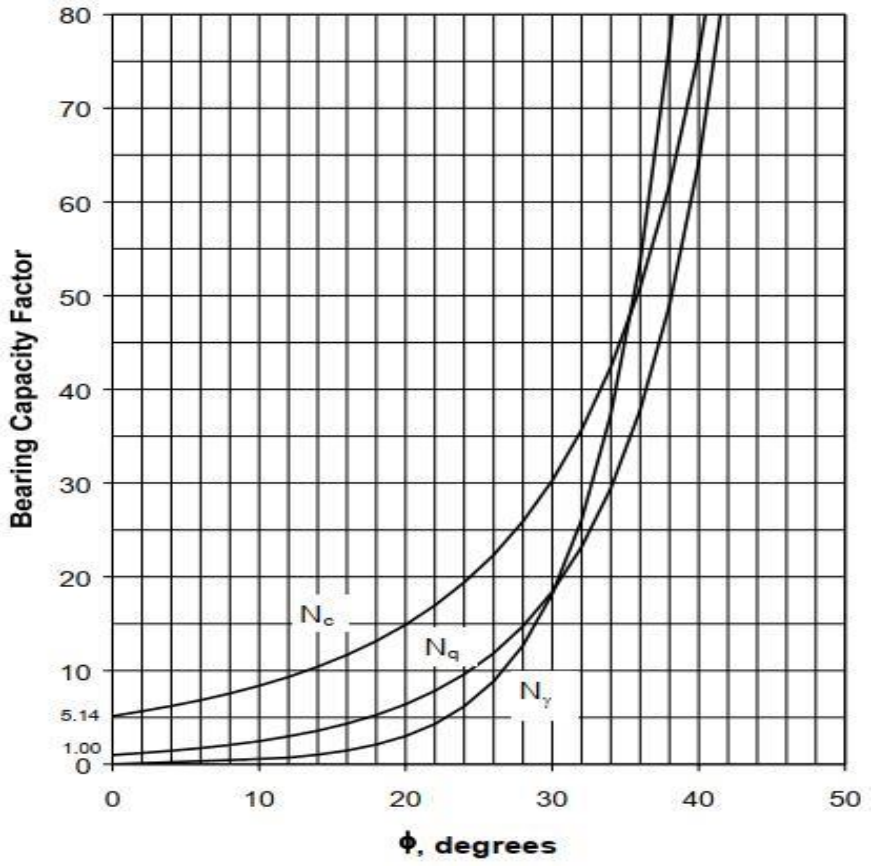

Figure 2.3: Plotted value of bearing capacity factors (N_c, N_q and N_γ) (ALA, 2005)

2.3.4 Pipe-Soil Interaction (PSI) element modeling

A pipe-soil interaction (PSI) element available in Abaqus, a finite element software, is increasingly being used recently to model the behaviour of buried pipe. Abaqus provides two-dimensional (PSI24 and PSI26) and three-dimensional (PSI34 and PSI36) pipe-soil interaction elements to model the interaction between a buried pipeline and the surrounding soil. The pipeline is modeled as a beam using pipe elements (available in Abaqus). A PSI element is a special type of quadrilateral element that interacts with a structural beam element. One side of each PSI element shares nodes with all nodes of a beam or pipe element it is interacting with (Figure 2.4). The other side represents a far-field or ground surface. The depth of the PSI element is kept equal to the

height of the ground surface above the pipe springline, *H*. The element only has the displacement degree of freedom at its nodes. As the actual domain of the surrounding soil is not discretized for using the PSI elements, the actual condition of the surrounding medium (soil) is not explicitly modeled. The effects of the soil medium are implicitly represented by the model parameters (i.e., spring constants).

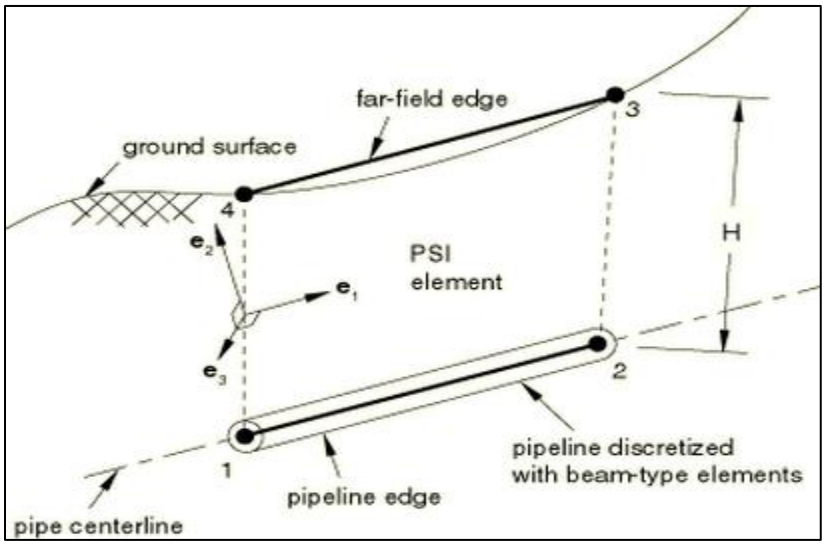

Figure 2.4: Pipe-Soil Interaction (PSI) element development technique (Abaqus, 2014)

The deformation of the PSI element is described by relative displacements between the nodes on the two opposite edges of the element. The elements are strained by the relative displacements that depend on their constitutive model parameters. Positive strains are described as:

$$\varepsilon_{ii} = \Delta u \times e_i \qquad [2.13]$$

where $\Delta u = u_{far} - u_{pipe}$ are the relative displacements between the two edges with u_{far} being the far-field displacement and u_{pipe} being the displacement of the pipe. The term e_i indicates the local directions, where the index value of i ($i = 1, 2, 3$) refers to the three local directions. The strain components of ε_{11} and ε_{22} are available in two-dimensional and the strain component of

ε_{11}, ε_{22} and ε_{33} are available in three-dimensional elements. The symbols e_1, e_2 and e_3 are used to define the three different local directions: e_1 presents the axial direction, e_3 presents the transverse horizontal direction and $e_2 = e_3 \times e_1$ defines the transverse vertical behaviour.

The PSI elements are strained when subjected to the applied load or displacement and the forces are transmitted to the pipeline nodes. These forces can be a linear function (elastic) or a nonlinear function (elastic-plastic) of the strains in accordance with the type of constitutive model that the element uses. At each point along the pipeline, relative displacement, or strain, ε_{jj} induce force per unit length, q_i between that point and the point on the far-field surface, which is defined below.

$$q_i = q_i\,(\varepsilon_{jj}, s_\alpha, f_\beta) \qquad [2.14]$$

Here s_α and f_β define the state variables and field variables, respectively. The force per unit length (q_i) is controlled by the constitutive model.

For defining the constitutive behaviour of the PSI element, two methods are generally used in Abaqus: (1) defining the q_i relationship directly in a tabular format, (2) using the ASCE guideline (ASCE, 1984), which describes the relationship for sands and clays having different soil properties. A linear (Figure 2.5a) or non-linear (Figure 2.5b) constitutive behaviour can be defined using tabular input with various positive and negative tension behaviours. To define a nonlinear behaviour, both for positive and negative displacements, field variables can be used as a function of force per unit length (q_i). Data are given in the ascending order of relative displacement and are provided over an adequately large range of relative displacement values such that the behaviour is properly described. Outside the range of data points, the force remains unchanged.

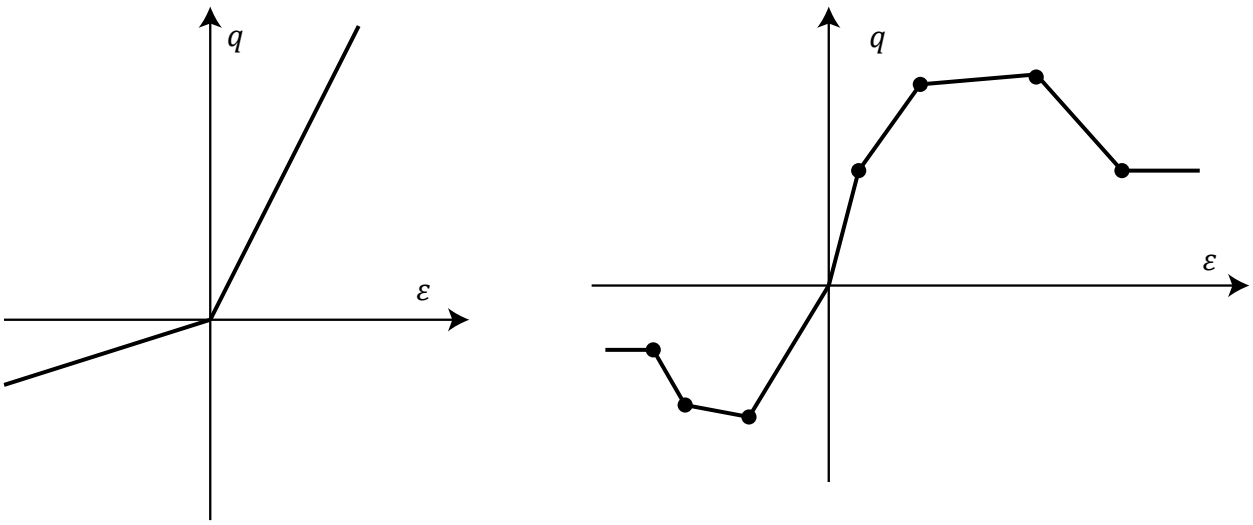

(a) (b)

Figure 2.5: Constitutive behaviour: (a) Linear, and (b) Nonlinear

2.4 Review of experimental studies

The present understanding of lateral ground movement effects on pipelines is predominantly based on the experimental results from small-scale lateral pullout tests of pipe segments or anchors. The very first lateral pullout test was conducted on vertical plate anchors to obtain the horizontal force-displacement characteristics (Casbarian et al., 1966; Choudhary and Dash, 2017; Das, 1975; Das and Seeley, 1975; Neely et al., 1973; Rowe and Davis, 1982). These studies aimed to perform experimental investigation and develop analytical models of lateral resistance of vertical anchors. However, pipelines subjected to ground movements involve a more complex interaction with the surrounding soil. The pipe behaviour also depends on the orientation of the ground movements with respect to the pipe axis and the boundary conditions of the pipe. Researchers conducted physical model tests and numerical models to develop an improved understanding of the soil-pipe interactions during relative ground movements in the longitudinal

direction of the pipes (Audibert and Nyman, 1977; Muntakim et al., 2018; Paulin et al., 1995; Reza et al., 2019; Sheil et al., 2018; Weerasekara, 2011; Weerasekara and Wijewickreme, 2008; Wijewickreme et al., 2009; Wijewickreme and Weerasekara, 2015).

Full-scale lateral and vertical uplift pullout tests were conducted by Trautmann and O'Rourke (1983) on steel pipes with 102 mm and 324 mm diameters with three different densities of sand (14.8, 16.4, and 17.7 kN/m^3). A total of 30 lateral loading tests were conducted with three densities and five burial depths to diameter ratios (H/D) equal to 1.5, 3.5, 5.5, 8, and 11. Displacements associated with maximum force were found to be about 0.13H, 0.08H, and 0.03H for loose, medium, and dense sand, respectively. A dimensionless depth versus normalized horizontal force graph was developed for different internal friction angles of the soil. The goals of the study were to measure maximum soil force, evaluate force-displacement characteristics as a function of soil density and H/D results which were used as a basis of the design guidelines for calculating the lateral pullout resistance in ASCE (1984).

Hsu (1993) conducted an extensive full-scale testing program (120 tests) examining the effects of several variables such as burial depth, soil density, pulling rate, pipe diameter, and soil density, focusing on the behaviour of rigid pipe. Hsu et al. (2001) conducted an experimental study to investigate the friction load of soil due to oblique pipe movements in loose sand. Hsu et al. (2006) also conducted another test on dense sand for investigating soil friction load. Then, analytical models were used to evaluate the longitudinal and lateral soil load.

Paulin et al. (1998) conducted an extensive testing program to investigate the pipe-soil interaction using sand and clay. Two pipe-soil loading conditions: lateral movement and axial movement were considered. To understand the flexural behaviour of buried pipe, a number of investigations were conducted at the Centre for Cold Ocean Resources Engineering (C-CORE) by Konuk et al. (1999).

Two large-scale tests were conducted to investigate the bending behaviour of buried pipes due to lateral loading in dense sand, measuring the pipe profile deflection, ovalization effect and pipe force-induced soil deformation. Yoshizaki et al. (2001) conducted laboratory lateral pullout tests to study the permanent ground displacement (PGD) effects on a steel pipe of 100 mm diameter and 4.1 mm thickness with a composition of a 90-degree elbow connection. They also conducted finite element analysis (FEA) with a Hybrid Model that showed a perfect agreement with the deformation and axial strain in the longitudinal direction.

A full-scale laboratory lateral pullout test was performed using a branched polyethylene pipe with three different diameters in dense and loose sand at the University of British Columbia (Anderson et al., 2004). The contribution of the branch pipe to soil resistance was studied, and complex interaction between the branch pipe and soil was observed. The study showed that a small diameter trunk pipe is more vulnerable due to the presence of branched pipe, in contrast to the larger diameter pipe where the branch pipe is more vulnerable, subjected to permanent ground movement. A reduced soil resistance was noticed due to the arching effect providing a peak value of the load-displacement response. To study the lateral and axial pipe-soil interaction for large diameter rigid steel pipelines (324 mm and 457 mm), a full-scale testing program was conducted at the University of British Columbia by Karimian (2006). The aim of the study was to investigate the response of buried steel pipeline subjected to lateral and axial loading and study the effect of trenching.

To obtain the force-displacement behaviour under various conditions, Liu et al. (2011) conducted vertical, lateral, and axial pullout tests at different burial depth to diameter ratios between 1 and 9. Stainless steel pipes with a length of 1200 mm and diameters of 30 mm, 50 mm and 80 mm were chosen for the tests at a constant pullout rate of 0.06 mm/sec. The sand density was kept at 16.6

kN/m^3. They used a model tank of 1 m × 1 m × 3 m (length × width × depth) dimensions made of PVC plates for their tests. It was found that the soil resistance became flat after the peak value for all the tests, and the displacement corresponding to peak force was pipe diameter dependent. Thermal effect and internal pressure were also monitored, concluding that the lateral soil resistance is more than twice that for uplift resistance for the same covered depth, and that the soil failure modes with smaller depth of cover are greatly different from those with larger cover depth.

At Queen's University, Almahakeri et al. (2012) conducted tests with three small-diameter steel pipes and two different GFRP laminate structure pipes. The nominal diameter was 102 mm. The tests were conducted in dense sand with H/D ratios from 3 to 7. This study mainly focused on load-displacement behaviour and bending deflection of steel and GFRP pipes subjected to lateral ground deformation. Later Almahakeri et al. (2014) conducted nine full-scale lateral pullout tests on buried 105 mm diameter steel pipes with H/D ratios ranging from 3 to 7. Both studies summarized that the bending deflection of the pipe is not linear with the pulling forces even within the elastic range of the material tested.

A large-scale test was conducted by Wang et al. (2018) with a 200 mm diameter PVC pipe to study the lateral resistance of a shallow-embedded pipeline using a model test tank (3 m × 1.1 m × 1 m). The pipe was buried in marine sand with a density of 1455 kg/m^3 and an internal friction angle of 30.9 degrees. Two different series of tests were conducted: (1) large amplitude motion tests to study the lateral soil response under different pipe weights and embedment ratios up to the displacement of 6D and, (2) breakout observation tests to investigate the deformation mechanism of soil during the breakout stage during small displacement. A softening response of lateral resistance was observed at an embedment ratio of 0.5. Breakout was observed for the lightweight

pipe in a deep embedment condition, whereas for heavy pipe, the breakout was observed in a shallow embedment condition.

Raheem (2019) conducted a large-scale physical model test to examine the behaviour of lateral pipe-soil interaction for PVC and steel pipes in ultra-soft clayey soil. The pipes of 90 mm diameter and 120 mm length were tested at three different displacement rates (0.04 mm/sec, 0.4 mm/sec and 2.1 mm/sec). The effects of fixed-end, free-end boundary conditions of the pipe and the lateral pipe-soil interaction behaviour in ultra-soft clayey soil were investigated. It was noticed that fixed-end boundary conditions could increase the lateral resistance up to 50% more than the free-end conditions. The study concluded that PVC pipe could have a higher lateral resistance than steel pipe in ultra-soft clay as the coefficient of adhesion of the PVC pipe is higher than for the steel pipe.

This review reveals that most experimental studies focused on steel pipes, with limited studies of polyethylene and PVC pipes. There are research gaps in understanding the behaviour of polymer pipes using experimental observations.

2.5 Review on numerical modeling

Different numerical modeling techniques were employed to estimate the ultimate pullout capacity of anchor plates. The finite element method of strip anchor was employed using different constitutive models (Vermeer and Sutjiadi 1985, Tagaya et al. 1983, and Sakai and Tanaka 2007) to observe the horizontal pullout capacity. Murray and Geddes (1987) and Smith (1998) performed lower bound limit analysis to determine the capacity of horizontal and vertical anchor plate strips. Dickin and Laman (2007) determined the pullout capacity of a strip anchor (1 m wide) in both

loose and dense sand using finite element software PLAXIS (plane strain analysis). The studies concluded that the ultimate pullout resistance of the anchor plate is related to the embedment ratio and sand packing. Instead of a single anchor strip, Kumar and Bhoi (2008) used multiple strip anchor plates and converted multiple strips to a single strip using a proper boundary (considering plane of symmetry) condition through numerical analysis. The interference effect due to multiple anchor plates in the granular medium was investigated. Roy et al. (2018) performed finite element analysis for lateral loading response of vertical strip anchors and compared the result with those of buried pipes. They identified the limitations of the conventional Mohr-Coulomb model for the soil and found a Modified Mohr-Coulomb model to better represent the soil behaviour. It was observed that the normalized peak resistance is related to the embedment ratio. However, at a large burial depth, the peak resistance became constant. The anchor plate provided around 10% higher peak lateral resistance than buried pipe when the pipe diameter and height of the anchor were the same.

Yimsiri et al. (2004) employed two soil models (Mohr-Coulomb and Nor-Sand model) for FE analysis of 102 mm diameter pipe with embedment ratios of 2 to 100. The model was developed based on the experimental data provided by Trautmann (1983). The simulation was further extended up to the embedment ratio of 100. A design chart for deep embedment pipelines was proposed based on the numerical simulations. To explore the soil-pipe interaction from a micromechanics perspective, Yimsiri and Soga (2006) conducted Distinct Element Method (DEM) analysis of a shallow embedment depth, based on the test results of Trautmann (1983). They reported that the peak dimensionless forces are almost similar in both DEM and FEM for medium dense sand. However, for the dense sand, DEM analysis showed a higher value due to its ability to simulate the large soil movement near the pipe.

Guo and Stolle (2005) examined the lateral force for a wider range of pipe diameters (33-3300 mm) and burial depths (embedment ratio of 1.03 to 10) using continuum-based finite element analysis. They investigated the effects of the stress level and model scale on lateral pipe-soil interaction using ABAQUS/Standard. It was concluded that lateral ground-induced maximum pipe force depends on the pipe's size and the burial depth. Based on the numerical study and in comparison with published laboratory test results, a relation was established between pipe diameter, dimensionless force, and H/D ratio.

Karimian (2006) performed a numerical analysis of buried steel pipe with a diameter of 460-mm and H/D ratio of 1.92 using FLAC 2D finite-difference software. Two different soil models were considered: Mohr-Coulomb model and Hyperbolic model. The conventional Mohr-Coulomb model was found to provide a 17% higher peak load than the observed experimental results. The hyperbolic model showed good agreement with the experimental results.

While most of these studies focused on the analysis of rigid pipes under plane strain conditions, Daiyan et al. (2011) investigated the bending behaviour under axial-lateral pipe-soil interaction using 3D finite element analysis. In the 3D continuum model, solid elements (C3D8R) were used for the soil domain, and shell elements (S4R5) were used for the pipe. Jung et al. (2013 and 2016) analyzed the lateral pipe-soil interaction in dry and partially saturated sand and the multi-directional force-displacement response using finite element models under plane strain conditions. The model was validated against large-scale test results. Based on the analysis, a dimensionless force-depth relationship was developed for dry medium, dense, and very dense sand.

A few studies are also available in the literature that have investigated the soil-pipe interaction for polyethylene pipes. Naeini et al. (2016) performed finite element analysis of High-Density Polyethylene (HDPE) pipe to investigate the effect of diameter, thickness, burial depth, friction

angle, the density of surrounding soil, and the bending strain. A three-dimensional model was developed using solid elements (C3D8R) for the soil and shell elements (S4R) for the pipe, using Abaqus. The results of the analysis were compared with the experimental results, and these were calculated using a Winkler-based two-dimensional analysis. For the Winkler-based analysis, beam elements (B32) were used to idealize the pipe, and soil-structure interaction elements (PSI36) were used to represent the soil-pipe interaction. The finite element model reasonably predicted the experimental bending strains. However, the Winkler based model overpredicted the bending strain. The difference increased with the increase of fault displacement. The authors also suggested that in order to reduce bending strain on the pipe, it is necessary to bury the pipe at a shallower depth.

Almahakeri et al. (2016) and Almahakeri et al. (2019) also examined the bending deformations and strains on buried pipes using the finite element method. The effect of internal friction angle, selection of proper element type and modulus of elasticity dependent stress variation within the soil were investigated. A constitutive non-associated Mohr-Coulomb model and an elastoplastic model were used for dense sand and the steel pipe, respectively, and were used to observe the bending behaviour and the strain along the pipe.

2.6 Analytical models

Flexural analysis of a foundation is often conducted on granular soil by simulating either as a beam or a plate on an elastic medium. The beam on a flexible foundation has given the fundamental auxiliary model for a range of problems, including pipelines. The continuous pipeline system can generally be analyzed as a beam on an elastic medium. The well-known closed-form solutions of the beam having a finite and infinite length on an elastic foundation were provided by

Hetényi (1946) using Winkler's hypothesis (Winkler, 1867). It considered the soil as an infinite number of independent springs based on the constant subgrade modulus and uniform beam cross-section assumptions (Winkler, 1867). The solutions of Hetényi (1946) were developed for small deformation problem only and, therefore, are not applicable for the pipelines subjected to ground movements where the deformation is large. Liu and O'Rourke (1997) revealed that for pipelines subjected to ground movements, a continuous pipe behaves like a beam over a small width of the deformation zone where the flexural stiffness controls response. A cable-like behaviour was observed over the rest of the pipe length, where both axial force and bending deformation control the pipe responses.

Weerasekara and Wijewickreme (2010) developed an analytical model for calculating the pipe wall strain of MDPE pipes considering the axial force and bending deformation. They studied the behaviour of buried pipe subjected to abrupt ground movement perpendicular to the pipe axis. The pipe's load-displacement responses were divided into two different regions: the small deformation region where only pipe bending governs the lateral deformation and the large deformation region where both axial force and pipe bending act together.

2.7 Summary

Pipelines subjected to lateral ground deformation may cause damage to the pipe due to increased loading from the surrounding soil. A review of existing experimental and numerical/analytical investigations on the effects of lateral ground movements is presented in this chapter. The existing design guidelines (ASCE 1984, ALA 2005), as well as various proposed methods of pipe analysis, are discussed. The review reveals that most of the investigations

available in the literature focus on rigid pipe, with particular attention to steel pipe. The numerical analysis conducted for the pipe-soil interaction focused on the beam-on-spring type of idealization due to the simplicity of the method. The major challenge in this method is to define the spring parameters appropriately to represent the soil-pipe interaction correctly. The spring parameters were reported to depend on the pipe material and its flexural rigidity, which can be developed based on extensive experimental investigations of the pipe behaviour. Only a limited number of studies are available in the literature on investigating the behaviour of MDPE pipes. Further research is needed to understand the behaviour of MDPE pipes and develop numerical modeling technique to investigate the pipe-soil interaction for MDPE pipe.

CHAPTER 3

Experimental Investigation of the Ground Movement Effects

3.1 Introduction

Buried pipelines serve as the most convenient and economical means of transporting liquids and gases. Over the last several decades, plastic pipes have been increasingly used due to their various advantages, including low cost, corrosion-resistance, light weight, and flexibility. In North America, 90% of the natural gas pipelines are plastic pipes, of which 99% are polyethylene pipes (PIPA, 2001). Pipelines are often exposed to various hazards, including differential ground movements resulting from landslides, earthquakes, fault movements, and other sources. Ground movements have been identified as one of the major causes of pipeline failure (EGPIDA 2018). Assessment of the effects of ground movements on the performance of the pipeline is, therefore, an important consideration for pipeline integrity assessment.

The behaviour of pipelines subjected to the ground movements is governed by a complex interaction of the pipelines with the surrounding soil, which also depends on the orientation of the ground movements with respect to the pipe axis and the pipe's boundary conditions (i.e., joints or connections). Researchers have conducted physical model tests and numerical modeling to develop an improved understanding of the soil-pipe interactions during relative ground movements in the longitudinal direction of the pipes (Paulin et al., 1998; Wijewickreme et al., 2009; Daiyan et al., 2011; Sheil et al., 2018; Muntakim et al., 2018; Reza et al., 2019). Earlier works investigating pipelines subjected to lateral ground movement focused on examining the maximum lateral loads imposed on rigid pipes only (Audibert and Nyman, 1977). Audibert and Nyman (1977) conducted

tests with steel pipes having different diameters (25-mm, 60-mm, and 114-mm) and observed the soil behaviour against lateral displacements of the pipes. Pipes buried in the sand with various densities and with various burial depths were investigated. Based on the tests, force-displacement relations were expressed as hyperbolic functions. The hyperbolic functions support the relation provided in Das and Seeley (1975), who investigated the load-displacement relationship of a vertical anchor plate against the horizontal movement in the ground. Trautmann (1983) conducted full-scale experiments on pipes with two different diameters (i.e., 102-mm and 324-mm) subjected to lateral movements with sand of three different sand densities. Hsu (1993) undertook an extensive full-scale testing program examining several variables such as burial depth, pulling rate, pipe diameter, and soil density. It was shown that the soil resistance and corresponding pipe displacement exhibit a power-law relation against the velocity of movements.

Konuk et al. (1999) conducted two large-scale tests to investigate the bending behaviour of buried pipes due to lateral loading in dense sand. During each test, measurements were made of the deflected pipeline profile, pipeline ovalization, lateral forces, and the associated soil deformations. Almahakeri et al. (2012) and Almahakeri et al. (2014) also conducted tests with steel pipes and Glass Fiber Reinforced Polymer (GFRP) pipes, respectively, which had a nominal diameter of 100 mm in dense sand. The studies concluded that bending deflection of the pipe is not a linear function of the pulling force, even within the elastic range of the pipe stresses. The nonlinearity is attributed to the effect of the highly nonlinear behaviour of the surrounding soil. For the investigation of the flexural behaviour of buried pipe under lateral ground movement, Konuk et al. (1999) and Almahakeri et al. (2012 and 2014) pulled a buried pipe with parallel forces from two ends of the pipe. This simulates the responses between the inflection points during longitudinal bending of the pipe (Almahakeri et al., 2012). The tests correspond to the behaviour of a simply supported beam

subjected to the load from the soil. Thus, the stresses/strains developing in the pipe walls are expected to be influenced by the distance between the supports (span). Researchers also conducted two-dimensional and three-dimensional numerical analyses to examine the laboratory pullout test data on different types of pipes using various numerical modeling software (Yimsiri et al., 2004; Guo and Stolle, 2005; Karimian, 2006; Daiyan et al., 2011; Jung et al., 2013; Almahakeri et al., 2016 and Almahakeri et al., 2019).

Distribution pipelines are often connected with lateral branches or connections to supply natural gas to various points of interest. Figure 3.1 shows a lateral branch in a distribution system and a lateral connection to a house. The pipe system can be exposed to soil movement, with tension cracks shown using the dotted lines in the figure. The ground loads from such soil movement can cause bending deformation of the main pipe and axial force on the branch pipe. An excessive bending strain can cause leaking or rupture of the main pipe, while a high axial force on the branch pipe can cause leaking or joint failure. Figure 3.2 shows the bending deformation of a main pipe and the failure of a branch pipe observed in the field due to ground movements. No design method is currently available to assess the bending strain on the main pipe and the axial force on the branch pipe due to such ground movements.

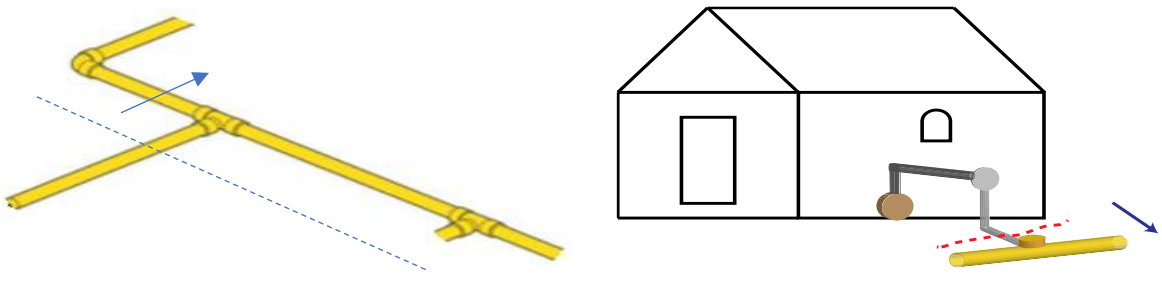

(a) Lateral branch (b) Connection to the client

Figure 3.1: Distribution pipes with lateral connection subjected to ground movement

(a) Bending deformation

(b) Joint break

Figure 3.2: Bending deformation and joint failure due to pipes subject to ground movement (Photo courtesy: FortisBC Energy Inc.)

This chapter presents an investigation of the bending strains on a pipe subjected to lateral ground movement and the axial force on a branch pipe. A full-scale laboratory test method was designed to simulate the effects of the lateral ground movement on a pipe near a connection. Pipe tests were conducted using the test method, measuring the pipe wall strains to capture the deformation mechanism. The solution of the beam-on-elastic foundation was applied for the preliminary evaluation of the measured pipe strains.

Flexural behaviour of foundations on granular soil are often analyzed idealizing a beam resting on an elastic medium. The closed-form solution of the beam with a finite and infinite length on an elastic foundation is provided by Hetényi (1946) using Winkler's hypothesis (Winkler, 1867). Lee and Harrison (1970) applied Hetényi's solution to evaluate the shear force, bending moment, and deflection at various points of the beam. The closed-form solutions of beam-on-elastic-foundation and numerical modeling using the finite element (FE) method are employed in this study to

investigate the flexural behaviour of MDPE pipe at small displacements. A spring constant recommended in Vesic, (1961) is used to account for the soil-pipe interaction. Note that the spring constant in Vesic (1961) was developed based on a beam of infinite length resting on a semi-infinite elastic subgrade. The applicability of these parameters for MDPE pipes is examined through simulation of the pipe responses obtained from the laboratory tests.

3.2 Test method

A test method was designed to simulate the effect of ground movement on a distribution pipeline and the axial force on a lateral branch near a connection. Figure 3.3 shows a ground movement scenario near a pipe connection and its laboratory idealization. In Figure 3.3(a), an idealized prismatic soil mass moved perpendicular to a pipe axis where a branch is connected. The other end of the branch pipe is restrained in the stable ground. The relative movement of the pipe with respect to the surrounding soil was simulated in the laboratory by fixing the soil in a box and pulling a buried pipe by applying force at the location of the branch (Figure 3.3b). The pullout force represents the axial force on the branch pipe due to the relative ground movement. The bending deflection of the main pipe under the effect of soil-pipe interaction was monitored during the tests.

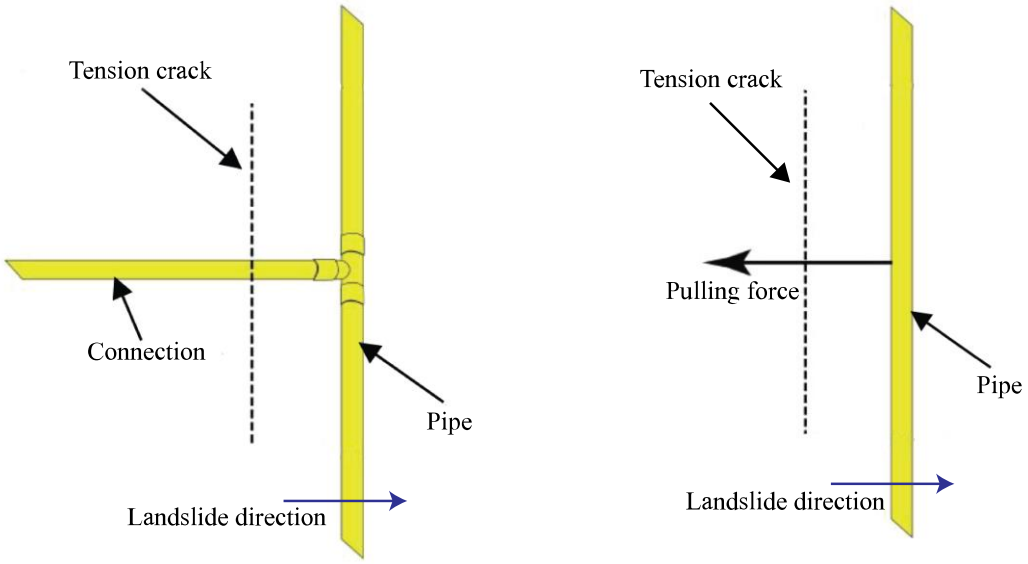

(a) (b)

Figure 3.3: Pipe condition and test idealization: (a) Pipe with lateral connection, (b) Test idealization

A full-scale laboratory test facility developed at Memorial University of Newfoundland (Murugathasan et al., 2020) was used for the tests. The facility is shown in Figure 3.4. The facility (test cell) consists of a steel chamber with dimensions of 4 m (length) × 2 m (width) × 1.5 m (height), having two circular openings on two opposite walls in the long direction. For each test, an MDPE pipe was buried at the desired depth in the test cell and pulled with a pulling cable connected to its midspan (Figure 3.5). The pulling cable passed through a circular opening on the wall to a hydraulic actuator. A mechanism was devised to grip the pipe at the center and pull the pipe laterally from a single point. Note that this grip doesn't represent the actual connection in the field but a mechanism to apply the lateral force. The pulling cable was enclosed in a 42.2-mm MDPE pipe, keeping a 120 mm gap to accommodate pipe movement, as shown in Figure 3.5, to avoid frictional resistance to the cable during pulling. Steel rods or cables are commonly used

encasing in plastic tubes in pipe pullout tests to reduce friction (Trautmann, 1983; Almahakeri et al., 2012). Almahakeri et al. (2012) used threaded rods enclosed in a PVC tube to pull pipes buried in sand. A load cell with a maximum capacity of 22.5 kN was attached between the hydraulic actuators and the pulling cable to measure the applied load (Figure 3.6). The actuator was connected to a steel frame attached firmly to a strong floor. The length of the test pipes was varied to examine the effect of pipe length on the bending mechanism and the test results.

Figure 3.4: Test facility for soil-pipe interaction testing

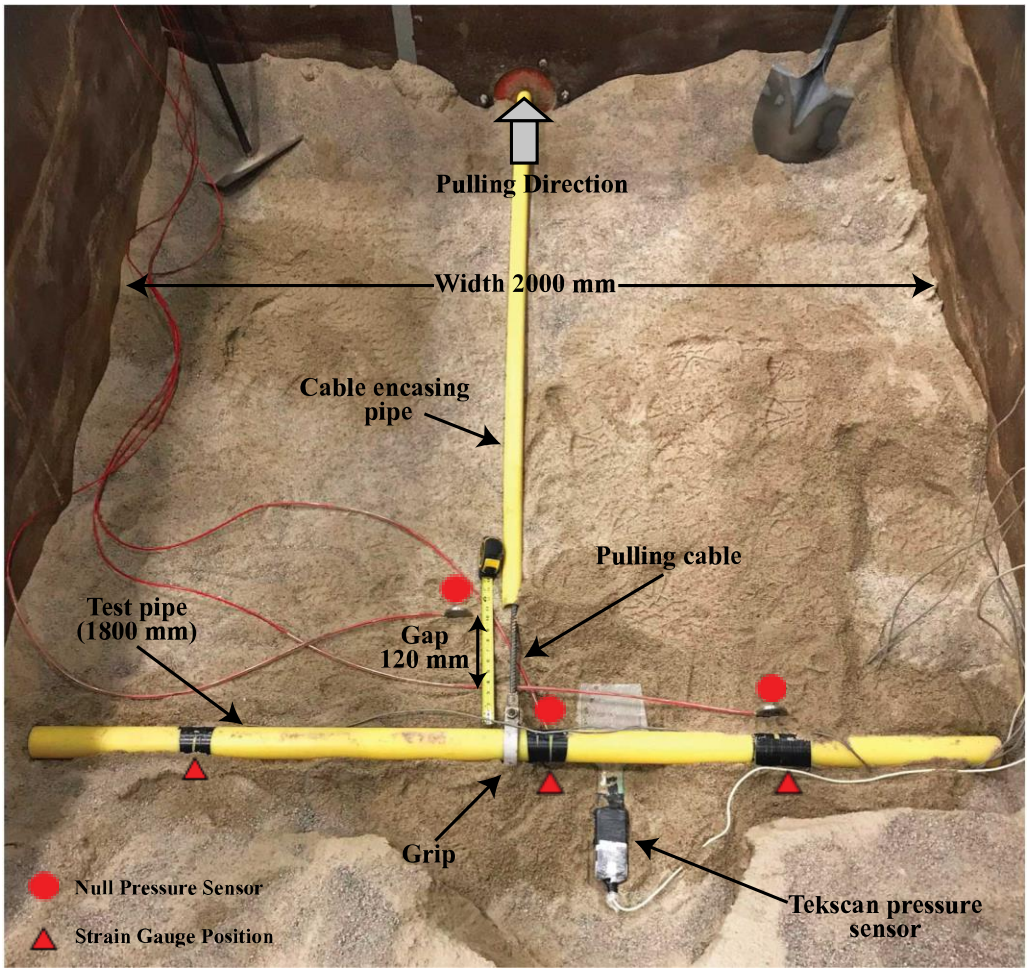

Figure 3.5: Mechanism of lateral pulling of pipe (1800 mm long)

Displacement controlled tests were conducted through pulling at a rate of 0.5 mm/min displacement for all tests. Tests were conducted to a maximum displacement of up to 120 mm, based on the space available for the cable for free movement. The lateral pullout force, lateral displacement, pipe wall strains, and soil stresses were measured during the tests. All data were collected using a data acquisition system. The tests were performed at room temperature (~22°C).

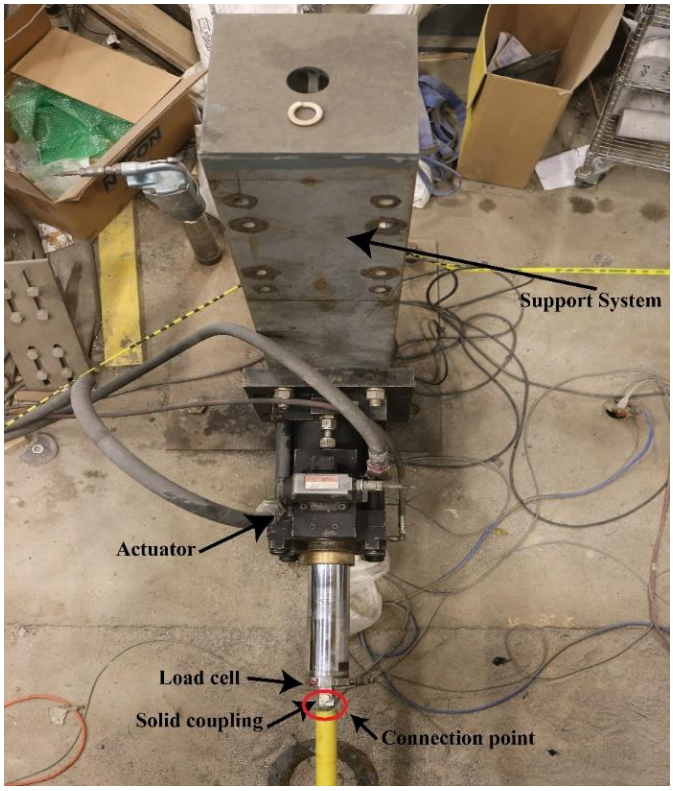

Figure 3.6: Loading mechanism

3.3 Test material

3.3.1 Backfill soil

Locally available well-graded clean sand was selected to backfill the pipes in the test cell. The sand contained about 98.7% of sand and 1.3% fine (Saha et al., 2019). The mean particle size was 0.742 mm. The grain size distribution test indicated the coefficient of uniformity (C_u) of 5.81 and the coefficient of curvature (C_c) of 2.08. Standard Proctor maximum dry unit weight of the sand was 18.0 kN/m^3. The sand was air-dried with an average moisture content of around 1% to avoid the effect of metric suction (Saha, 2021).

3.3.2 MDPE pipe

Medium Density Polyethylene (MDPE) pipes, common in natural gas distribution systems, were used for the tests. The MDPE pipe with two different diameters: (a) 60-mm, and (b) 42.2-mm were considered, which are most common in gas distribution systems. The thicknesses of the pipes were 5.5 mm and 4.22 mm, respectively. For a beam on-elastic-foundation subjected to a point load, the load's effect diminishes at a distance beyond four times the characteristic length (Hetényi, 1946). However, Hetényi's solution is only applicable to small displacement problems. For large displacements, the zone of influence may extend beyond that distance. Thus, the pipe specimens were kept much longer than the estimated four times the characteristic length which includes two different lengths: (a) 1800 mm, and (b) 1500 mm. The specimen lengths are smaller (100 mm on both sides for 1800 mm pipe, 250 mm on both sides for 1500 mm pipe) than the tank width. Therefore, no friction of the pipe ends with the test cell wall was expected. Note that the test condition represents the bending behaviour of the pipe having free-end conditions and does not represent the actual field condition. However, the mechanism observed could be useful for understanding the mechanics of pipe-soil interaction under lateral bending.

3.4 Installation

The sand was poured into the test cell in lifts of about 100 mm thickness, falling from a height of approximately 1 meter. An overhead crane was used to move the sandbags during placement. No sidewall treatment was applied to reduce wall friction between the cell wall and the soil as the effect of sidewall friction on pullout tests of the pipe is insignificant (Wijewickreme et al., 2009). For each lift, the soil surface was leveled using shovels and brooms and then compacted using a hand compactor of 3 kg weight for dense conditions of the soil. After placing a 600 mm thick layer of soil from the bottom of the test cell, the instrumented test pipe was placed. Then, the

soil was placed and compacted again up to the desired depth of soil cover. The density of the sand above the pipe was measured using the Sand Cone method (ASTM D1556-07).

3.5 Instrumentation

Test instrumentation included electronic strain gauges to measure pipe wall strains for capturing the bending mechanism and earth pressure sensors to measure soil pressures. Figure 3.7 shows the locations of the strain gauges. The strain gauge locations for 1800 mm and 1500 mm long pipe specimens are shown in Figure 3.7(a) and Figure 3.7(b), respectively. KYOWA strain gauges (5 mm length, 120 ohms) were used to measure the strains. Four uniaxial strain gauges were attached at four different locations at the pipe's springline (one immediately close to the pulling grip and the others at distances away from the pipe center) to measure the strain distribution. A pair of strain gauges was attached to the front (towards the direction of movement) and rear (opposite side of the direction of movement) sides of the pipe to examine the bending strains (Figure 3.7). Each strain gauge was directly connected with a connector and wired to the data acquisition system.

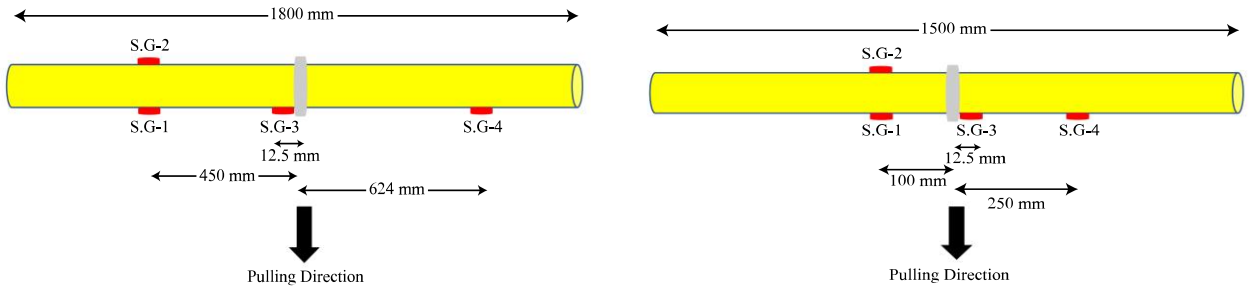

(a) (b)

Figure 3.7: Pipe wall strain measurement: (a) 1800 mm pipe, and (b) 1500 mm pipe

Four null pressure sensors (Talesnick et al., 2014) were used to measure soil stresses (Figure 3.8). The pressure sensors were installed horizontally and vertically in the soil to measure the vertical and horizontal soil pressures, respectively. In Figure 3.8, MU1 measured the vertical soil pressure, and MU2, MU3, and MU4 measured the horizontal soil pressures.

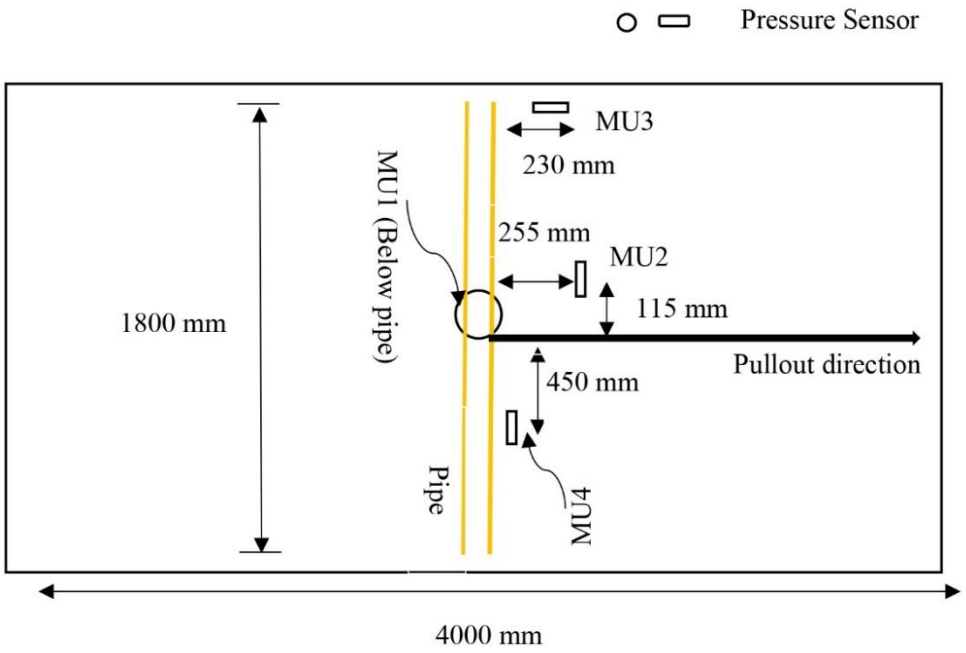

Figure 3.8: Test instrumentation (1800 mm Pipe): Pipe wall strain measurement

3.6 Test program

Ten (10) tests were performed on 42.2-mm and 60-mm diameter pipes buried in dense and loose conditions of the soil. Table 3.1 provides a summary of the test program. For each test, the pipe was pulled at a rate of 0.5 mm/min. The soil cover above the pipe springline was kept at 600

mm or an H/D ratio of 8. Two pipe lengths, i.e., 1800 mm and 1500 mm, were considered to examine the effects of the specimen length on the test results. The unit weights for the dense soil ranged from 15.5 kN/m^3 to 17 kN/m^3 and for the loose soil from 12 kN/m^3 to 13.5 kN/m^3

Table 3.1: Details of the testing program

Test No.	Pipe length (mm)	Pipe diameter (mm)	Rate of pulling (mm/min)	Soil condition	Height of soil above spring line (mm)
D-1	1800	42.2	0.5	Dense	337
D-2					600
D-3		60			480
D-4					600
L-1		42.2		Loose	600
L-2		60			
D-5	1500	42.2		Dense	600
D-6		60			
L-3		42.2		Loose	
L-4		60			

3.7 Test results

3.7.1 Load-displacement response

Figure 3.9 shows the load-displacement responses observed during the tests for 1800 mm long samples in dense sand. The pullout force corresponds to the resistance offered by the soil against the pipe movement and is therefore termed herein as the pullout resistance. The pullout resistance against the pipe displacement at the mid-span is plotted in Figure 3.9. Figure 3.9(a) reveals that the observed pullout force increases nonlinearly with the pipe's mid-span displacement. The rate of increase of the pulling force is less at large displacements. For the 42.2-

mm pipe with the burial depth of 337 mm (Test D-1), the pullout resistance reaches a peak value when the maximum capacity of the soil resistance is reached (discussed later). Thus, the soil resistance appears to depend extensively on the burial depth of the pipe.

For the 42.2-mm diameter pipes (Tests D-1 and D-2), the maximum pullout resistances during the tests were 3.44 kN and 8.88 kN for the burial depths of 337 mm and 600 mm, respectively (depth to diameter (H/D) ratio of 8 and 14.2, respectively). Approximately 159% of the pulling force was increased due to the increase of the H/D ratio from 8 to 14.2. For the 60-mm diameter pipes (Tests D-3 and D-4), the maximum pullout resistances are 9.37 kN and 11.03 kN for the burial depths of 480 mm and 600 mm (H/D of 8 and 10), respectively (Figure 3.9a). The pullout force increased by 17.7% for the 60-mm diameter pipe after increasing the burial depth from H/D = 8 to H/D = 10. As expected, the maximum pullout forces are higher for the pipes with larger diameters. However, the pullout forces normalized by the pipe diameter and the burial depth almost match each other (Figure 3.9b). Thus, the effect of burial depth and pipe diameter can be accounted for using the normalized pulling force if the backfill soil conditions are the same (dense in the current case).

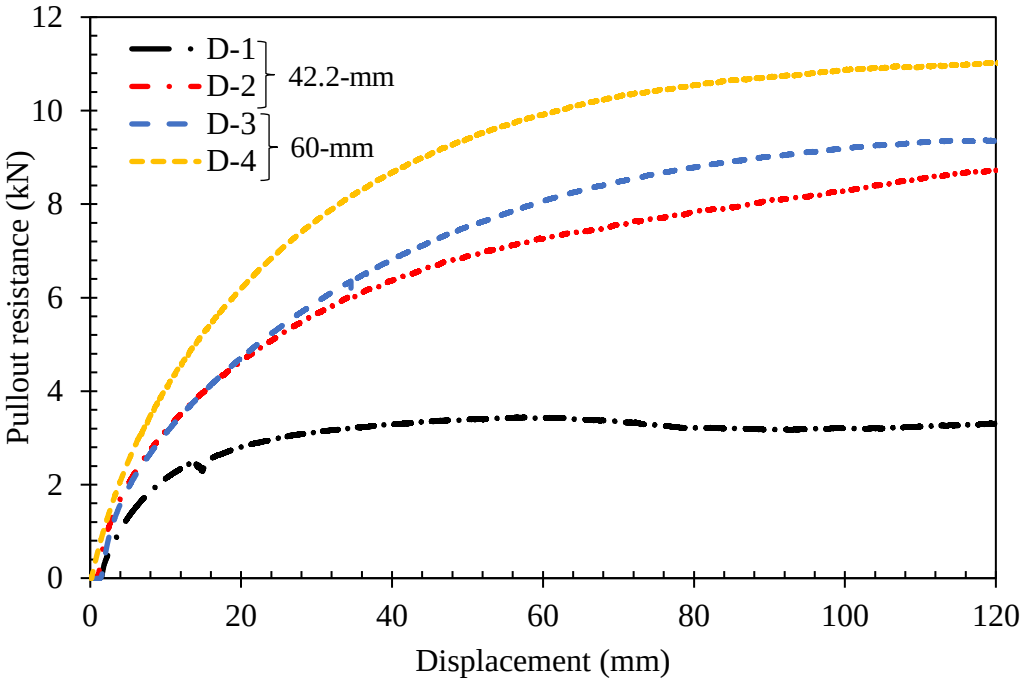

(a)

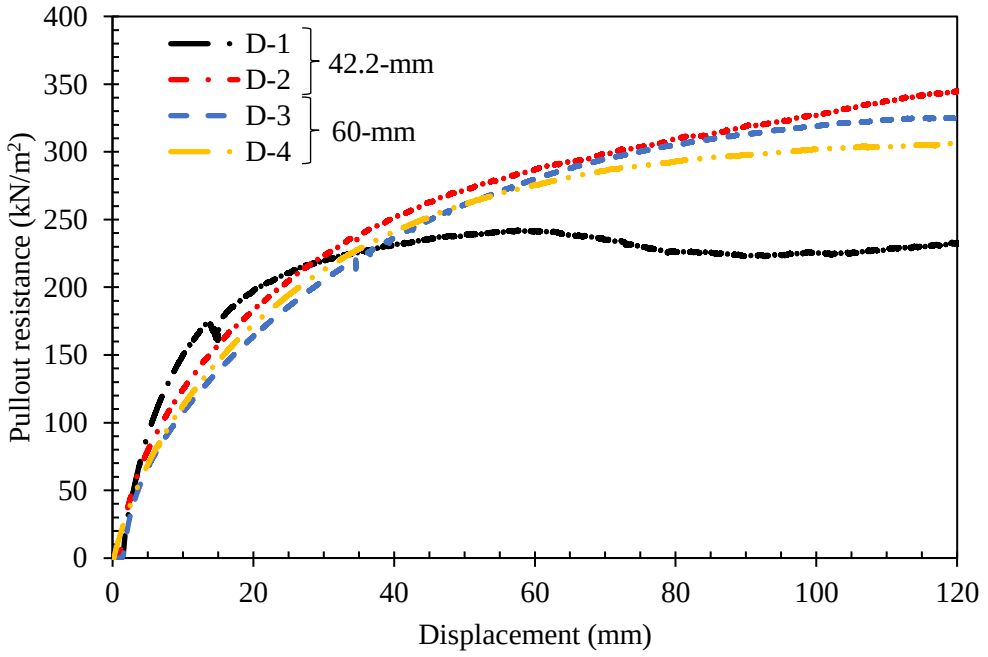

(b)

Figure 3.9: Load-displacement responses for 1800 long specimens: (a) observed, (b) normalized

In Test D-1 (42.2-mm pipe with a burial depth of 337 mm), the peak pullout resistance was observed at the (mid-span) displacement of around 59 mm, beyond which the resistance decreased (Figure 3.9). In this test, cracks on the soil surface were observed, as shown in Figure 3.10, indicating that the peak soil resistance was reached during the test with a shallow burial depth (i.e., 337 mm). However, no mechanical failure/fracture on the pipe specimen was observed after the test. Although no soil surface crack was observed in Test D-3 (60-mm pipe with a burial depth of 480 mm), the peak pullout resistance is noticed at the displacement of around 120 mm (Figure 3.9). Thus, the peak soil resistance is mobilized at a larger displacement if the burial depth is higher.

For the pipes buried at 600 mm (Tests D-2 and D-4), the peak pullout force continues to increase beyond the (mid-span) displacement of 120 mm, (the maximum displacement applied during the tests), indicating that the peak soil resistance was not reached in these tests. Depending on the magnitude of the pulling force, structural failure can occur on the main pipe and at the joint of the branch pipe (as shown in Figure 3.2b). However, the displacement corresponding to the structural failure couldn't be measured.

Figure 3.10: Soil failure mode observed (Test D-1)

Figure 3.11 shows the structural bending mechanism observed in the specimens after completion of the tests. The 42.2-mm diameter pipe with 600 mm burial depth (in Test D-2) experienced structural failure as local buckling (Figure 3.11a). While no local buckling was observed for the 60-mm diameter pipes, due to higher flexural rigidity, permanent bending deformation was observed in the pipes used in Tests D-3 and D-4 (Figure 3.11). No cracks on the soil surface were observed in these tests with higher burial depths of the pipes.

(a)

(b)

(c)

Figure 3.11: Bending mechanism of pipe (a) Test D-2, (b) Test D-3, (c) Test D-4

Figure 3.12 compares the force-displacement responses of the 1800 mm and 1500 mm long specimens. Test results of 42.2-mm and 60-mm diameter pipes in dense sand are compared in the figure. It shows that the maximum pullout forces of the 1500 mm long pipes are higher than those of the 1800 mm long pipes for each pipe diameter. The differences in the results are apparently not due to the length of the specimens, as a shorter specimen would normally provide a lower pulling force if there were an effect of the specimen length. No effects of pipe length on the test results are expected as the specimens were longer than four times the characteristic length. The higher pullout forces for the 1500 mm long pipes are attributed to a higher soil density of the backfill soil. Although a similar method was manually applied to compact the soil in the test cell, the same density was not obtained in the tests conducted on different days. This can be due to the differences in the moisture contents of the soil and/or different persons worked on the soil placements. The density measurement using Standard Proctor tests during the experiments also confirms the same. The dry unit weights measured after tests D-4 and D-6 are about 15.6 kN/m^3 and 16.0 kN/m^3, respectively.

Note that the initial load-displacement responses are stiffer due to the higher density of the backfill soil for the 1500 mm long specimens compared to the 1800 mm long specimens (Figure 3.12). After reaching the peak values, the responses for the 1500 mm long pipes become flat, which is due to the mobilization of the maximum soil resistance. Cracks on the ground surface for both tests (Tests D-5 and D-6) were observed, as shown in Figures 3.13 and 3.14, respectively, confirming the soil failure. Thus, in denser soil, the peak soil resistance may be mobilized at a lower relative ground displacement. However, the magnitude of the maximum pulling force is higher for a pipe buried in a denser backfill soil. For the 42.2-mm pipe, structural failure was

observed due to the high pulling force, as in Test D-2 (Figure 3.13b). The maximum pulling forces for the 42.2-mm and 60-mm diameter pipes were 9.6 kN and 11.3 kN, respectively.

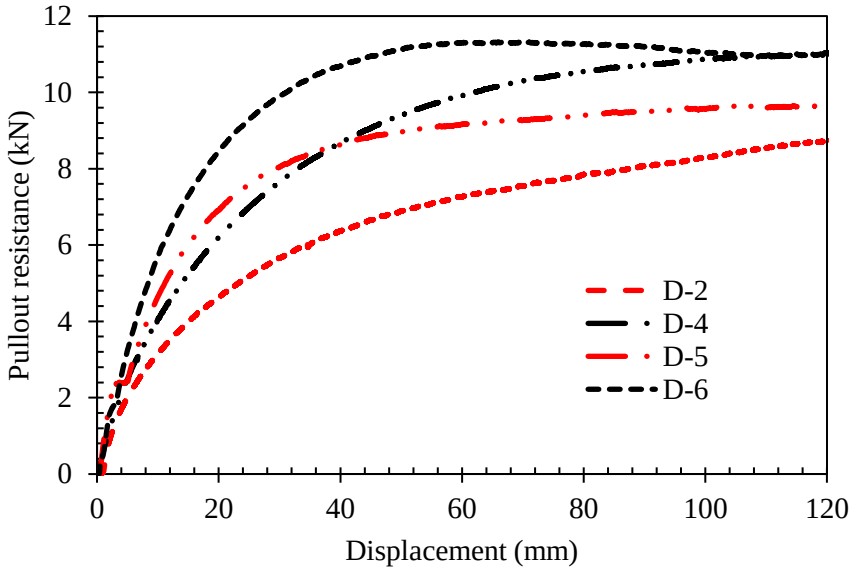

Figure 3.12: Comparison of load-displacement responses for 1800 mm and 1500 mm test specimens

(a) (b)

Figure 3.13: Failure mode for 42.2-mm diameter pipe (1500 mm long specimen: Test D-5): (a) soil failure, (b) pipe failure

Figure 3.14: Soil failure for 60-mm diameter pipe (1500 mm long specimen: Test D-6)

Figure 3.15 shows the lateral pullout resistance of 42.2-mm and 60-mm pipes with different lengths buried in loose sand. All the tests were conducted at 600 mm of burial depth in loose sand. Figure 3.15(a) shows the pullout resistance of 1800 mm long pipe having diameters of 42.2-mm and 60-mm, and Figure 3.15(b) shows the results for 1500 mm long pipes. As seen in the figure, the pullout forces increase continuously for both cases up to the maximum displacement applied during the tests (i.e., 120 mm). Note that a small jump in test results were observed due to slippage of pulling grip (Figure 3.15a). The pullout forces are less than those for the pipes in dense sand, discussed above. The forces are higher for the 1800 mm long pipe than those for the 1500 mm long pipe. However, the differences might be due to the differences in the density of the backfill soil. For the loose backfill, it was challenging to maintain the same density in multiple tests. The pipes in loose sand did not experience any structural failure. The longitudinal bending profile observed after completion of the tests are shown in Figure 3.16.

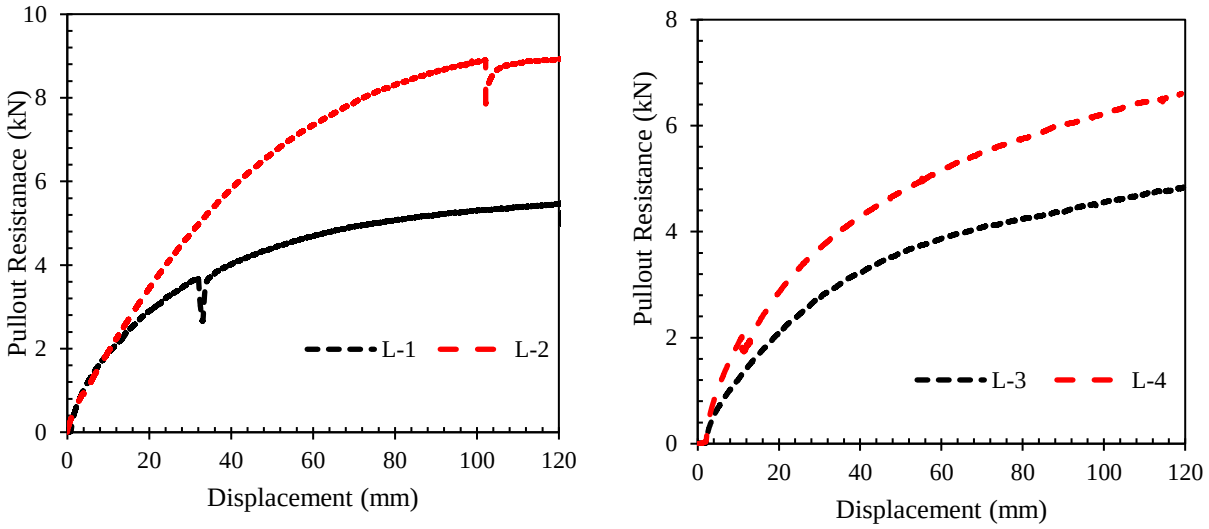

(a) (b)

Figure 3.15: Tests in loose sand: (a) pipe length 1800 mm, (b) pipe length 1500 mm

(a) (b)

Figure 3.16: Bending profiles: (a) Test L-1, (b) Test L-2

3.7.2 Pipe wall strains

In all tests, the highest axial strains were measured near the pulling force at the mid-span (strain gauge S.G.-3 in Figure 3.7), as expected. The strains measured using the other strain gauges were significantly lower. Figure 3.17 shows the axial strains measured during Tests D-1 and D-2 (42.2-mm diameter pipes). The figure shows that the maximum axial strain near the pulling force is higher for the shallow buried pipe (Test D-1), although the pulling force was less (Figure 3.9). For the shallow buried pipe, the soil support was less, which was further reduced due to soil failure propagating to the ground surface. As a result, the pipe had higher bending deformation under a lower pulling force. For the pipe with a greater burial depth (Test D-2), the pipe was well-supported by the soil, and the bending deformation of the pipe was less. The maximum strain near the pulling force was stabilized beyond 25 mm of displacement, which is likely due to the development of local buckling on the pipe wall (Figure 3.11a). In strain gauges S.G.-1 and S.G.-2, located 450 mm away from the pulling force, the strains are significantly less and almost zero for the pipe at a higher burial depth. This implies that the effect of the pulling force is insignificant beyond that distance. This confirms again that the pipe length considered in the tests is sufficiently long to study the pipe behaviour under the concentrated load. The bending deformation at the distance of 450 mm was higher for the shallow buried pipe due to lower soil resistance. Note that strain gauge S.G.-3 measured tensile strains while S.G.-1 measured compressive strains, despite that both of the strain gauges being on the same side of the pipe surface. Strain gauge S.G-2, placed on the opposite side of the pulling direction, provides tensile strains. Thus, the pipe underwent a curvature change within the distance of 450 mm from the load. The curvature change was observed when the pipe was exposed after the test (Figure 3.11c). The axial soil resistance also contributed to the

axial strains of the pipe. As a result, the tensile strains measured by S.G.-2 are greater than the compressive strains measured by S.G.-1 (Figure 3.17).

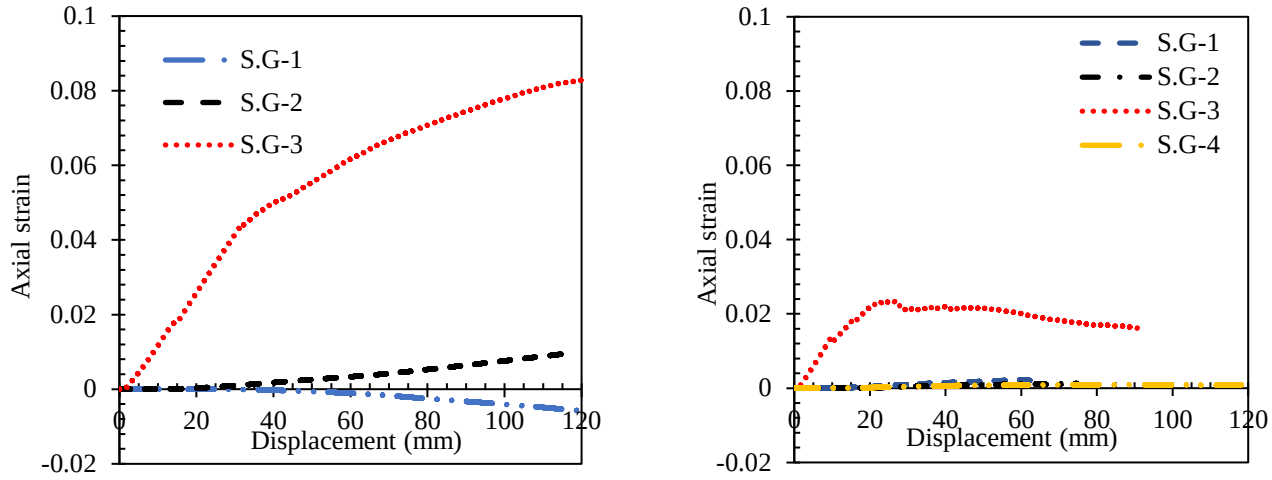

(a) (b)

Figure 3.17: Wall strains for 42.2-mm diameter pipes: (a) Test D-1, (b) Test D-2

Axial strains measured for the 60-mm diameter pipes (in Test D-3 and D-4) were similar to those for the 42.2-mm diameter pipes (Figure 3.18). However, the bending strains were larger for the 60-mm diameter pipes at the same level of pulling displacements. This might be due to the larger diameter pipe having a similar curvature change under the combined effect of axial force and lateral force. The bending strain at a distance of 624 mm (in strain gauge S.G.-4) was negligible for the pipe. The strain readings were sometimes not available or discontinued at large displacements, likely due to disconnection of the gauges during pipe movements through the soil.

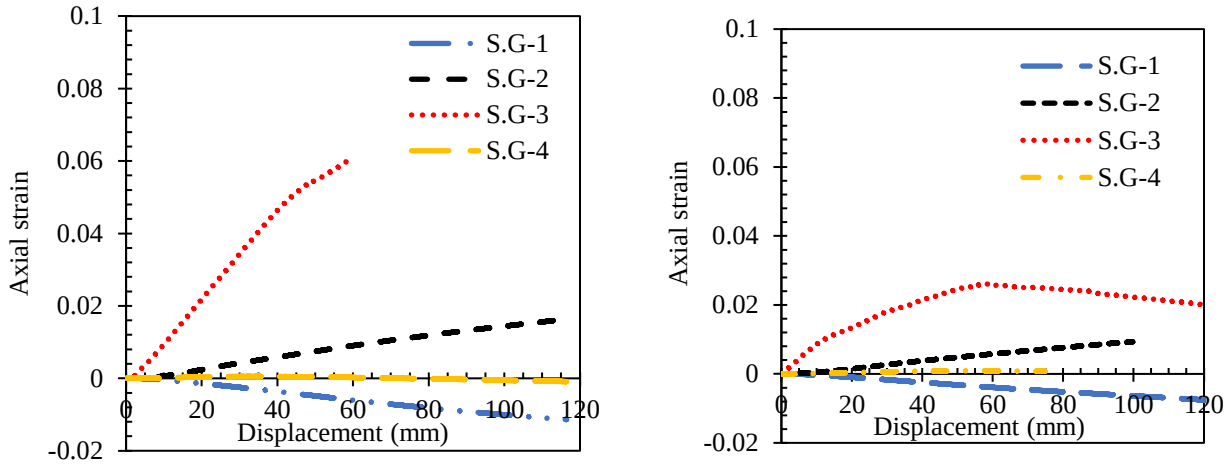

Figure 3.18: Wall strains for 60-mm diameter pipes: (a) Test D-3, (b) Test D-4

3.7.3 Soil stress measurements

Earth pressure sensors were placed at different locations in the test cell to study the load transfer mechanism between the soil and the pipe. It was challenging to measure the earth pressures encountered during the tests correctly as the soil pressures were too small to be measured using conventional vibrating wire earth pressure cells. Therefore, null pressure sensors (Talesnick et al., 2014) were employed. These sensors were successfully used to measure earth pressures in Chakraborty et al. (2020). However, some of the sensors were non-responsive during the tests conducted in this study. Figure 3.19 shows the earth pressures measured at different locations from various tests. As seen in the figure, the earth pressure near the pulling force (measured by MU2) increased with the pipe displacement. The earth pressures did not significantly change at any other locations (the one underneath the pipe, one located by the cell boundary, and the other located at a distance of 450 mm from the pulling force). The pipe wall strains were also insignificant at a distance of 450 mm from the pulling force, confirming the minimum effect of the pulling force beyond that distance.

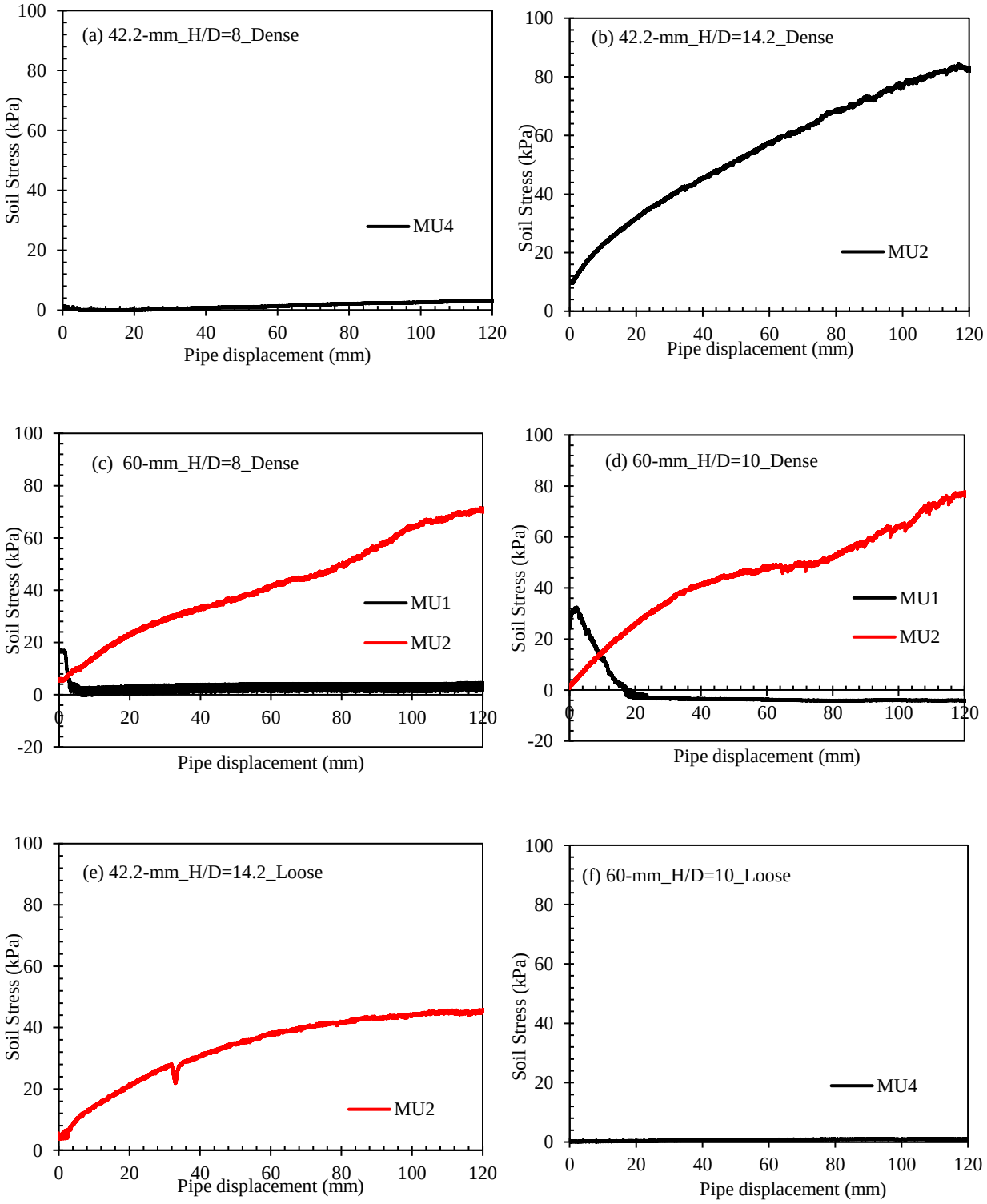

Figure 3.19: Earth pressure measurement: (a) Test D-1, (b) Test D-2, (c) Test D-3, (d) Test D-4, (e) Test L-1, and (f) Test L-2

The maximum earth pressure was around 80 kPa in dense soil and around 45 kPa in the loose soil near the pulling force at the displacement of 120 mm. The information on the soil pressure would be valuable for estimating the soil parameters to use in the analysis of the pipe.

3.8 Analysis of bending strains

The test results presented above revealed that ground movements in the lateral direction of a pipe can cause axial force on the branch pipe anchored in stable ground. The magnitude of the axial force depends on the extent of ground movement, pipe diameter, and pipe burial condition (i.e., burial depth and backfill soil density) for the main pipe. Due to the effect of axial force on the branch pipe, the main pipe experiences bending deformation. An excessive bending strain can lead to leakage or a break in the pipe and, therefore, should be evaluated. The existing analytical and numerical methods, based on beam-on-spring idealization, are examined in this chapter for a preliminary evaluation of the bending strains observed during the tests. A more detailed analysis is provided in Chapter 4.

3.8.1 Analytical model

The flexural behaviours of buried pipe can be analyzed through beam-on-spring idealization (Figure 3.20). The analytical solution of the beam-on-elastic-foundation by Hetényi (1946) based on Winkler's hypothesis (Winkler, 1867) was used here to calculate the pipe wall strains and compare with the test results. For a straight beam supported on an elastic foundation (spring) and subjected to a single concentrated force at the midpoint, the strain at any point is given by Equation (3.1), Hetényi (1946).

Strain, $\varepsilon = \frac{Py}{4\lambda}\frac{C_{\lambda x}}{EI}$ [3.1]

where

$$C_{\lambda x} = e^{-\lambda x}(\cos \lambda x - \sin \lambda x)$$

$$\lambda = \left[\frac{k}{4\,EI}\right]^{1/4}$$

Here, *P* is the load applied at the center point of the beam/pipe, *k* is the Winkler's modulus in MPa (Winkler, 1867), *EI* is the flexural stiffness of beam/pipe, *x* defines the distance along the length of pipe from the load, and *y* is the deflection.

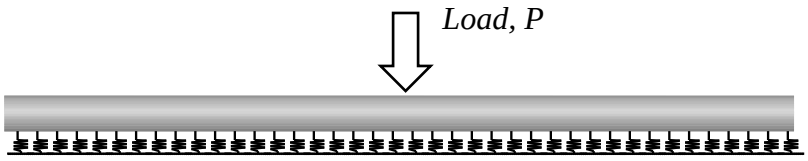

Figure 3.20: Beam on spring idealization

The equation of Vesic (1961) for calculating the coefficient of subgrade reaction can be used to calculate the spring stiffness, *K*. One of the advantages of using Vesic's equation is that it accounts for the flexural stiffness of the pipe-soil system in calculating the spring stiffness. However, the equation was developed for small displacement problems. Vesic's equation for spring stiffness is given in Equation (3.2) below.

$$K_{\propto} = 0.65 \sqrt[12]{\frac{E_S B^4}{E_b I}} \times \frac{E_S}{1-{\nu_S}^2} \quad [3.2]$$

Here, *B* = pipe diameter, E_s = Modulus of elasticity of sand, E_b = Modulus of elasticity of pipe material, ν_s = Poisson's Ratio of Sand and *I* = Moment of inertia of the pipe section. Assuming E_s = 11.5 MPa for dense sand, E_s = 5 MPa for loose sand, E_b = 550 MPa, B = 60-mm and 42.2-

mm, spring constants of 8 kN/m and 3.3 kN/m were obtained for both 42.2-mm and 60-mm diameter MDPE pipes in dense sand and loose sand, respectively.

Note that the solution of Hetényi (1946) is only applicable to the linear soil-pipe interaction problem. However, the behaviour of the soil and the MDPE pipe is nonlinear. Numerical modeling techniques can be used to capture the effects of nonlinearity in the pipe response (discussed in Chapter 4). In this chapter, a numerical modeling technique is employed to analyze the linear soil-pipe interaction using Vesic's spring constants.

3.8.2 Numerical model

Two-dimensional FE analysis was conducted using Abaqus/Standard to investigate the lateral pipe-soil interaction. Both 60-mm and 42.2-mm pipes with the length of 1800 mm and 1500 mm, were modeled using PIPE21 element. The modulus of elasticity of E_p = 550 MPa and the Poisson's ratio of ν_s = 0.45 was selected for the pipe material. Spring element (SPRING1) available in the Abaqus spring element library, was chosen as an elastic foundation to simulate soil reactions. SPRING1 element works between the nodes on the pipe and the ground, acting in a fixed direction. The direction can be defined by giving the degree of freedom (DOF) at each node of the element. To define the spring along longitudinal and lateral directions of the pipes, the DOF of 2 was chosen. Note that the contribution of the longitudinal spring is insignificant for the pipes subjected to lateral load at small displacements; however, it is included here to examine the effect. A value of constant spring stiffness (8 kN/m and 3.3 kN/m) was selected based on Vesic's (1961) equation, as discussed above.

The FE mesh was developed with an element size of 1 mm in length, which is very small. For linear analysis, the use of small element size did not cause any issue with the computational time;

however, it could improve the accuracy of the results. The springs were assigned at each node (located 1 mm apart). A concentrated load was applied at the center point of the pipe. Figure 3.21 shows the FE model used.

Figure 3.21: Numerical modeling of MDPE pipe

3.8.3 Comparison of results

Figures 3.22 to 3.31 show comparisons of experimental results with those from the analytical and numerical analyses. Strains corresponding to two pulling forces, one within the initial linear part of the load-displacement responses and the other in the nonlinear part of the load-displacement responses observed during the tests (i.e., Figure 3.9), were calculated and compared in the figures. Figure 3.22 and Figure 3.23 show the axial strain comparisons for the 42.2-mm diameter pipes buried at 337 mm and 600 mm depths (Tests D-1 and D-2), respectively. The strains at the displacements of 6 mm and 2.2 mm within the linear range of load-displacement relations were compared for Tests D-1 and D-2, respectively. Within the nonlinear load-displacement relations, the strains at the displacement of 50 mm were compared for both tests. Figures 3.22 and 3.23 show that the strains from the analytical and numerical solutions are in good agreement with the experimental strains for the displacements corresponding to the linear load-displacement relation. However, at the displacement of 50 mm (when the load-displacement relation is nonlinear), the analytical and numerical solutions underpredict the axial strains compared with the experimental results, as expected. These are also observed for the 60-mm diameter pipes buried at

the depths of 600 mm and 337 mm (Figure 3.24 and Figure 3.25). Figure 3.24 plots the strains at the displacements of 2.5 mm and 50 mm, and Figure 3.25 plots the strains at the displacements of 4 mm and 80 mm when the load-displacement relations are linear and nonlinear, respectively. The measured strains reasonably matched the values predicted using the analytical and numerical methods at small displacements in the figures, while the measured strains were underpredicted by the method at large displacements.

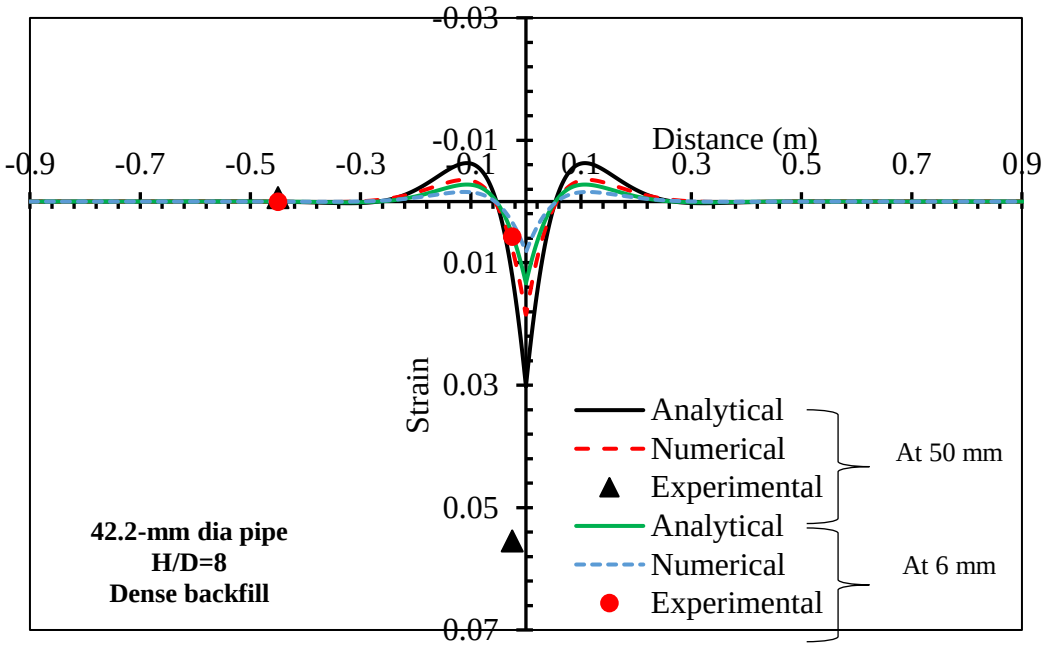

Figure 3.22: Comparison of axial strains along the pipe length: Test D-1

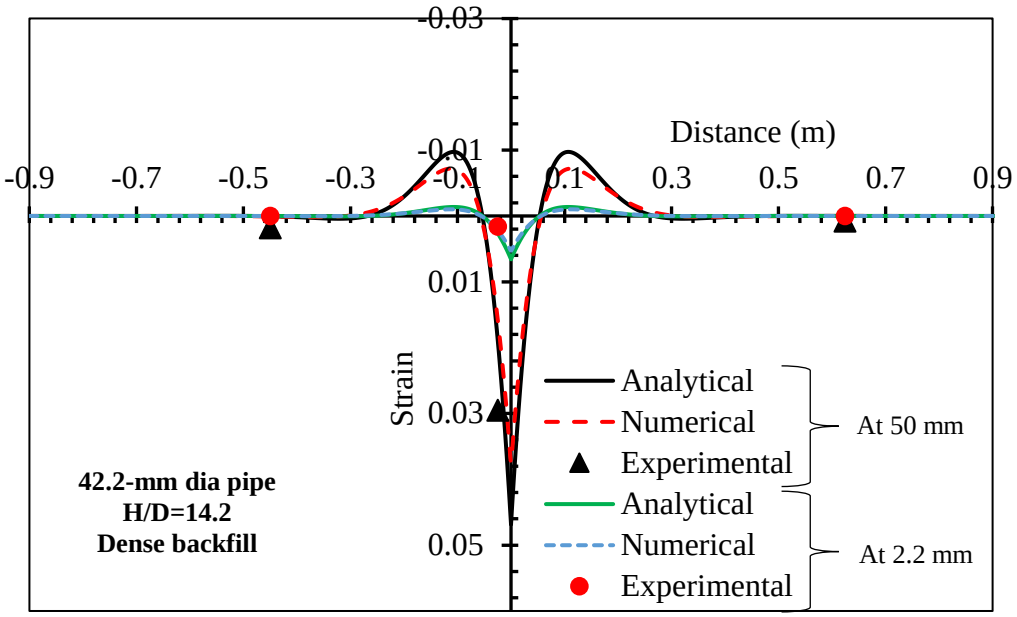

Figure 3.23: Comparison of axial strains along the pipe length: Test D-2

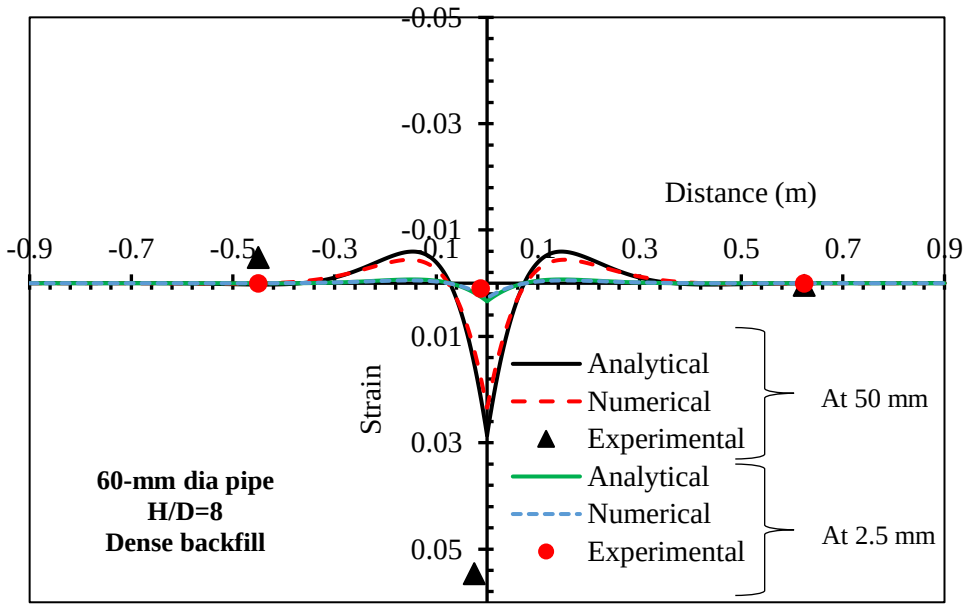

Figure 3.24: Comparison of axial strains along the pipe length: Test D-3

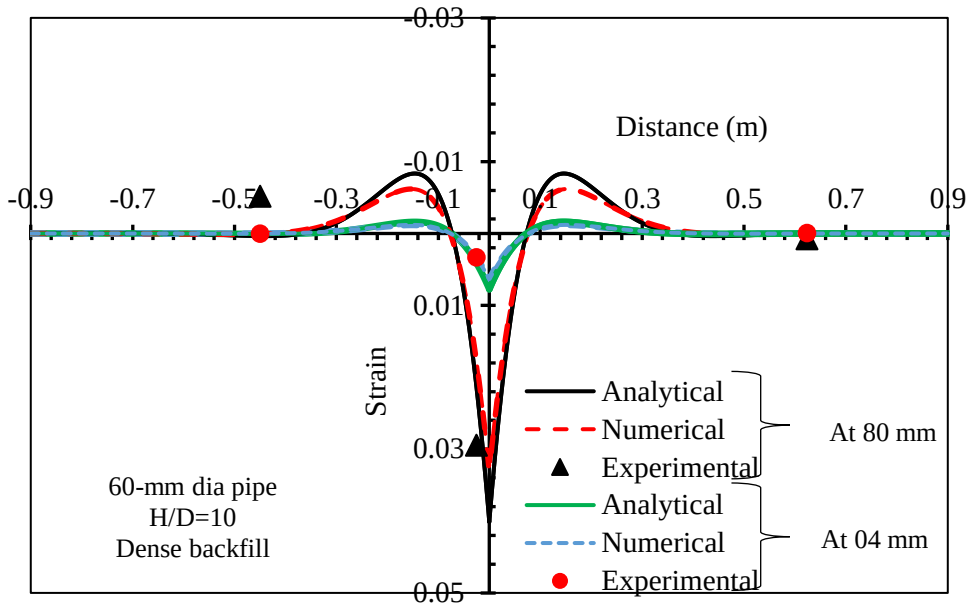

Figure 3.25: Comparison of axial strains along the pipe length: Test D-4

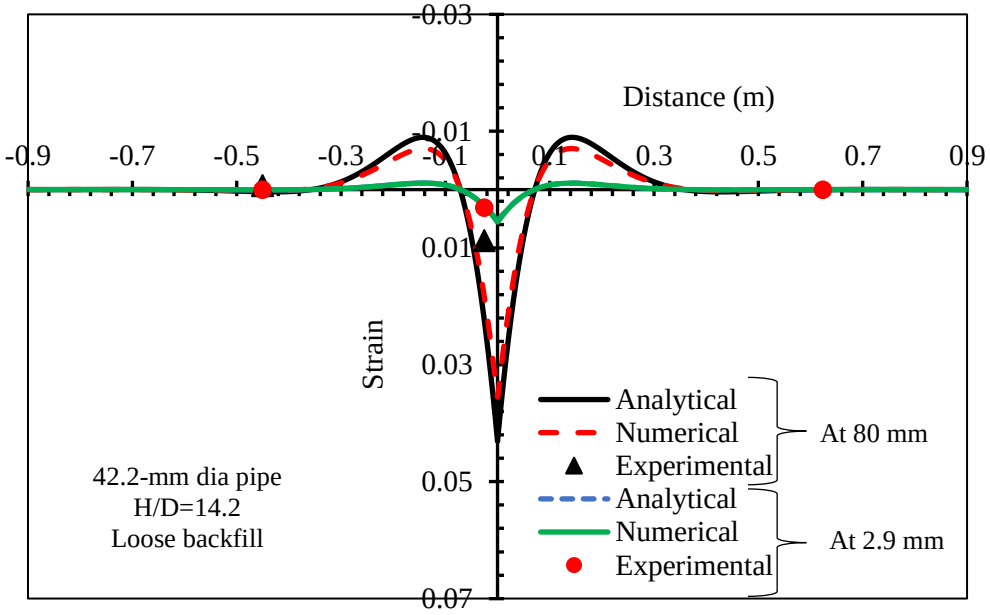

Figure 3.26: Comparison of axial strains along the pipe length: Test L-1

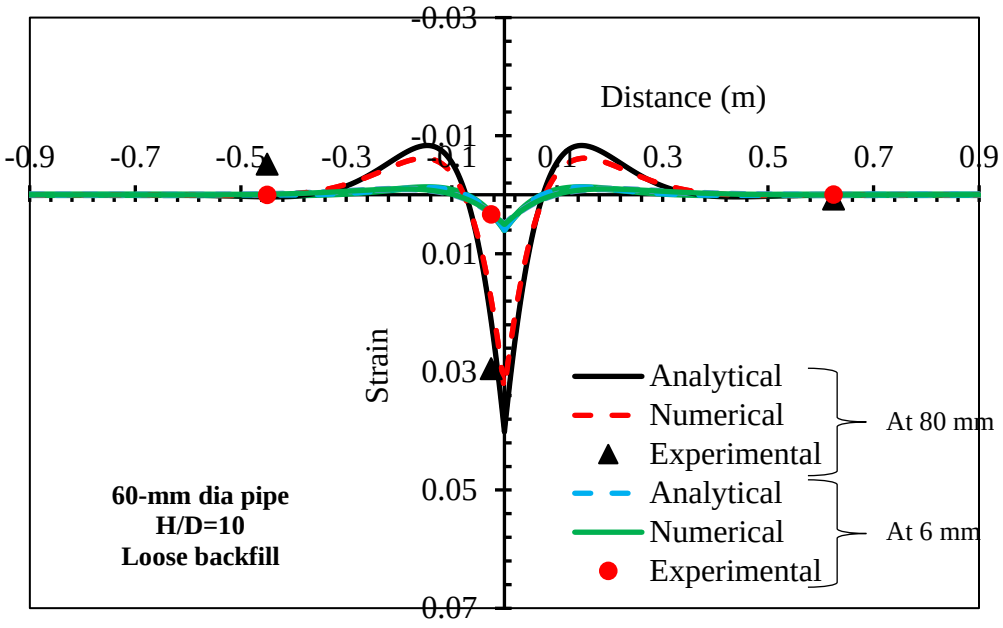

Figure 3.27: Comparison of axial strains along the pipe length: Test L-2

Comparisons of axial strains for 42.2-mm and 60-mm diameter pipes with 1800 mm of specimen length in loose sand are shown in Figure 3.26 and Figure 3.27, respectively. Figure 3.26 shows the strains at the displacements of 2.9 mm and 80 mm, and Figure 3.27 shows the strains at the displacements of 6 mm and 80 mm (within the linear and nonlinear load-displacement relation, respectively). For Test L-1, the analytical and numerical methods underpredict the midpoint axial strain at the large displacement (Figure 3.26). The midpoint strain gauge was detached after 15 mm of displacement. However, both loose sand tests (tests L-1 and L-2) show a reasonable match of the experimental strains with those from the analytical and numerical methods at small displacements.

Figures 3.28 and Figure 3.29 compare the axial strains for Tests D-5 and D-6 (1500 mm long specimens buried in dense sand). Displacements of 80 mm and 60-mm were selected for the nonlinear range and displacements of 5.3 mm and 8 mm were selected within the linear range

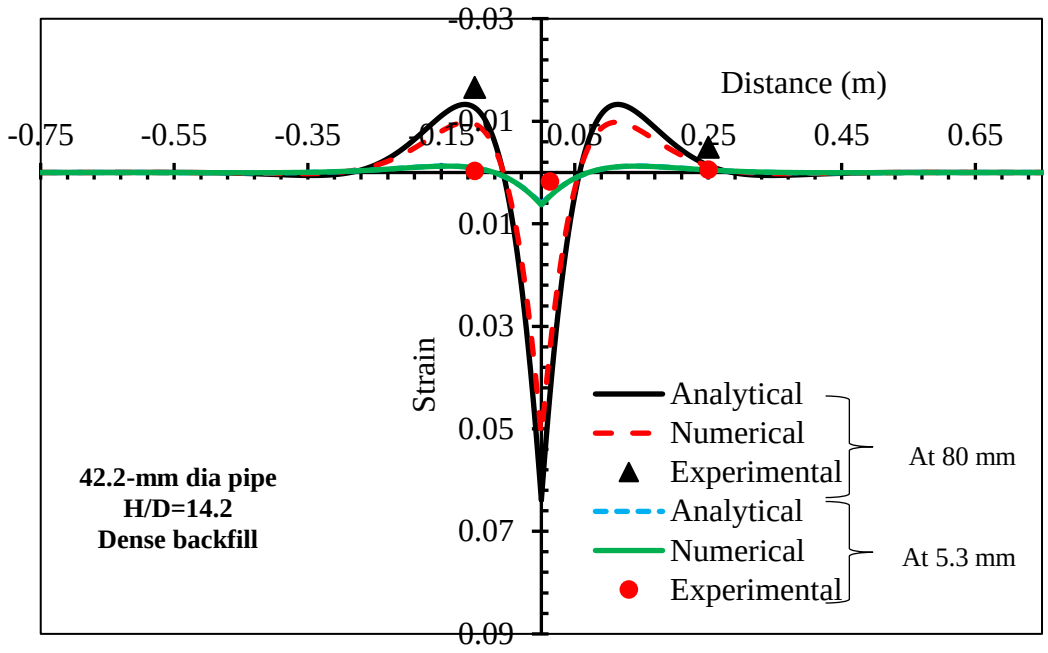

Figure 3.28: Comparison of axial strains along the pipe length: Test D-5

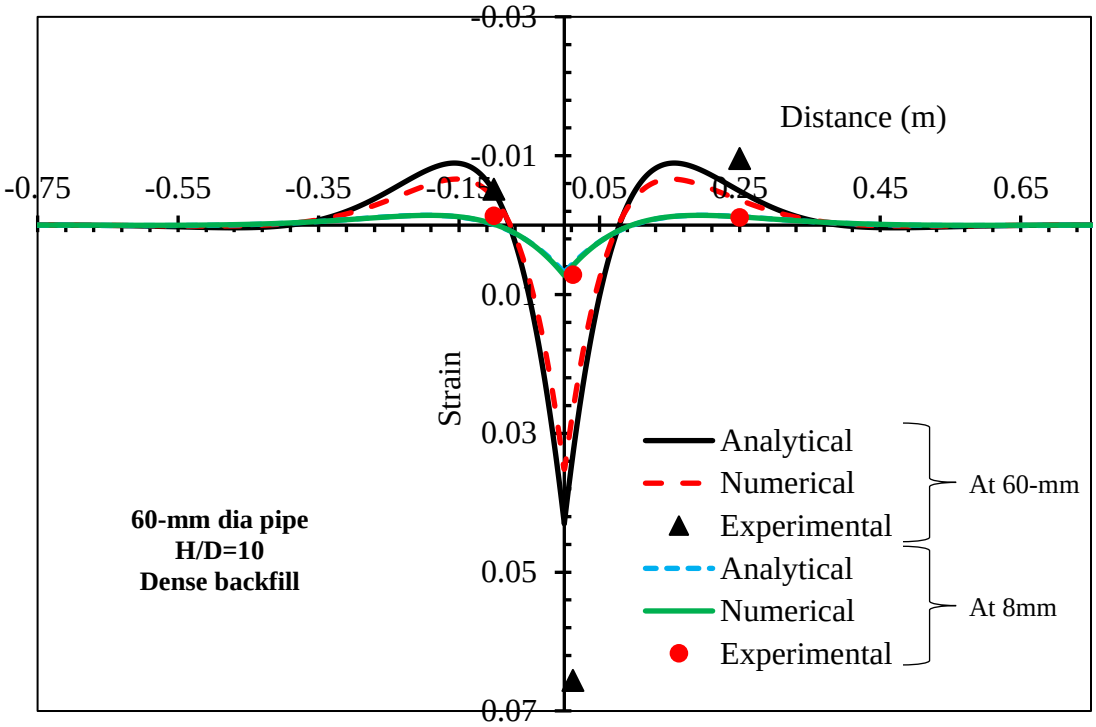

Figure 3.29: Comparison of axial strains along the pipe length: Test D-6

for Tests D-5 and D-6, respectively. Figures 3.30 and 3.31 plot the axial strain comparisons for Tests L-3 and L-4 (1500 mm long specimens buried in loose sand), respectively. Similar to the results for 1800 long specimens, the strains for 1500 mm long specimen match reasonably with the prediction at small displacements. However, the strains are underpredicted by the analytical and numerical methods at larger displacements. An analysis with nonlinear spring constants could be used to capture the nonlinearity in the measured responses at large displacements (discussed in Chapter 4). It is also observed that the axial strain is the highest near the pulling force and it reduces with distance from the force. After a certain distance away from the loading point, the value of strain is almost zero, which indicates no bending. For a beam-on-elastic foundation subjected to a concentrated load, the bending deformations are minimized at a distance of 1.25 π/λ from the load (Hetényi, 1946), which is consistent with results obtained from this study for small displacements.

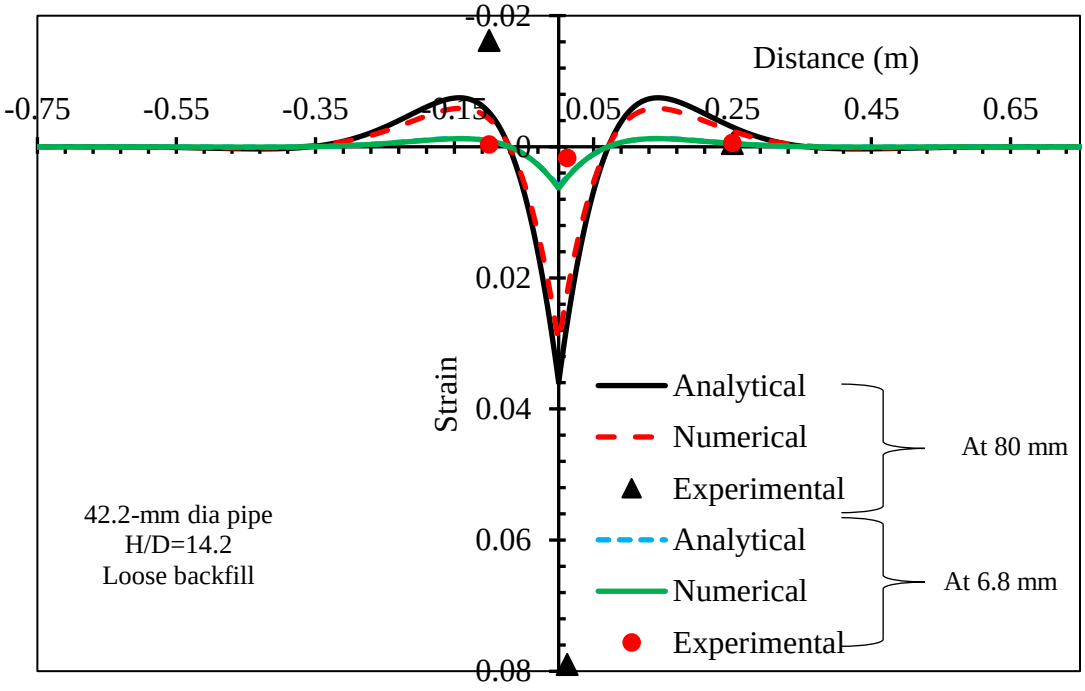

Figure 3.30: Comparison of axial strains along the pipe length: Test L-3

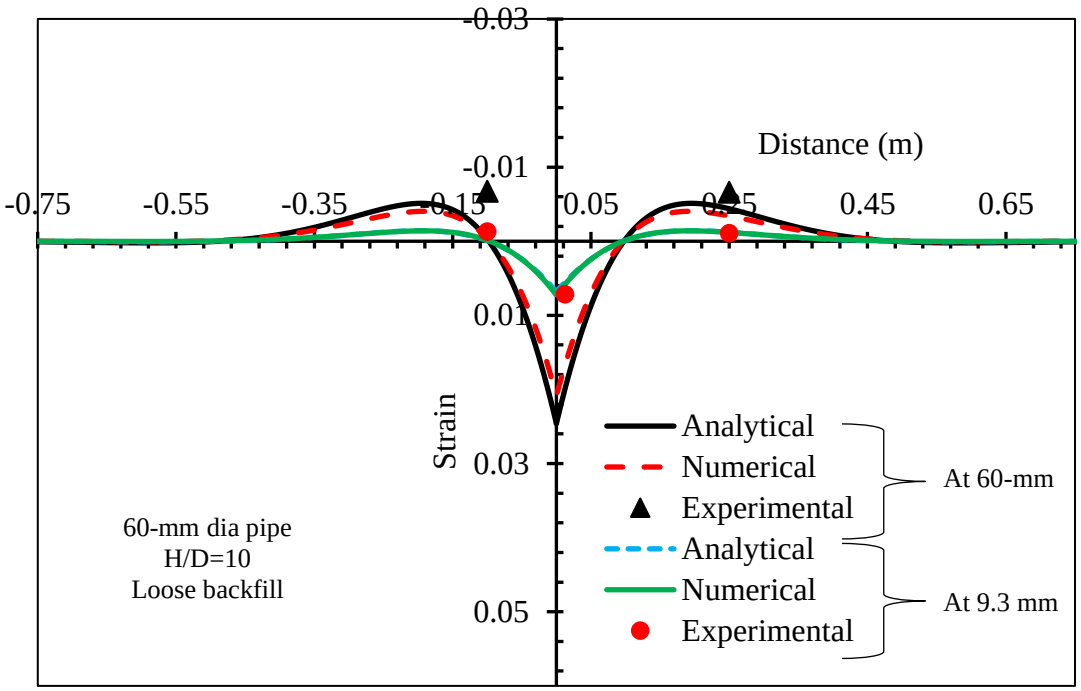

Figure 3.31: Comparison of axial strains along the pipe length: Test L-4

3.9 Conclusion

The flexural behaviour of buried 42.2-mm and 60-mm diameter MDPE pipes subjected to a concentrated load is investigated in the study presented in this chapter. Lateral ground movement near the connection of the pipe can cause such a loading scenario. Pipes buried in dense and loose sands with various burial depths (337 mm, 480 mm, and 600 mm) are studied. The conclusions from the study are summarized below:

- For the MDPE pipes tested, the load-deflection response is nonlinear at large displacement and depends on the resistance offered by the soil. Soil support is greater for the deeply buried pipe than for the shallow buried pipe. In general, the axial force on the lateral branch increases with the increase of relative ground movement. The axial pulling force is higher for the larger diameter and higher burial depth of the main pipe. The pulling forces normalized by the pipe

diameter and the burial depth are the same for similar soil conditions unless the maximum soil resistance is mobilized. The maximum pulling forces for the 42.2-mm and 60-mm diameter pipes were 9.6 kN and 11.3 kN, respectively, for the pipes buried at a depth of 600 mm in dense sand. For the pipes buried in loose sand, the maximum pullout forces were 5.4 kN and 8.9 kN, respectively.

- For the pipe buried at shallow depth, the maximum pullout force on the lateral branch can be less due to the full mobilization of soil resistance with the propagation of cracks to the ground surface. As a result, structural distress may not be expected at the joint with the branch or at the main pipe in terms of cracking or local buckling. However, the bending deformation of the pipe can be larger.
- The pulling force continues to increase with the ground movement for pipes buried at greater depths. The pipe can experience structural failure at a high pulling force, which depends on the flexural rigidity of the cross-section. Structural failure in the form of local buckling was observed during the test for the 42.2-mm pipe. In denser soil, the peak soil resistance was mobilized at a lower relative ground displacement.
- The effect of the concentrated load is insignificant at a distance beyond 624 mm from the load. Thus, there is no effect of specimen length on the test results for the test specimens with lengths of 1500 mm and 1800 mm. The pulling forces are higher for the pipes in dense sand than those in loose sand.
- Measurement of earth pressure at different points shows a good agreement with the load-displacement response and bending behaviour of the pipe.
- The beam-on-elastic-foundation solution is found to reasonably estimate the pipe-soil interaction behaviour within the linear elastic range. Nevertheless, the solution underpredicts

the axial strain at large displacements. An analysis with nonlinear spring parameters can be used to account for the nonlinear pipe-soil interaction at large displacements.

CHAPTER 4

Modeling MDPE Pipe Behaviour Under Lateral Ground Movement

4.1 Introduction

Pipelines are used extensively for transporting water and hydrocarbons, which form an essential part of lifeline infrastructure. Any disruption of the pipeline performance can create an unacceptable effect on the economy, environment, and society. The performance of a buried pipeline system can be affected when a component is broken by any factors such as human activities (i.e., excavation, tunneling, directional drilling) or any geotechnical hazards (e.g., landslides, rockfall, land subsidence, etc.). The geohazard, such as lateral ground movement, is one of the common hazards that the pipelines experience. Lateral ground movement can induce excessive pipe wall strains that can lead to leakage or breakage. It is important to estimate the pipe wall strains due to the ground movement when evaluating the pipeline performance exposed to the hazard.

Various analytical models were developed based on simplifying assumptions for calculating the wall strains for pipelines subjected to ground deformation resulting from fault movements or landslides (e.g., Kennedy et al., 1977; Rajani et al., 1995; Takada et al., 2001; Trifonov et al., 2010; Sarvanis et al. 2017). It is, however, difficult to capture the complex soil-pipe interaction during ground movements within the framework of analytical solutions. Numerical modeling using the finite element (FE) method offers a viable alternative to examine complex pipe-soil interaction. However, although a pipeline subjected to lateral ground movement is a three-dimensional (3D) problem, a rigorous 3D continuum-based FE modeling of the pipe-soil system

is often challenging due to the large scale of the problem and the uncertainties associated with the input parameters. Some researchers employed 3D continuum-based FE modeling only for small-scale pipe-soil interaction simulations (Mahdavi et al., 2013; Almahakeri et al., 2016; and Sarvanis et al., 2017). An alternative to 3D continuum-based FE modeling is to employ a simplified FE modeling approach where the pipe is idealized as a beam, and the surrounding soil is represented using appropriate springs. In this approach, the major challenge is to identify the proper spring parameters to describe the soil-pipe interactions correctly. The spring parameters recommended in design guidelines for steel pipes (e.g., ASCE, 1984; ALA, 2005; PRCI, 2017) are widely used for soil-pipe interaction analyses. In these guidelines, the spring parameters are defined using the maximum soil reactions as the spring forces and the displacements corresponding to the maximum spring forces.

Many studies were conducted over the last few decades to evaluate the maximum soil reactions on steel pipes using experimental and numerical methods (e.g., Trautmann and O'Rourke, 1985; Yimsiri et al., 2004; O'Rourke et al., 2016 and others). An extensive review of these works is available elsewhere (e.g., Almahekari et al., 2019) and, therefore, not repeated here. In general, these studies investigated the load-displacement relations and the maximum soil reactions under plane strain loading conditions. Guo and Stolle (2005) summarized data from different studies and showed that the peak soil reactions depend on soil properties, the diameter of the pipe, burial depth, and loading scenarios. However, no such study is available to examine the load-displacement responses for flexible polyethylene pipes. As testing under the plane strain condition is not feasible for flexible pipes (Almahekari et al., 2016), researchers performed large-scale or reduced-scale (centrifuge) tests that could be used to calibrate the existing models for the flexible pipes (Ha et al., 2008; Weerasekara and Wijewickreme, 2010; Wham et al., 2017; Ni et al., 2018b). Based on

the centrifuge modeling of a high-density polyethylene (HDPE) pipeline crossing a strike-slip fault, Ha et al. (2018) showed that the force-displacement relationships vary along the length of the pipe with stiffer responses near the fault line and softer responses further away from the fault. The maximum spring force was found to compare favorably with those given by the existing design guidelines for steel pipes. Ni et al. (2018a) found a spring stiffness value of one-third of that for steel pipe to provide better results for their full-scale laboratory tests with polyvinyl chloride (PVC) pipes, crossing a normal fault. A similar finding was reported in Almahekari et al. (2016): the displacements for GFRP (glass-fiber-reinforced polymer) flexible pipe at the peak pulling force are ~3.5 times those for steel pipes, reducing the spring stiffness. Wham et al. (2017) conducted full-scale strike-slip fault rupture tests with biaxially oriented polyvinyl chloride (PVCO) pipes and demonstrated that the axial load capacity significantly influences the pipe's performance under lateral ground movement, which was also recognized earlier in Weerasekara and Wijewickreme (2010). Weerasekara and Wijewickreme (2010) developed an analytical method to calculate the pipe wall strains considering the axial tension and bending. Note that only limited studies were conducted for the flexible pipes subjected to ground movements. The major focus of the studies was on pipelines exposed to fault movement. With the increasing demand for polyethylene pipe in liquid and gas transportation worldwide, there is a growing need to understand the behaviour of pipes under the more complex loading conditions expected in the field.

Distribution pipelines are often connected with lateral branches and connections. Ground movement near the connection can cause bending deformation on the pipe perpendicular to the direction of movement (called herein the "distribution main" pipe) and axial force on the pipe running parallel to the direction of the movement (called herein the "branch" pipe), as in Figure 4.1. A laboratory test program carried out to examine the bending deformation of medium-density

polyethylene (MDPE) main pipe, and axial force on the branch pipe, is presented in Chapter 3. This chapter presents a numerical modeling technique developed to assess the bending deformation and axial forces on the pipes. FE analysis was performed using the Abaqus software. The pipe was modeled using beam elements and the pipe-soil interaction was modeled using pipe-soil interaction (PSI) element, available in Abaqus. The results obtained from FE analysis were validated using the experimental results obtained from laboratory tests discussed in Chapter 3. The applicability of soil springs recommended in the design guidelines (ALA, 2005; ASCE, 1984) for the MDPE pipe was examined. Finally, a parametric was conducted to develop a design guideline for assessing the effects of ground movement near the connection.

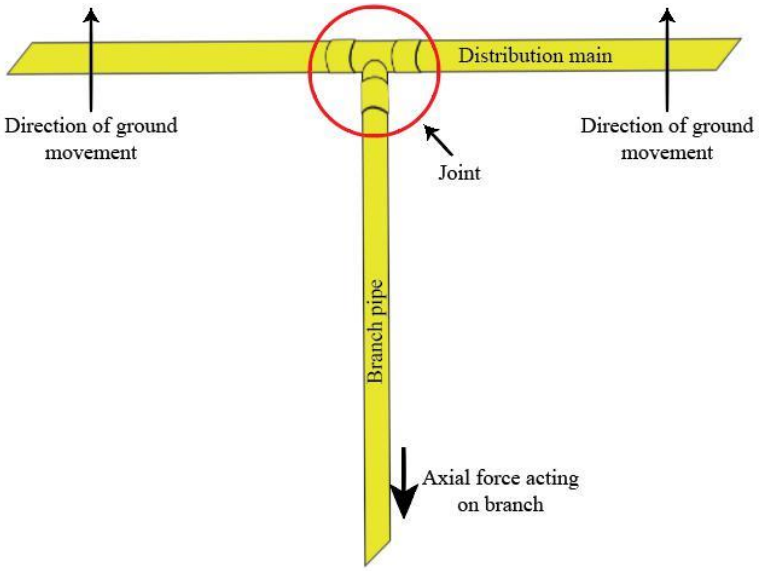

Figure 4.1: Effect of ground movement of pipe with a lateral branch connection

4.2 Soil pipe interaction (PSI) modeling

As discussed earlier, three-dimensional soil-pipe interaction analysis is computationally challenging for buried pipelines. The beam on the Winkler foundation (Winkler, 1867) with the

linear spring (known as the Winkler model) is the simplest form of soil-pipe interaction analysis. The conventional study of beams on elastic foundations considers that the contact pressure to deflection ratio is constant at all points in the beam and can be written as (Equation 4.1):

$$\frac{p}{w} = k \qquad [4.1]$$

where p = pressure at any point (N/mm^2), w = deflection at the same point of the beam (mm) and, k = coefficient of subgrade reaction (N/mm^3).

The spring constant or the coefficient of subgrade reaction can be defined along the axial and lateral directions of the pipelines. There are several guidelines available to calculate the spring constants. Vesic (1961) developed a model for the elastic spring constant based on Biot's solution (Biot, 1937) for the bending of a beam of infinite length under a concentrated load. The spring constant obtained from Vesic's expression (Vesic, 1961) can reasonably estimate the pipe-soil interaction behaviour within the elastic range of deformation. However, in real life, the pipe's deformations extend beyond the elastic range, making the pipe-soil interaction complex and nonlinear. Extensive studies have been conducted to investigate the nonlinear soil-structure interaction with attention to laterally loaded pipes and piles. Nonlinear load-displacement relationships, termed as *p-y* relations, were developed to represent the soil responses to the laterally loaded piles and pipelines, as discussed below.

4.2.1 Current design guidelines

Current pipeline design guidelines, such as ALA (2005) and PRCI (2017), proposed bilinear (elastic-perfectly plastic) relations to represent the nonlinear soil spring characteristics for

soil-pipe interaction modeling. These guidelines follow the original recommendation in ASCE (1984) design guidelines. In this method, the spring parameters are defined using the maximum soil reaction forces and the displacement corresponding to the maximum soil forces. Spring parameters in longitudinal, lateral, and vertical directions (Figure 4.2) are recommended.

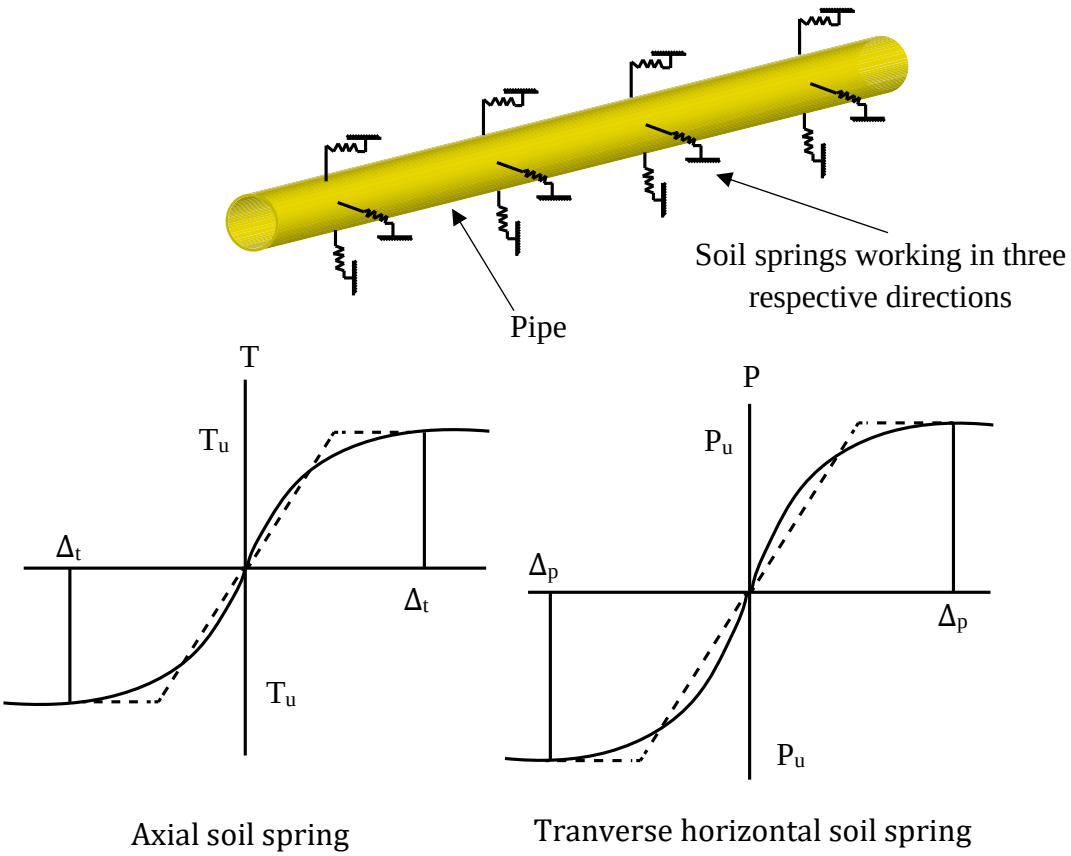

Figure 4.2: Pipe-soil interaction modeling approach

4.2.1.1 Axial soil springs

To calculate the maximum axial soil load on the pipeline along the longitudinal (axial) direction, the equation proposed in the design guidelines (ALA, 2005; ASCE, 1984; PRCI, 2017) for sand is as below (Equation 4.2).

$$T_u = \pi D \gamma H \frac{1+K_0}{2} \tan(f\phi) \quad [4.2]$$

Here,

$T_u =$ Peak soil resistance in the axial direction, γ = unit weight of soil, H = height of soil from the surface to the pipe centerline, K_0= coefficient of earth pressure at rest, f = coating factor relating the internal friction angle of soil to the friction angle at the soil-pipe interface, and ϕ = internal friction angle of soil.

The yield displacement (corresponding to the peak soil resistance) for the axial soil spring depends on the type of surrounding soil, i.e., Δ_t= 3 mm for dense sand, Δ_t = 5 mm for loose sand (ALA, 2005).

4.2.1.2 Lateral soil springs

Lateral pipe-soil interaction occurs where there is a relative horizontal displacement of the pipeline and the soil. The maximum lateral soil force for pipes in the sand was proposed in the design guidelines as in Equation (4.3) (ASCE, 1984; ALA, 2005; PRCI, 2017).

$$P_u = N_{qh} \gamma H D \quad [4.3]$$

Here,

P_u is the peak load per unit length of the pipe, H is the depth to pipe centerline, γ is the effective unit weight of soil, D is the outside diameter of the pipe. N_{qh} is the dimensionless parameter (known as "horizontal bearing capacity factor") that depends on internal friction angle and burial depth to diameter ratio. The value of N_{qh} can be obtained from the design chart provided in the guidelines (ALA, 2005; ASCE, 1984), developed based on the experimental investigation of Hansen (1961). The yield displacement for the lateral soil spring can be obtained using Equation (4.4).

$\Delta p =$ displacement at P_u

$$= 0.04\left(H + \frac{D}{2}\right) \leq 0.10D \; to \; 0.15D \qquad [4.4]$$

where H and D represent the soil cover depth and the pipe diameter, respectively.

4.2.2 Murchison and O'Neill procedure

The bilinear spring parameters discussed above (recommended in the pipeline design guidelines) provide a constant slope of the force-deformation responses corresponding to the maximum forces. However, plastic deformation of the soil starts considerably before the maximum soil force is reached. The initial slope of the force-deformation response is much stiffer during purely elastic deformation, which nonlinearly changes to the value at the maximum soil force. To account for the nonlinearity, the *p-y* relationship iss characterized by a continuous hyperbolic tangent curve in Murchison and O'Neill (1984) for piles in sand. The hyperbolic relation is shown

in Equation (4.5). In this method, the deformation at the peak force is not constant but can be obtained from the curve fitting using Equation (4.5).

$$p = p_u \tanh\left[\frac{k_i}{p_u} y\right] \quad [4.5]$$

where

k_i = initial modulus of subgrade reaction (initial slope) and p_u = peak force and y = lateral displacement.

4.2.3 Liang et al. (2010) procedure

Liang et al. (2010) proposed a different hyperbolic equation (Equation 4.6) to describe the nonlinear *p-y* curve that relates the initial slope and the peak force.

$$p = \frac{y}{\frac{1}{k_i} + \frac{y}{p_u}} \quad [4.6]$$

where

k_i = initial modulus of subgrade reaction, p_u = peak force and y = lateral displacement.

In the current study, the bilinear and nonlinear spring models are examined for soil-pipe interaction modeling under lateral ground movements.

4.3 FE Modeling

4.3.1 Model development

A two-dimensional FE analysis was performed using ABAQUS/Standard to simulate the pipe responses under the lateral loads applied during the tests (Chapter 3). The pipe was modeled in Abaqus using the PIPE21 element which is a type of beam element. The soil reactions to the pipe were modeled using a pipe-soil interaction element (PSI24 element in Abaqus).

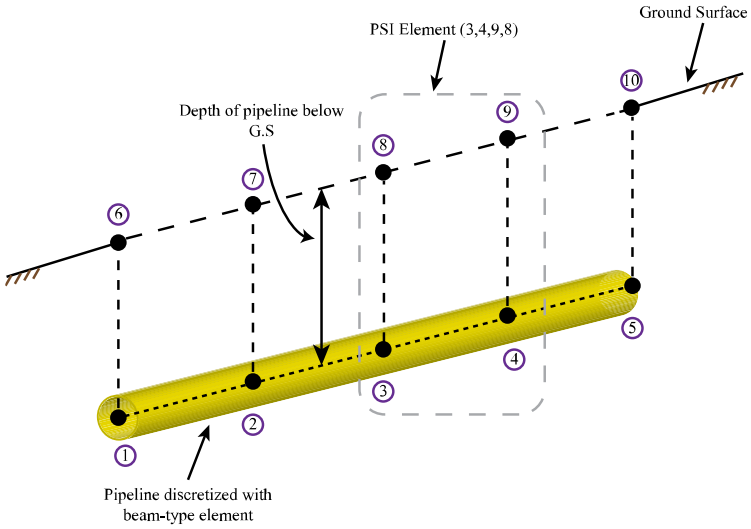

Figure 4.3: Pipe-soil interaction (PSI) element modeling approach

As discussed in Chapter 2, Abaqus provides two-dimensional quadrilateral-shaped pipe-soil interaction (PSI) elements (i.e., PSI24 and PSI26) for modeling the interaction between a buried pipeline and the surrounding soil (Figure 4.3). One side of the PSI element shares nodes with the beam or pipe elements. The other side represents the far-field or ground surface and has independent nodes. The depth of the element is kept equal to the height of the ground surface from the pipe springline, H. The elements only have displacement degrees of freedom at the nodes. The PSI elements, representing the surrounding soil, are "strained" by the relative movements of the

nodes at the far end and the near end and apply nodal forces to the pipe elements. Positive strains in the PSI element are defined by

$$\varepsilon_{ii} = \Delta u . e_i \quad [4.7]$$

where $\Delta u = u_f - u_p$ are the relative displacements between the two edges (u_f and u_p are the far-field displacements and pipe node displacements, respectively). The term e_i indicates the local directions, where the index value of i ($i = 1, 2, 3$) refers to the three local directions.

The material parameters for the PSI element are the spring constants along each of the local directions. The parameters can be defined using the force per unit length of pipe and the corresponding displacement. A linear or nonlinear constitutive behaviour can be defined using tabular input.

A pipe with a length of 1800 mm (the same length used in the experiment discussed in Chapter 3) was modeled using the FE method. A total of 120 mm lateral displacement was applied in increments at the pipe center over the width of 25 mm (Figure 4.4). The 25 mm width corresponds to the grip width used for the laboratory tests for pulling the pipe. The pipe was discretized with very small elements (5 mm long) to capture the nonlinearity, particularly near the applied load. The width of the PSI elements is the same as the length of the pipe element, as the PSI elements share the same nodes with the pipe elements. A mesh sensitivity analysis was conducted varying the element sizes, and no remarkable difference in pullout resistance and pipe strain was noticed for element size less than 5 mm.

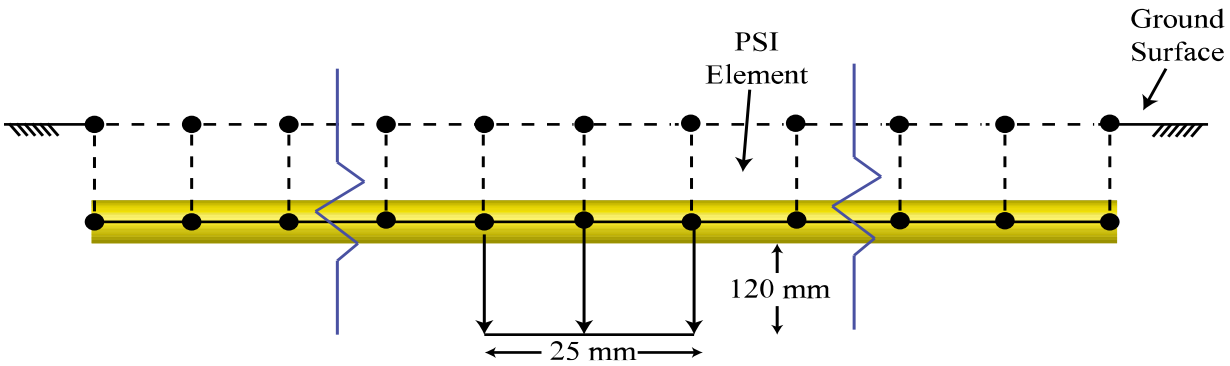

Figure 4.4: Numerical modeling technique of MDPE pipe using PSI element

4.3.2 Pipe material model

MDPE pipe material exhibits a nonlinear time-dependent property. Das and Dhar (2021) developed strain-rate-dependent stress-strain relations for MDPE pipe materials to account for the time-dependent material behaviour (Figure 4.5). Stress-strain response corresponding to the strain rates observed during the tests in Chapter 3 is used in the analysis. Figure 4.6 shows the moving average values of the strain rates calculated from the measurements of strains on the pipe walls. It reveals that the strain rate during the tests was close to 10^{-5}/sec. Therefore, the stress-strain response corresponding to the strain rate of 10^{-5}/sec is considered. Note that the stress-strain response of the material is highly nonlinear (Figure 4.5). The nonlinear stress-strain relation is defined using a constant initial modulus, yield stress and a nonlinear true-stress versus plastic-strain relation (Abaqus, 2014).

The true stress and logarithmic plastic strain were calculated using Equations (4.8) and (4.9).

True stress, $\sigma_{true} = \sigma_{eng} \times (1 + \varepsilon_{eng})$ [4.8]

Logarithmic plastic strain, $\varepsilon_{ln}^{plastic} = \ln(1 + \varepsilon_{eng}) - \frac{\sigma_{true}}{E}$ [4.9]

where

σ_{eng} is the engineering stress, ε_{eng} is the engineering strain, and E is the initial modulus of elasticity.

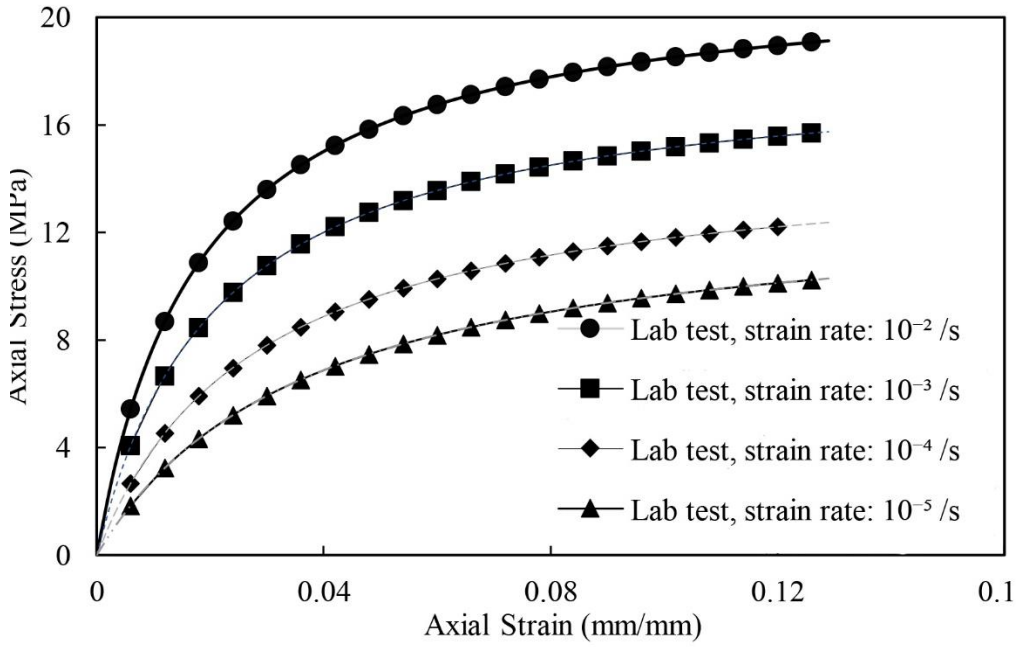

Figure 4.5: Engineering stress–strain results of uniaxial tensile tests at different strain rates (after Das and Dhar, 2021)

The first data point of the nonlinear true stress-plastic strain relation corresponds to the yield point (yield stress when plastic strain = 0). The subsequent strains are calculated using Equation (4.9). The initial modulus of elasticity and the ultimate yield stress are obtained from the strain-strain relation in Figure 4.5 as 413 MPa and 11.14 MPa, respectively. Figure 4.7 plots the true stress vs. logarithmic plastic strain for the strain rate of 10^{-5}/s. The Poisson's ratio and density of the MDPE pipe are assumed to be 0.45 and 940 kg/m^3, respectively. The parameters used in the numerical modeling are summarized in Table 4.1.

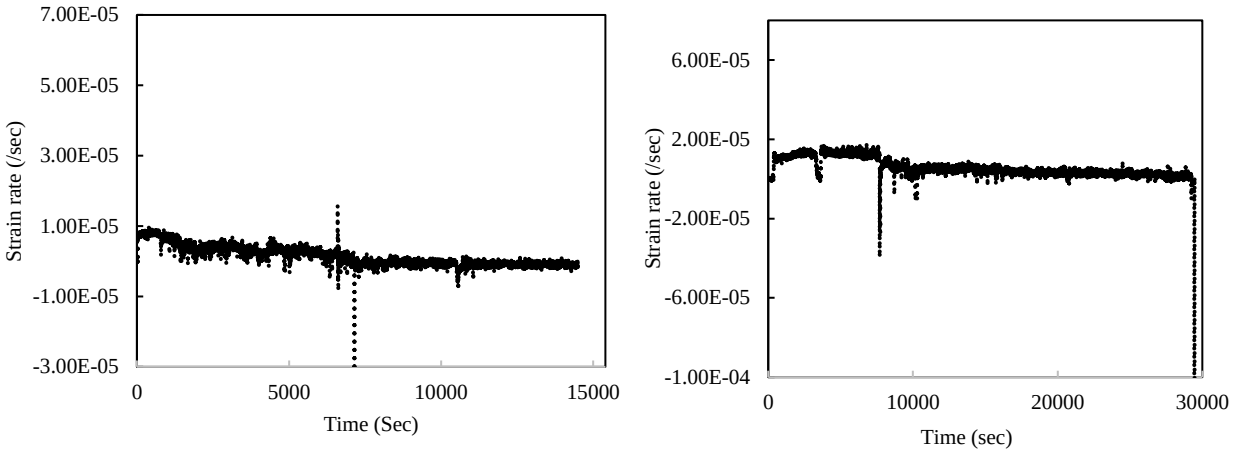

(a) (b)

Figure 4.6: Strain rate during lateral pullout test: (a) 60-mm pipe, and (b) 42.2-mm pipe

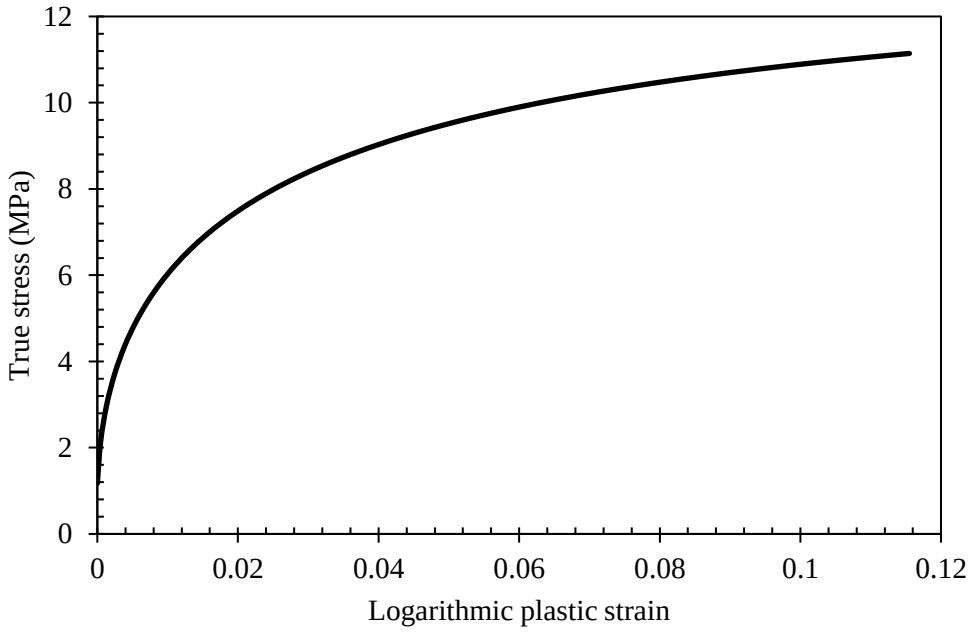

Figure 4.7: True stress- logarithmic plastic-strain curve of MDPE pipe (strain rate = 10^{-5}/s)

Table 4.1: Parameters used in numerical modeling

Parameters	Value(s)
Pipe Length	1800 mm
Pipe Diameters	42.2-mm and 60-mm
Material Density	940 kg/m^3
Initial Modulus of Elasticity	413 MPa
Poisson's ratio	0.45
Coating factor	0.60

4.3.3 Selection of PSI model

The deformations/strains of the PSI element are defined using spring parameters in three orthogonal directions (axial, lateral, and vertical directions). As discussed earlier, current pipeline design guidelines (ALA, 2005; PRCI, 2017) recommend methods for calculating spring parameters for steel pipes. No recommendation currently exists for flexible polyethylene pipes. Researchers revealed that the displacements corresponding to the maximum spring force for flexible GFRP, and PVC pipes are much higher than those for steel pipes (Almahekari et al., 2016; Ni et al., 2018a). It is also recognized that the maximum axial force recommended in the design guideline does not account for the effect of soil dilation during pipe movements. Weerasekara and Wijewickreme (2010) employed cavity expansion theory to predict the increase of normal stress on the pipe due to dilation (Equation 4.10).

$$\Delta\sigma_d = \frac{2G(\gamma)\Delta t_d}{D}\tan\psi_{max} \quad [4.10]$$

Here, $\Delta\sigma_d$ is the increase in normal stress due to dilation, G is the shear modulus of the soil, γ is the unit weight of the soil, Δt_d the thickness of the shear band and ψ_{max} is the maximum dilation angle. For a 42.2-mm pipe buried at a depth of 600 mm, the stress increase due to dilation is calculated to be 7 times higher than the maximum axial force given by Equation (4.2), based on G = 4 MPa, γ = 17 kN/m^3, Δt_d = 2 mm and ψ_{max}=8°.

It is, therefore, difficult to obtain the spring parameters that accurately represent the soil-pipe interaction. The spring parameters for the MDPE pipe discussed in this study were obtained using iterations to simulate the test results. A high displacement at the maximum pulling force is expected for the pipes, which was determined through the iterations. Furthermore, the maximum spring force developed for the steel pipe may also not be applicable for flexible pipes. The force-displacement responses with various magnitudes of the peak spring forces and corresponding displacements were calculated and compared with the experimental data to obtain the appropriate spring parameters. An example of iterations with the variation of axial spring parameters is shown in Figure 4.8. Figure 4.8 shows that the force-displacement response significantly depends on the maximum spring forces and the corresponding displacements. The pulling force was underpredicted if the maximum spring force was too low and overpredicted if the maximum spring force was too high for a constant yield displacement, i.e., 5 mm (Figure 4.8b). The spring constant (force per unit displacement) is higher for higher peak forces with a constant yield displacement, which contributes to a higher soil resistance. However, the spring constant was not the only factor controlling the pipe behaviour. Yield displacement also significantly influences the pipe-soil interaction. Figure 4.8a plots the results of analyses with a fixed spring constant but different yield displacements. For low yield displacements, a softening response is observed in Figure 4.8a. The

results of the analysis with the maximum axial spring force of 5310 N/m with yield displacement of 20 mm match most reasonably with the test results.

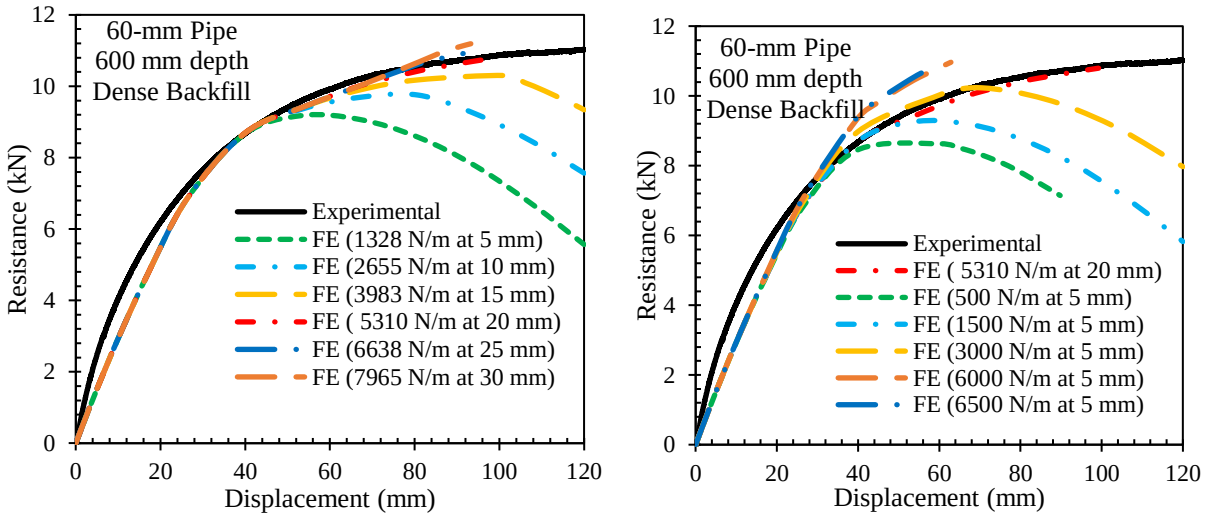

(a) Effect of maximum spring force (b) Effect of displacement

Figure 4.8: Iterations of varying axial spring parameters to simulate experimental responses

Based on the trials, the spring parameters were estimated that simulated the test conditions most reasonably. The following presents how the lateral and axial spring parameters were determined for the analysis.

- The maximum lateral spring force given by the design guidelines for steel pipes (Equation 3) was used with appropriate values of the horizontal bearing capacity factor, N_{qh}. The N_{qh} was increased from the one recommended in the ALA (2005) guidelines, based on Hansen (1961), by a factor of 1.17 and 2.36 for dense and loose sand, respectively. The same factor for each soil condition was applied regardless of pipe diameter and burial depth.
- The yield displacement (displacement at the maximum spring force) for the lateral spring was kept at 30 mm. The yield displacement is much greater than that recommended in the

design guidelines (ALA, 2005). A larger yield displacement for the flexible pipe was also recommended in Almahekari et al. (2016) and Ni et al. (2018a).

- The maximum axial spring force given by Equation (2) was multiplied by ~7 for both dense and loose sand. The high multiplying factor for the axial spring force is likely due to the increase of normal pressure on the pipe surface by the lateral load and soil dilation, increasing the axial resistance. This is consistent with the increase of normal stress calculated based on the cavity expansion theory (Weerasekara and Wijewickrement 2010), discussed earlier. The design guidelines do not account for the increase of the normal pressure.
- The yield displacement for the axial spring was 20 mm.

The spring parameters were then defined using the bilinear model recommended in pipe design guidelines (ALA, 2005; PRCI, 2017) and nonlinear models of Murchison and O'Neill (1984) and Liang et al. (2010). For the nonlinear models, the value of the initial subgrade moduli (k_i) (the slope of the force-displacement curve) was taken as 4000 kPa (Reese et al., 1975) and 800 kPa (Wong, 1992) for the dense and loose sand, respectively. Figure 4.9 shows the estimated spring parameters and a comparison of pulling force versus displacement responses for different approaches of defining the PSI parameters.

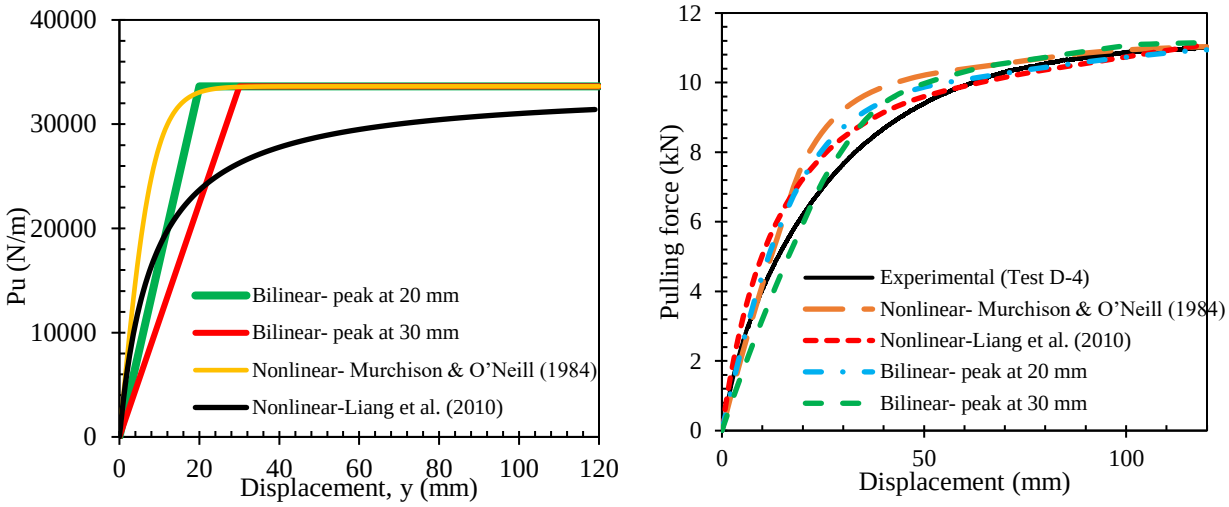

(a) p-y relations (b) Load-displacement responses

Figure 4.9: Spring parameters and load-displacement responses

The comparison reveals that the bilinear *p-y* relation with the yield displacement at 30 mm closely matches the experimental result. Thus, the bilinear *p-y* relation has been used for the analyses presented here. The coefficient of earth pressure at rest, $K_{0,}$ was calculated based on an estimated Poisson's ratio, ν, i.e., $K_0 = \nu/(1-\nu)$ (Tschebotarioff, 1973). The estimated lateral earth coefficient at rest, K_0 was 0.42, based on a Poisson's ratio of 0.3. The angles of internal friction 45° and 34° were selected for the dense and loose sand, respectively, based on the test results provided in Saha (2021). Table 4.2 shows the detailed estimations of the spring parameters corresponding to the test conditions discussed in Chapter 3.

Table 4.2: Estimation of spring parameters

Test	Pipe		Soil properties			Springs			
	Dia., (m)	Burial depth, (m)	Unit weight, γ (N/m^3)	Friction angle, ϕ (°)	Horizontal bearing capacity factor, N_{qh}	Peak Axial resistance, T_u (N/m)	Axial yield displacement, Δt (m)	Peak Lateral resistance, P_u (N/m)	Lateral yield displacement, Δp (m)
D-1	0.042	0.337	17000	45	48	1966.25	0.020	11210.5	0.030
D-2	0.042	0.600			75	3750.1		32995.24	
D-3	0.060	0.480			48	3865.14		24406.27	
D-4	0.060	0.600			55	5310.29		33627.37	
L-1	0.042	0.600	13500	34	53	2200.2		18510	
L-2	0.060	0.600			38	3011.5		18000	

4.4 Comparisons with test results

4.4.1 Load-displacement responses

Pullout forces versus lateral pipe displacements are calculated using FE analysis for the test conditions discussed in Chapter 3. As presented in Table 4.2, six tests are conducted with four in a dense backfill soil and two in a loose backfill soil at different burial depths. Figure 4.10 shows a typical deflection profile of the pipes calculated using the FE analysis.

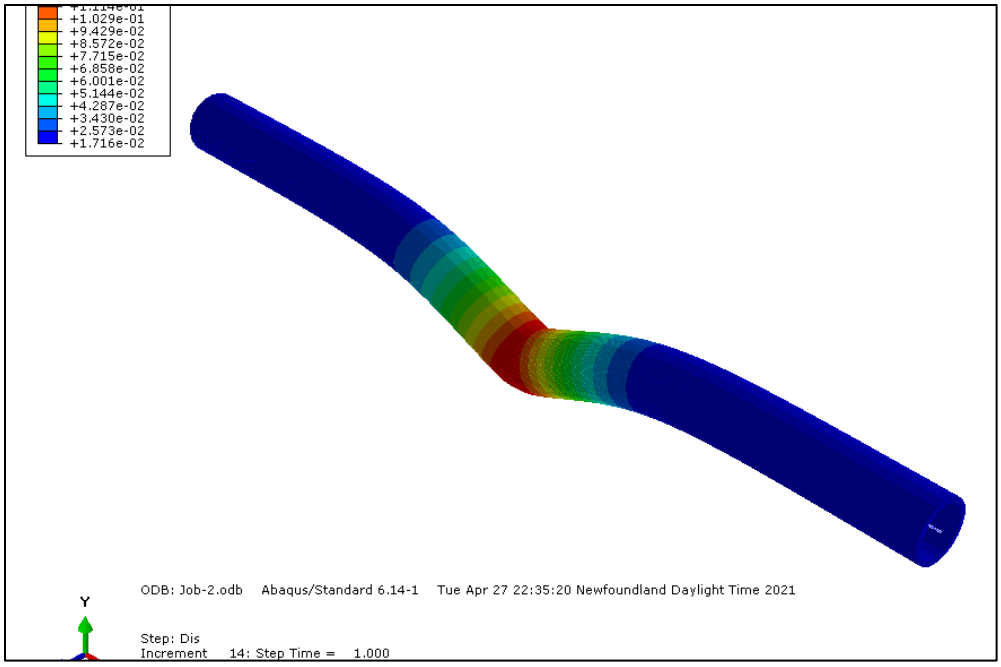

Figure 4.10: Calculated deflection profile

Figures 4.11 and 4.12 compare the calculated pullout resistance-displacement responses with the experimental measurements for the pipes in dense and loose sand, respectively. The FE calculations match reasonably with the measurements in the figure. For tests D-1 and D-2 with 42.2-mm diameter and embedment ratios of 8 and 14.2, respectively, the pullout force is significantly higher for the pipe with the higher embedment ratio (Figure 4.11a). The FE model captured the difference well, except that the FE calculated pullout force continues to increase with the displacement for test D-1. The spring parameters for the analysis are calculated using the same soil properties and different burial depths (Table 4.2). The horizontal bearing capacity factor is calculated considering the embedment ratio. Note that the horizontal bearing capacity factors are higher than the values recommended in ALA (2005) design guidelines based on Hansen (1961). Figure 4.11b shows similar findings for tests D-3 and D-4, using 60-mm diameter pipe with the embedment ratios of 8 and 10, respectively.

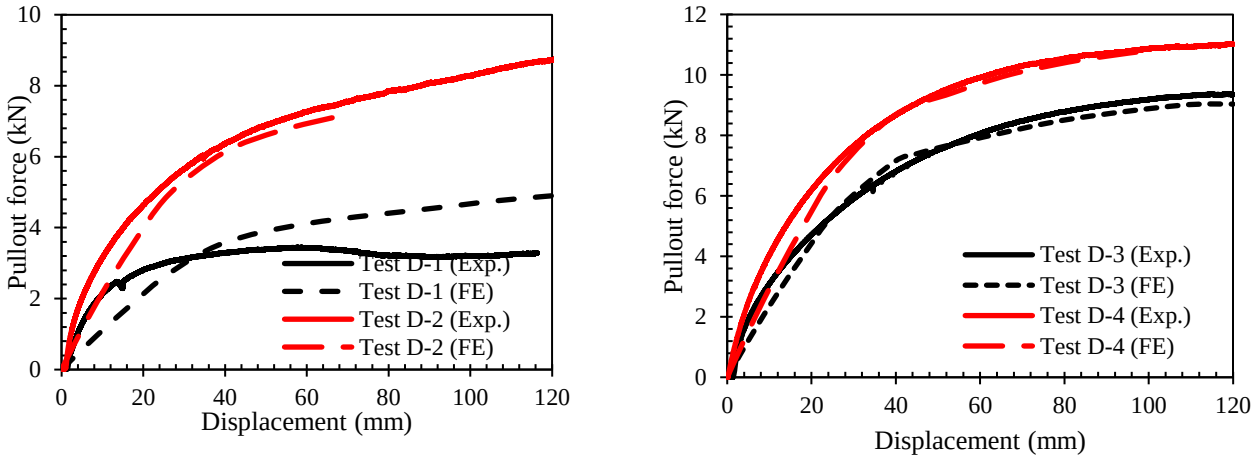

(a) (b)

Figure 4.11: Comparison of load-displacement responses for pipes in dense sand: (a) 42.2-mm pipe, and (b) 60-mm pipe

FE results based on loose sand properties also showed a good match with the experimental data (Figure 4.12). Figure 4.12 shows the comparison for pipe with two different diameters (60-mm and 42.2-mm) and two embedment ratios (10 and 14.4, respectively). The spring parameters were calculated independently of the pipe diameter and embedment ratio using the method discussed above. Thus, the proposed methods of calculating spring parameters appear to reasonably account for the soil-pipe interaction for the MDPE pipes observed during the tests.

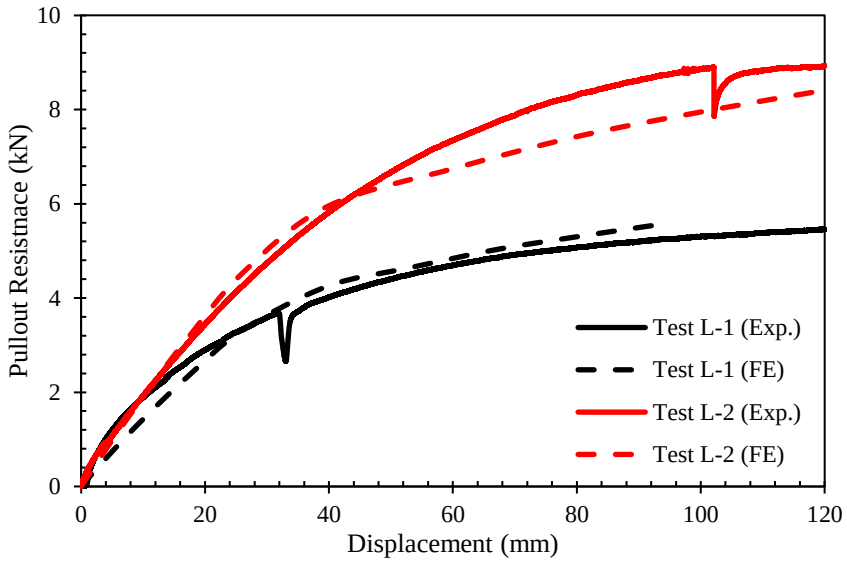

Figure 4.12: Comparison of load-displacement responses for pipes in loose sand

4.4.2 Comparison with pipe wall strains

Pipe wall strains were measured using electrical resistance strain gauges at different locations during the tests (Chapter 3). Measured strains were compared with the FE calculations in Figures 4.13– 4.15. The inset in Figure 4.13a shows the schematic locations of strain measurement. As the pipe was pulled laterally from its center, the highest strains were in the strain gauge located near the pulling force (S.G-3). At very high strains, the strain gauge could be detached, and therefore, the strain reading was stabilized, or no reading was available at the location of S.G.-3 for large pulling displacements, seen in Figures 4.13– 4.15. However, the calculated strains at this location continued to increase at large pulling displacements, while the calculations matched reasonably with the measurements at low displacements. Strains measured by the other strain gauges were less (<2%) and increased almost linearly with the applied displacements.

For the 42.2-mm pipes in test D-2 (600 mm burial depth), the calculated strains at the locations of S.G.-1 and S.G.-2 are almost zero (Figure 4.13b), indicating no effect of lateral pulling at this distance (450 mm). However, strain gauge "S.G.-1" measured compressive strains, and strain gauge "S.G.-2" measured the tensile strains, demonstrating a bending mechanism (Figure 4.13a). The magnitudes of the maximum measured strains are less (0.005 and 0.009, respectively, at 120 mm of displacement). The strains measured near the pulling force are in agreement with the FE calculations up to a displacement of around 60-mm. For the deeply buried pipe (Figure 4.13b), the FE calculations matched the measurement well, except at large displacement when the strain gauge "S.G.-3" likely lost bonding.

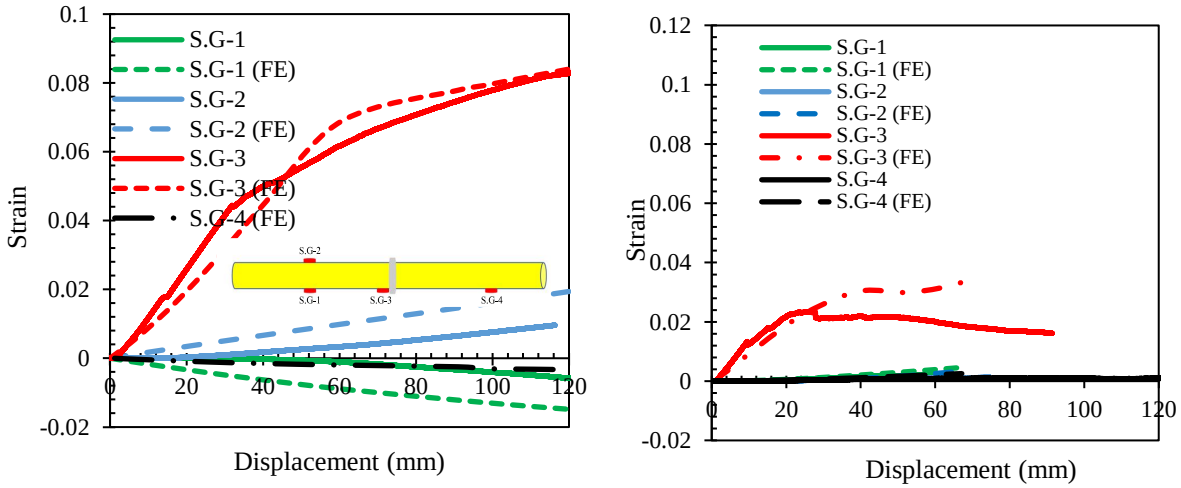

(a) (b)

Figure 4.13: Comparison of pipe wall strain for 42.2-mm diameter pipes in dense sand: (a) Test D-1, and (b) Test D-2

The FE method also underpredicted the strains at the distance of 450 mm from the load for the 60-mm pipes in dense sand (Figure 4.14). The strains near the pulling force were well predicted until

the strain gauges lost bonding at large displacements. The proposed FE method predicted the measured strains very well for the pipe in loose sand (Figure 4.15).

The comparisons of pipe wall strain with the measurements (discussed above) revealed that although some discrepancies exist between the calculated values and the measured values, the proposed model can be used for preliminary assessment of the pipe wall strains subjected to lateral ground movements. A parametric study is conducted using this method to investigate the effects of different parameters on the pipe wall stress and the pulling force.

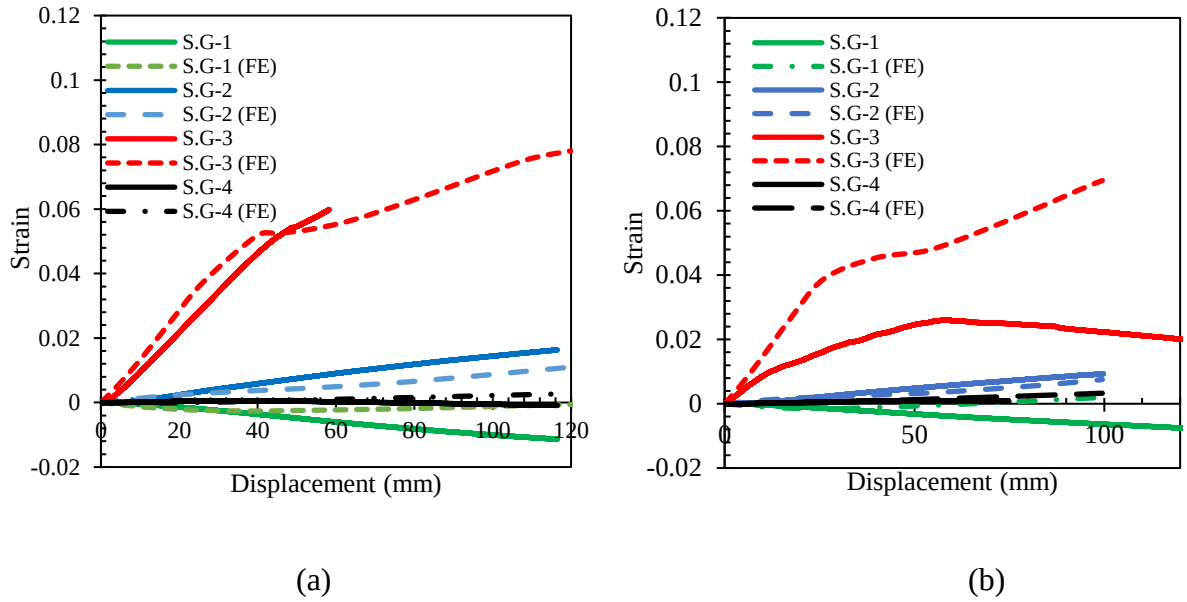

(a) (b)

Figure 4.14: Comparison of pipe wall strain for 60-mm diameter pipes in dense sand: (a) Test D-3, and (b) Test D-4

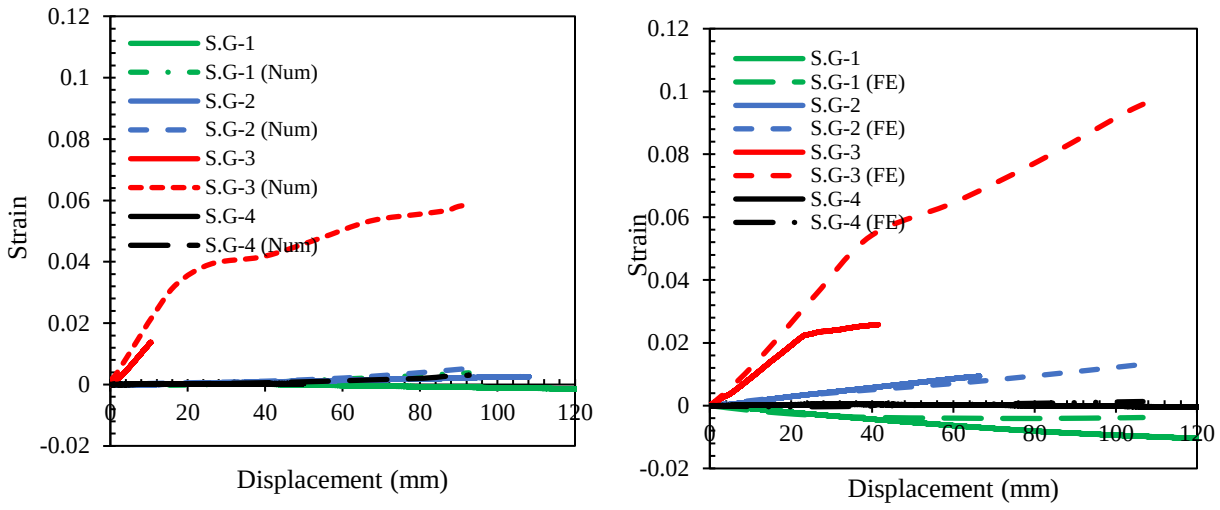

(a) (b)

Figure 4.15: Comparison of pipe wall strain for the pipes is loose sand: (a) Test L-1, and (b) Test L-2

4.5 Parametric study

A parametric study has been conducted to investigate the effect of burial depth, soil density, soil friction angle and landslide scale on the pipelines through the development of various FE models. The models were developed using Abaqus/Standard, and pipe-soil interaction was defined using the pipe-soil interaction (PSI) element (described above). Different input parameters were selected for numerical analysis, and corresponding maximum pullout force and strain were calculated. For analysis purposes, two different diameters (D) of pipe, i.e., 60-mm and 42.2-mm, were considered and modeled separately. Different burial depths (H) of pipes were selected, and the maximum H/D of 20 was investigated for each pipe diameter. The soil type was categorized based on the unit weight (γ) into loose sand, medium dense sand, and dense sand. The corresponding internal soil friction angles (ϕ) were defined. The effect of landslide scale had been studied; a maximum of 150 mm lateral landslide impact had been analyzed for 60-mm pipe. On

the other hand, lateral displacement of 100 mm had been analyzed for 42.2-mm to reduce the convergence issue of smaller diameter pipe. The ranges of input parameters considered for the parametric study are summarized in Table 4.3.

Table 4.3: Input parameter range

Input type	Range
Pipe diameter, D (mm)	• 60 • 42.2
Lateral displacement, δ (mm)	• 0~150 (60-mm pipe) • 0~100 (42.2-mm pipe)
Burial depth of pipe, H (mm)	• 600, 800, 1000, 1200 (60-mm pipe) • 500, 600, 700, 800 (42.2-mm pipe)
Unit weight of soil, γ (kN/m^3)	• Loose sand (11-13) • Medium dense sand (13-17) • Dense sand (17-20)
Soil internal friction angle, ϕ (°)	• Loose sand (28-34) • Medium dense sand (35-37) • Dense sand (38-45)
Amplification coefficient (Lateral)	• 2.36 (Loose sand) • Between 1.17-2.36 (Medium dense sand) • 1.17 (Dense sand)

An Abaqus Python script was developed using PyCharm Community Edition 2020 to conduct the parametric study based on the above parameter ranges. The Python script helped in the development of the models efficiently and saved the associated time with model development. The required output data could also be extracted easily without digging into the output data file. Some specific benefits of using the Python script are: (a) it automatically generates the FE model, (b) it

automatically defines the material property, mesh, and boundary conditions, including spring parameters, (c) it extracts output data in the required form.

Six variables were defined based on the input parameters within the loose, medium dense, and dense sand. These variables can generate a random combination within the specified parameters' ranges (Table 4.3) for different sand densities. The corresponding axial and lateral soil spring stiffnesses are then calculated based on the parameters. The python script was written to define automatically the parts, material properties, section, assembly, steps, mesh, boundary, PSI element property, and job submission. For each job, the corresponding output database (ODB) file was called, and the maximum pullout force and the maximum strain were saved in a text file (using the python script). A total of 448 numerical models was developed, and 2268 data points were analyzed. The mean values and standard deviations of the pulling forces and the maximum pipe wall strain for various burial depths and soil densities were then examined.

4.5.1 Load-displacement response

Figure 4.16 shows the mean values and standard deviation of the load-displacement response of 60-mm pipe with different burial depths in loose sand. It shows higher mean pulling forces for deeper pipes at the same level of relative displacements. However, the standard deviations of the pulling forces are higher for shallow buried pipes, indicating higher effects of parameter uncertainties for shallow buried pipes. The standard deviations are higher (13% to 18%) at lower displacements that decrease with the increase the displacements. The pulling forces on the branch pipe increase with the increase of relative ground displacements. The rate of increase is higher at a small displacement that stabilizes at large displacements (Figure 4.16a). The maximum pulling forces of 8 KN to 10 kN are observed for the range of ground displacement considered.

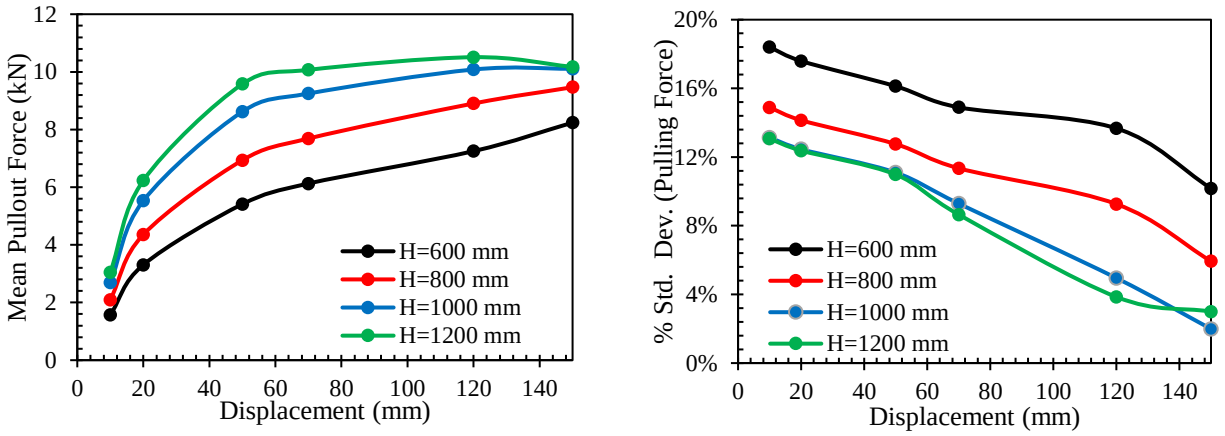

(a) (b)

Figure 4.16: Load-displacement response for 60-mm pipe in loose sand: (a) mean pulling force, and (b) standard deviation

Figure 4.16 reveals that even with a small relative ground displacement of 10 mm, the branch pipe can experience an axial pulling force of 1.5 kN to 3.0 kN. This axial force can cause 12 MPa to 24 MPa stresses on 16 mm diameter service piping, commonly used in the gas distribution system, resulting in axial strains beyond the allowable limit of the pipe material. Weerasekara and Rahman (2019) classified the MDPE pipe with 8% axial strain to have a high likelihood of failure. The 8% of axial strain is equivalent to the axial stress of 8 MPa under slow-moving ground, based on the test results of Das and Dhar (2021). Thus, the MDPE branch service piping would fail even with minimal ground displacement, which should be considered during design. The branch pipes could be designed to carry the pulling force expected from the ground movements. Note that under the axial force, the flexible MDPE pipe will elongate. Thus, the relative movement, which is the difference between the absolute ground movement and the elongation of the branch pipe, would be less, reducing the axial force.

Figures 4.17 and 4.18 show the mean load-displacement responses for the pipes in medium dense and dense sand, respectively. The average pullout forces in medium dense and dense sand increased continuously with the burial depth up to the lateral displacement of 60-mm. However, for higher burial depths, i.e., 1000 mm and 1200 mm, the average pullout forces started reducing after the displacement of 60-mm. The failure mechanisms of the soil surrounding the pipe are different for low and high embedment ratios. For the shallow burial depth, the passive earth pressure failure wedge extends to the soil surface, but local shear failure is predominant when the burial depth is high (Phillips et al., 2004). The failure mechanism for the MDPE pipe requires further investigation to understand it properly. The maximum pulling forces of 13 kN (Figure 4.17a) and 16 kN (Figure 4.18a) were calculated for the medium dense and dense sand. The standard deviations of calculated pullout forces were relatively less for the pipes in medium dense and dense sand (Figure 4.17b and 4.18b) compared to the pipes in loose sand (Figure 4.16b). Note that the mean pullout forces are reduced at higher displacement at H= 1000 mm and 1200 mm, which is likely due to the selection of the parameters randomly for the parametric study.

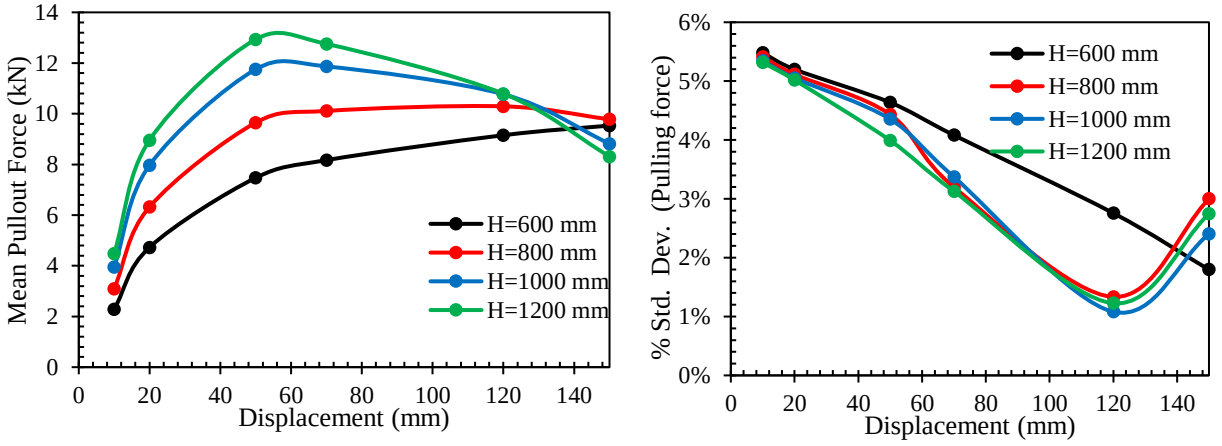

Figure 4.17: Load-displacement response for 60-mm pipe in medium dense sand: (a) mean pulling force, and (b) standard deviation

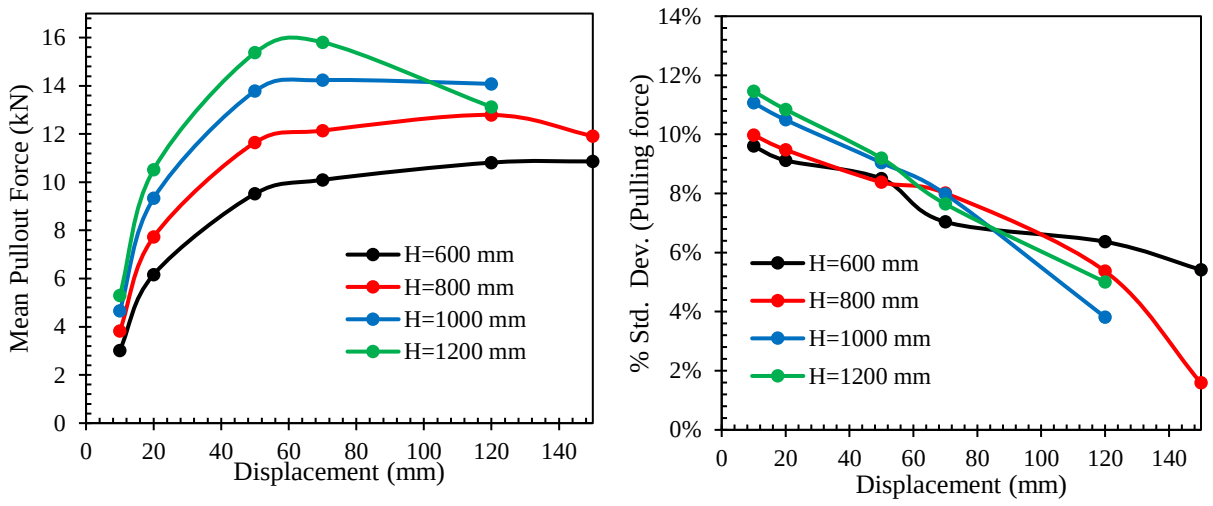

(a) (b)

Figure 4.18: Load-displacement response for 60-mm pipe in dense sand: (a) mean pulling force, and (b) standard deviation

Figures 4.19-4.21 present the load-displacement responses for the 42.2-mm pipe in loose sand, medium dense sand, and dense sand, respectively. The load-displacement responses for the 42.2-mm pipes are similar to those for the 60-mm pipes, except for the pipes in medium dense sand and dense sand. In medium dense sand and dense sand, the average pulling force increases continuously with the increase of displacement for the 42.2-mm diameter pipe regardless of the burial depth. However, for the 60-mm diameter pipes, the average force pulling force reached a peak value and then decreased with the increase of ground displacement. As expected, the maximum pulling forces were less for the 42.2-mm diameter pipes. The maximum pullout resistance was about 6 kN, 7 kN, and 9 kN for the pipe in loose sand, medium dense sand, and dense sand, respectively. Standard deviation plots show a higher deviation at the initial lateral displacement that reduces with the displacement (Figure 4.19b-4.21b), indicating a lower impact of parameter uncertainties at large displacement.

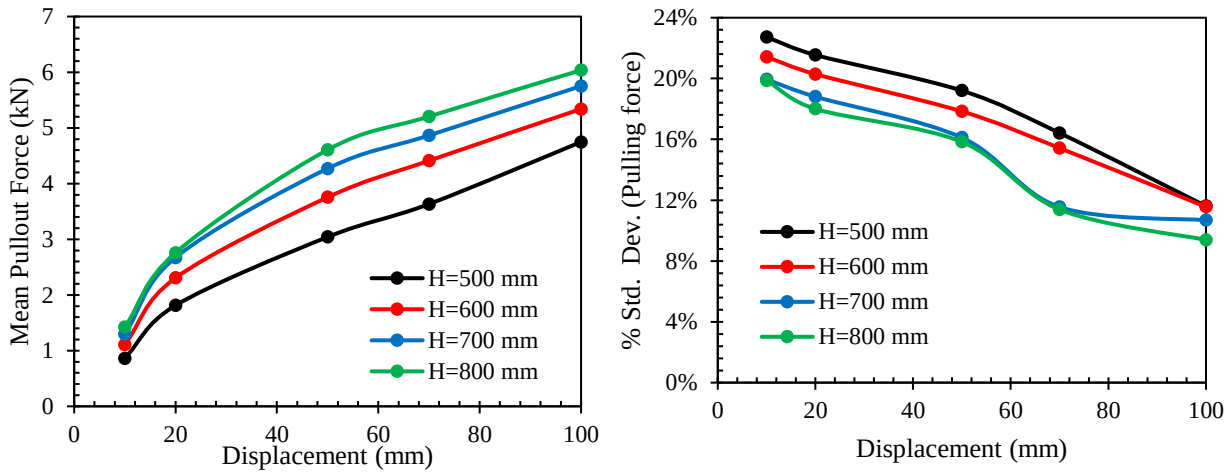

(a) (b)

Figure 4.19: Load-displacement response for 42.2-mm pipe in loose sand: (a) mean pulling force, and (b) standard deviation

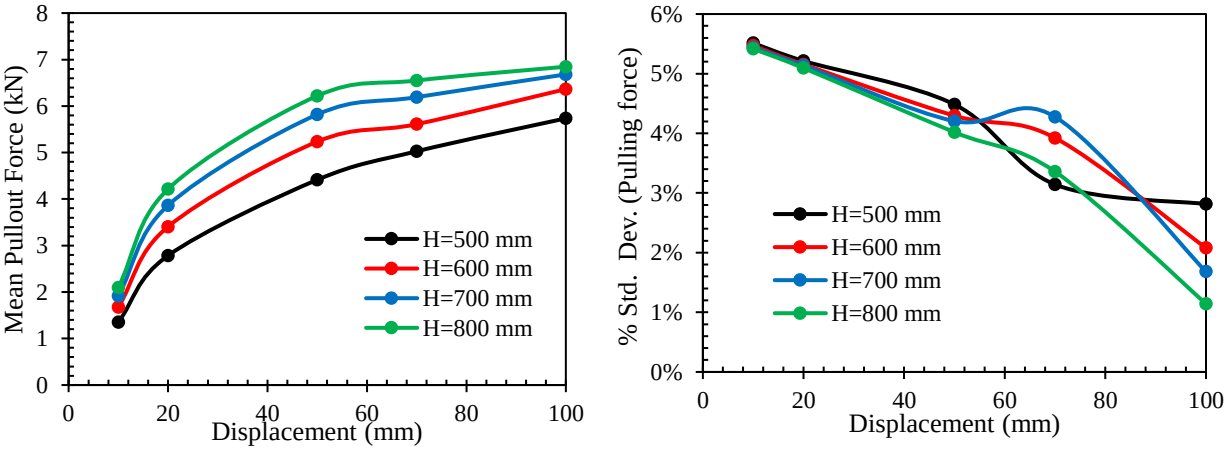

(a) (b)

Figure 4.20: Load-displacement response for 42.2-mm pipe in medium dense sand: (a) mean pulling force, and (b) standard deviation

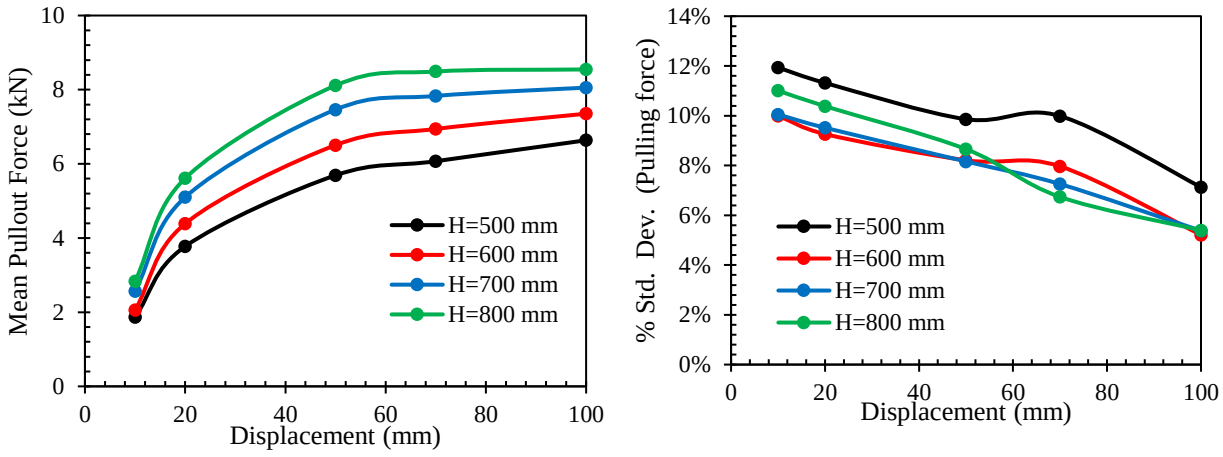

(a) (b)

Figure 4.21: Load-displacement response for 42.2-mm pipe in dense sand: (a) mean pulling force, and (b) standard deviation

4.5.2 Maximum strains on main pipe

As discussed earlier, the main pipe experiences bending strains near the branch pipe when subjected to relative ground movements. The maximum strain develops near the pulling force. Figures 4.22 and 4.23 plot the maximum strains for the 60-mm and 42.2-mm pipes, respectively, against the displacement. Only pipe strains in dense sand are plotted, as the strain distribution pattern is the same for all cases. The figures show that the maximum strain is higher for the pipe at lower burial depths (Figure 4.22a and 4.23a). Pipes with higher burial depths show comparatively less strain. The maximum strain is about 8 percent at 100 mm of lateral displacement for both 60-mm and 42.2-mm pipes (Figure 4.22a and 4.23b). The maximum standard deviation of strains is around 10%.

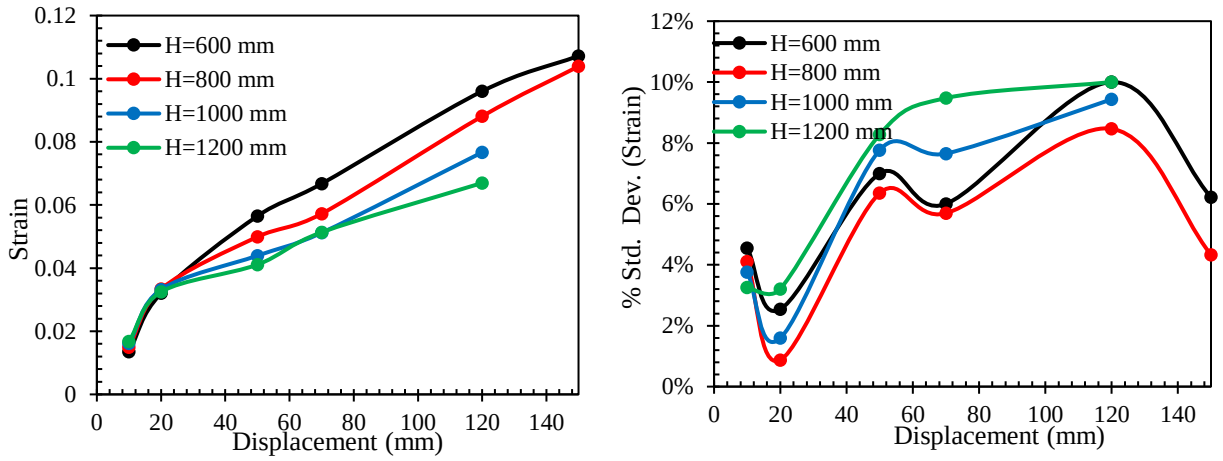

(a) (b)

Figure 4.22: 60-mm pipe in dense sand: (a) strain at different burial depths, and (b) percentage standard deviation measured

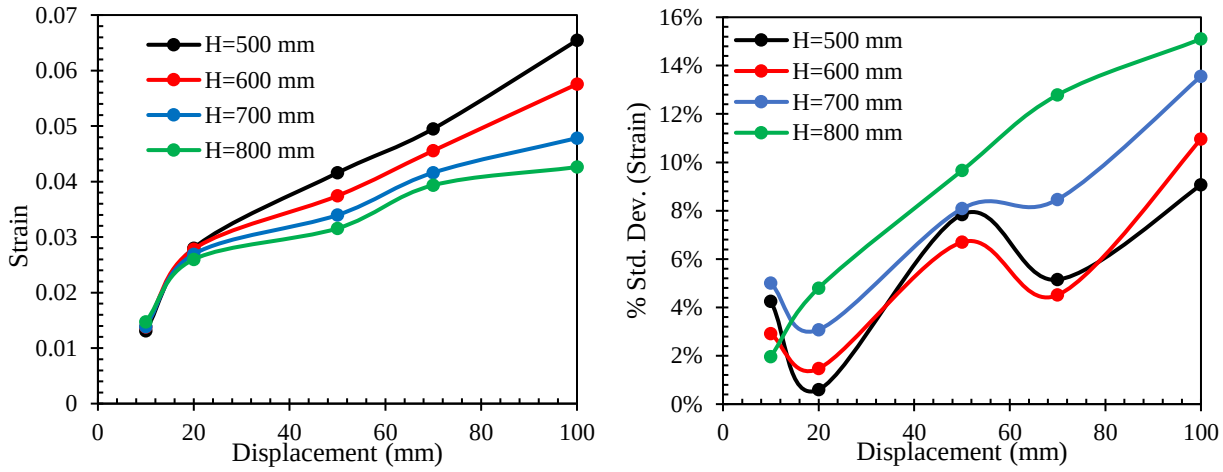

(a) (b)

Figure 4.23: 42.2-mm pipe in dense sand: (a) strain at different burial depths, and (b) percentage standard deviation measured

4.6 Conclusion

MDPE pipes subjected to lateral ground movement were analyzed based on the beam on spring idealization using the FE method. The FE analysis was performed using the software Abaqus. The pipe was idealized using the beam (pipe) element, and the soil was modeled using the PSI element. The spring parameters were determined to simulate the pipe responses observed during laboratory tests. The validated model was then used to conduct a parametric study. The following are the major findings of the investigation.

1. The beam-on-spring idealization can be used to simulate pipe behaviour with the appropriate choice of spring parameters. The design guidelines recommended in ALA (2005) can be modified to obtain the spring parameters for MDPE pipes.
2. For the MDPE pipes considered, the maximum horizontal spring force can be obtained by increasing the horizontal bearing capacity factor N_{qh} by a factor of 1.17 and 2.36 for dense and loose sand, respectively, from the values recommended in ALA (2005) guidelines. Similarly, the maximum axial spring force can be obtained by using a factor of 7.08 for both dense and loose sand due to the increase of normal pressure on the pipe by lateral load and the dilation of soil.
3. The yield displacement for both the axial and lateral spring is much greater than the values recommended guideline in ALA (2005). The yield displacements of 20 mm and 30 mm for the axial and lateral spring, respectively, successfully simulated the experimental results for both dense sand and loose sand. The numerical model can capture the load-displacement and the strain-displacement responses of pipe reasonably at different burial depths, pipe diameters, and soil densities using the spring parameters.

4. The bending effect due to concentrated load is minimized at a distance of 450 mm to 600 mm from the loading point.
5. Parametric studies show that mean pulling forces are higher for the deeper pipes subjected to the same level of relative displacements. However, the standard deviations of the pulling forces are higher at initial displacement, indicating higher effects of parameter uncertainties for the lower level of displacement.
6. Even at a small relative displacement of 10 mm, the branch pipe can experience an axial strain beyond the allowable limit (8%). Thus, the MDPE branch pipe may fail even with a small ground displacement, which should be considered during the design.
7. The reduction of the peak forces was observed at the higher burial depths due to different failure mechanisms between the shallow and deep burial depths. For the lower burial depth, the passive earth pressure failure wedge extends to the soil surface, but local shear failure is predominant when the burial depth is high.
8. The peak bending strain and stress were higher for the lower burial depth and decreased with the burial depth of the pipe. The distribution of stress and strain along the length of the pipe decreases significantly after the length of 450 mm from the pulling point of the pipe.

CHAPTER 5

Conclusion and Recommendations for Future Work

5.1 Overview

MDPE pipes are used widely in the gas distribution system in Canada and worldwide. However, limited studies are available in the literature on understanding the behaviours of buried MDPE pipes subjected to various hazards, including geohazards. Full-scale laboratory experiments are an efficient method for understanding pipe–soil interaction. Ten full-scale laboratory lateral pullout tests were conducted in this research to investigate the effect of ground movement on MDPE pipes near a connection. The goal of the experiments was to measure the load-displacement behaviour and the bending strain of buried MDPE pipe. Pipes of two different diameters (i.e., 60-mm and 42.2-mm diameter) were considered in the study, which are commonly used in the gas distribution systems.

Numerical modeling of the pipe behaviour was performed using the pipe-soil interaction (PSI) element in ABAQUS/Standard. The models were developed using PSI24 and PIPE21 elements and verified with the experimental data. A parametric study was performed using the numerical approach to study the effect of pipe burial depth, soil density, soil internal friction angle, and landslide magnitudes.

The findings from the experimental and numerical investigations are discussed in Chapters 3 and 4. This chapter includes an overall summary of the conclusions and recommendations for future research.

5.2 Conclusions

The following are the key findings of the study conducted on the behaviour of the MDPE pipeline with a lateral branch subjected to lateral ground deformation.

- The lateral load-displacement behaviour of buried MDPE pipe is nonlinear and depends on the soil support, which is greater for the deeply buried pipe than for the shallow buried pipe.
- The axial force on the lateral branch depends on the pipe diameter and the burial depth of the main pipe. The axial force on the lateral branch pipe is higher for a larger diameter and higher burial depth of the main pipe, and vice-versa.
- For pipe with shallow burial depth, the maximum pullout force may be less due to full mobilization of soil resistance, with the crack propagation to the ground surface.
- The effect of the concentrated load is insignificant at a distance beyond 624 mm from the point of load.
- Beam-on-elastic-foundation solution can estimate the pipe-soil interaction behaviour within the elastic range only. However, for the nonlinear range with larger displacements, the solution underpredicts the axial strains on the main pipe.
- Beam-on-spring idealization of the buried pipe using the PSI element can reasonably be used to account for the pipe-soil interaction. However, spring parameters appropriate to the pipe should be used.
- A modification of the spring parameters recommended in ALA (2005) guidelines is proposed for the MDPE pipelines. An increase of the horizontal bearing capacity, N_{qh} factor, by a factor of 1.17 and 2.36 for dense and loose sand, respectively, calculated the maximum lateral spring force that simulated the test results. For the maximum axial spring

force, a modification factor of 7.08 was found most suitable. The high axial spring force is associated with the high normal stress caused by the lateral load and the dilation of the interface soil.

- The yield displacements for lateral and axial springs for the MDPE pipe are much greater than those recommended for steel pipes in ALA (2005) design guidelines. The yield displacements of 20 mm and 30 mm for the axial and lateral spring, respectively, were successfully used to simulate the test results.

5.3 Recommendations for future study

This thesis presents a study of a pipeline subjected to ground movement near a joint. To the best knowledge of the author, no such study is currently available in published literature. Therefore, this research is the first of this kind and requires further studies to address the problem. The following are recommendations for future works to improve understanding of pipe behaviour.

- The present study develops a small database by investigating 60-mm and 42.2-mm diameter pipes. The database should be extended with additional testing under various conditions to assist in developing numerical models through validation.
- The pipe was pulled at the midpoint using a cable, and the effect of the pullout behaviour of the pipe connected with the lateral branch was studied in this research. However, applying pullout force at both ends of the pipe can be considered to study the bending deformation of due to geotechnical hazards pipe subjected to ground movements.

- The movement of pipe at different points during the tests was not measured due to the lack of proper equipment. However, measuring the movement of pipes at different locations can be considered, to capture the bending behaviour more accurately.
- The strain distribution along the pipe length for the pipeline subjected to ground movement is nonuniform. The distribution of strain could not be measured using discrete strain gauges at four locations (used in this study). Measuring the pipe strain at multiple locations could be considered to identify the correct bending behaviour and strain distribution. Fibre optic sensors could be used to measure the continuous strain.
- The finite element modeling techniques are only validated with the current test results. The applicability of the modeling techniques should be examined with additional test results.
- Parametric studies were undertaken using the numerical approach to investigate the effect of burial depth, embedment ratio, soil density, and landslide magnitude. However, the parameters were randomly selected in this study. The parametric study could be further extended to perform a reliability assessment of the pipeline through identifying the distribution patterns of the parameters. The developed database can be used to develop a model using the machine learning method.

References

Abaqus. (2014). *Theory Manual of ABAQUS*. Abaqus, Inc., Providence, RI. Available from http://130.149.89.49:2080/v6.14/ (citated January 2020)

ALA. (2005). *Guidelines for the design of buried steel pipe*. American Lifeline Alliance, available from https://www.americanlifelinesalliance.com/pdf/Update061305.pdf (cited July 2019).

Almahakeri, M., Fam, A., and Moore, I. D. (2014). Experimental investigation of longitudinal bending of buried steel pipes pulled through dense sand. *Journal of Pipeline Systems Engineering and Practice*, *5*(2), 4013014.

Almahakeri, M., Moore, I. D., and Fam, A. (2012). The flexural behaviour of buried steel and composite pipes pulled relative to dense sand: Experimental and numerical investigation. *Proceedings of the Biennial International Pipeline Conference, IPC*, *1*, 97–105. https://doi.org/10.1115/IPC2012-90158

Almahakeri, M., Moore, I. D., and Fam, A. (2016). Numerical study of longitudinal bending in buried GFRP pipes subjected to lateral earth movements. *Journal of Pipeline Systems Engineering and Practice*, *8*(1), 4016012.

Almahakeri, M., Moore, I. D., and Fam, A. (2019). Numerical techniques for design calculations of longitudinal bending in buried steel pipes subjected to lateral Earth movements. *Royal Society Open Science*, *6*(7), V. https://doi.org/10.1098/rsos.181550

Anderson, C. D. (2004). *Response of buried polyethylene natural gas pipelines subjected to lateral ground displacement*. Master's thesis. University of British Columbia, Canada.

Anderson, C., Wijewickreme, D., Ventura, C., and Mitchell, A. (2004). Full-scale laboratory testing of buried polyethylene gas distribution pipelines subject to lateral ground displacements. *Proceedings of the 13th World Conference on Earthquake Engineering, Vancouver, BC*, 1–6.

ASCE. (1984). *Guidelines for the seismic design of oil and gas pipeline systems, Committee on Gas and Liquid Fuel Lifelines*. Technical Council on Lifeline Earthquake Engineering, American Society of Civil Engineers (ASCE), New York, USA.

ASTM D1556-07. (2007). *Standard Test Method for Density and Unit Weight of Soil in Place by the Sand-Cone Method*. ASTM International, West Conshohocken, PA, USA.

Audibert, J. M. E., and Nyman, K. J. (1977). Soil restraint against horizontal motion of pipes. *Journal of the Geotechnical Engineering Division*, *103*(10), 1119–1142.

Biot, M. A. (1937). Bending of an Infinite Beam on an Elastic Foundation. *Journal of Applied Mechanics*, *4*(1), A1–A7. https://doi.org/10.1115/1.4008739

C-CORE, and Honegger, D. (2003). *Extended Model for Pipe-soil Interaction*. Design, Construction and Operations Technical Committee of Pipeline Research Council International (PRCI), Inc, Virginia, USA.

Casbarian, A. O. P., and others. (1966). Ultimate Lateral Resistance of Anchor Plates in Cohesionless Soils. *Society of Petroleum Engineers Journal*, *6*(04), 299–307.

Chakraborty, S., Dhar, A. S., Talesnick, M., & Muntakim, A. H. (2020). *Behavior of a branched buried MDPE gas distribution pipe under axial ground movement.* GeoVirtual 2020, September 14-16.

Choudhary, A. K., and Dash, S. K. (2017). Load-carrying mechanism of vertical plate anchors in sand. *International Journal of Geomechanics*, *17*(5), 4016116.

Daiyan, N., Kenny, S., Phillips, R., and Popescu, R. (2011). Investigating pipeline-soil interaction under axial-lateral relative movements in sand. *Canadian Geotechnical Journal*, *48*(11), 1683–1695. https://doi.org/10.1139/t11-061

Das, B. M. (1975). Pullout resistance of vertical anchors. *Journal of Geotechnical and Geoenvironmental Engineering*, *100*(Proc. Paper 11040 Tech. Note).

Das, B. M., and Seeley, G. R. (1975). Load-displacement relationship for vertical anchor plates. *Journal of Geotechnical and Geoenvironmental Engineering*, *101*(ASCE# 11402 Proceeding).

Das, S., and Dhar, A. S. (2021). Nonlinear Time-Dependent Mechanical Behaviour of Medium-Density Polyethylene Pipe Material. *Journal of Materials in Civil Engineering*, *33*(5), 4021068.

Di Prisco, C., and Galli, A. (2006). Soil-pipe interaction under monotonic and cyclic loads: experimental and numerical modelling. *1st Euro Mediterranean Symposium on "Advances in Geomaterials and Structures", c*, 755–760.

Dickin, E. A., and Laman, M. (2007). Uplift response of strip anchors in cohesionless soil. *Advances in Engineering Software*, *38*(8–9), 618–625.

Dinovitzer, A., Fredj, A., Weerasekara, L., Rahman, M., and Wijewickreme, D. (2014). *Performance Monitoring and Modeling of Small Diameter MDPE Natural Gas Pipelines Subject to Ground Movement*. https://doi.org/10.1115/IPC2014-33532

DNV (Det Norske Veritas). (2011). *On-Bottom Stability Design of Submarine Pipelines*, DNV-RP-F109, Det Norske Veritas, Baerum, Norway.

EGPIDA. (2018). *10th Report of the European Gas Pipeline Incident Data Group (period 1970 – 2016).* Doc. number VA 17.R.0395, European Gas Pipeline Incident Data Group, Groningen, The Netherlands.

EIA (Energy Information Administration). (2020). *Natural gas pipelines - U.S. Energy Information Administration (EIA)*. Energy Information Administration. https://www.eia.gov/energyexplained/natural-gas/natural-gas-pipelines.php.

Guo, P. J., and Stolle, D. F. E. (2005). Lateral pipe-soil interaction in sand with reference to scale effect. *Journal of Geotechnical and Geoenvironmental Engineering*, *131*(3), 338–349. https://doi.org/10.1061/(ASCE)1090-0241(2005)131:3(338)

Ha., D., Abdoun, T.H., O'Rourke, M.J., Symans, M.D., O'Rourke, T.D., Palmer, M.C. and Stewart, H.E. (2008). Centrifuge modeling of earthquake effects on buried high-density polyethylene (HDPE) pipelines crossing fault zones. Journal of Geotechnical and Geoenvironmental Engineering, ASCE, 134(10): 1501-1515.

Hansen, J. B. (1961). The ultimate resistance of rigid piles against transversal forces. *Bulletin 12, Danish Geotech. Institute*, 1–9.

Hetényi, M. (1946). *Beams on elastic foundation: theory with applications in the fields of civil and mechanical engineering* (Issue BOOK). University of Michigan Press, Ann Arbor, MI.

Honegger, D. G., Gailing, R. W., and Nyman, D. J. (2002). Guidelines for the seismic design and assessment of natural gas and liquid hydrocarbon pipelines. *Proceedings of the International*

Pipeline Conference, IPC, *A*, 563–570. https://doi.org/10.1115/IPC2002-27330

Horvath, J. S., and Colasanti, R. J. (2011). New hybrid subgrade model for soil-structure interaction analysis: foundation and geosynthetics applications. In *Geo-Frontiers 2011: Advances in Geotechnical Engineering* (pp. 4359-4368).

Horvath, J. S. (2002). Soil-structure interaction research project: Basic SSI concepts and applications overview. *Manhattan College School of Engineering: Bronx, NY, USA*.

Hsu, T.-W. (1993). Rate effect on lateral soil restraint of pipelines. *Soils and Foundations*, *33*(4), 159–169.

Hsu, T.-W., Chen, Y.-J., and Wu, C.-Y. (2001). Soil friction restraint of oblique pipelines in loose sand. *Journal of Transportation Engineering*, *127*(1), 82–87.

Hsu, T. W., Chen, Y. J., and Hung, W. C. (2006). Soil friction restraint of oblique pipelines in dense sand. *J. Transp. Eng*, *132*(2), 175–181.

Jung, J. K., O'Rourke, T. D., and Olson, N. A. (2013). Lateral soil-pipe interaction in dry and partially saturated sand. *Journal of Geotechnical and Geoenvironmental Engineering*, *139*(12), 2028–2036. https://doi.org/10.1061/(ASCE)GT.1943-5606.0000960

Jung, J. K., O'Rourke, T. D., and Argyrou, C. (2016). Multi-directional force--displacement response of underground pipe in sand. *Canadian Geotechnical Journal*, *53*(11), 1763–1781.

Karimian, S. A. (2006). *Response of buried steel pipelines subjected to longitudinal and transverse ground movement*. Ph.D thesis, University of British Columbia, Canada.

Katebi, M., Maghoul, P., and Blatz, J. (2019). Numerical analysis of pipeline response to slow landslides: Case study. *Canadian Geotechnical Journal*, *56*(12), 1779–1788.

https://doi.org/10.1139/cgj-2018-0457

Kennedy, Robert P., Robert A. Williamson, and Andrew M. Chow. (1977) "Fault movement effects on buried oil pipeline." Journal of Transportation Engineering, ASCE 103.5: 617-633

Konuk, I., Phillips, R., Hurley, S., and Paulin, M. J. (1999). Preliminary ovalisation of buried pipeline subjected to lateral loading. *Proceedings of the Offshore Mechanics and Arctic Engineering (OMAE), St. John's, NL*.

Kumar, J., and Bhoi, M. K. (2008). Interference of multiple strip footings on sand using small scale model tests. *Geotechnical and Geological Engineering*, *26*(4), 469.

Liang, R., Yang, K., and Nusairat, J. (2010). Closure to "p-y Criterion for Rock Mass" by Robert Liang, Ke Yang, and Jamal Nusairat. *Journal of Geotechnical and Geoenvironmental Engineering*, *136*(1), 274–275.

Liu, R., Guo, L., Yan, S., and Xu, Y. (2011). Studies on soil resistance to pipelines buried in sand. *Advanced Materials Research*, *243–249*, 3151–3156. https://doi.org/10.4028/www.scientific.net/AMR.243-249.3151

Liu, R., and Wang, X. (2018). Lateral global buckling of submarine pipelines based on the model of nonlinear pipe--soil interaction. *China Ocean Engineering*, *32*(3), 312–322.

Liu, X., and O'Rourke, M. J. (1997). Behaviour of continuous pipeline subject to transverse PGD. *Earthquake Engineering and Structural Dynamics*, *26*(10), 989–1003. https://doi.org/10.1002/(SICI)1096-9845(199710)26:10<989::AID-EQE688>3.0.CO;2-P

Luo, X., Ma, J., Zheng, J., and Shi, J. (2014). Finite element analysis of buried polyethylene pipe subjected to seismic landslide. *Journal of Pressure Vessel Technology*, *136*(3).

Mahdavi, H., Kenny, S., Phillips, R., and Popescu, R. (2013). Significance of geotechnical loads on local buckling response of buried pipelines with respect to conventional practice. *Canadian Geotechnical Journal*, *50*(1), 68–80.

Muntakim, A. H., Dhar, A. S., and Reza, A. (2018). *Modelling time dependent behaviour of buried polyethylene pipes using Abaqus*. GeoEdmonton 2018, Edmonton,Alberta,Canada.

Murugathasan, P., Dhar, A. S., and Hawlader, B. C. (2020). An experimental and numerical investigation of pullout behaviour of ductile iron water pipes buried in sand. *Canadian Journal of Civil Engineering*, *999*, 1–10. https://doi.org/10.1139/cjce-2019-0366

Murray, E. J., and Geddes, J. D. (1987). Uplift of anchor plates in sand. *Journal of Geotechnical Engineering*, *113*(3), 202–215.

Murchison, J. M., and O'Neill, M. W. (1984). Evaluation of py relationships in cohesionless soils. *Analysis and Design of Pile Foundations*, 174–191.

Murray, E. J., and Geddes, J. D. (1987). Uplift of anchor plates in sand. *Journal of Geotechnical Engineering*, *113*(3), 202–215.

Naeini, S. A., Mahmoudi, E., Shojaedin, M. M., and Misaghian, M. (2016). Mechanical response of buried High-Density Polyethylene pipelines under normal fault motions. *KSCE Journal of Civil Engineering*, *20*(6), 2253–2261. https://doi.org/10.1007/s12205-015-0695-3

NEB. (2017). *Incidents At NEB-Regulated Pipelines And Facilities*. National Energy Board of Canada. Retrived December 15, 2020, from https://open.canada.ca/data/en/dataset/fd17f08f-f14d-433f-91df-c90a34e1e9a6 https://doi.org/doi.org/10.35002/ycrm-a941

Neely, W. J., Stuart, J. C., and Graham, J. (1973). Failure loads of vertical anchor plates in sand.

Journal of Soil Mechanics and Foundations Div, *99*(Proc. Paper 9980).

Ni., P., Moore, I.D. and Take, A. (2018a). Distributeed fibre optic sensing of strains on buried full-scale PVC pipelines crossing a normal fault. *Geotechnique* 68(1):1-17.

Ni, P., Mangalathu, S., and Yi, Y. (2018b). Fragility analysis of continuous pipelines subjected to transverse permanent ground deformation. *Soils and Foundations*, *58*(6), 1400–1413. https://doi.org/10.1016/j.sandf.2018.08.002.

NRCAN (National Resources Canada). (2020). *Pipelines Across Canada*. Government of Canada. Retrieved February 1, 2021, from https://www.nrcan.gc.ca/our-natural-resources/energy-sources-distribution/clean-fossil-fuels/pipelines/pipelines-across-canada/18856

Oliveira, J. R. M. S., Almeida, M. S. S., Almeida, M. C. F., and Borges, R. G. (2010). Physical modeling of lateral clay-pipe interaction. *Journal of Geotechnical and Geoenvironmental Engineering*, *136*(7), 950–956.

O'Rourke, T.D, Jung, J.K. and Argyrou,C. (2016). Undergroundpipelineresponsetoearthquake-inducedground deformation. Soil Dynamics and Earthquake Engineering. 91(2016):272–283.

Paulin, M. J., Phillips, R., and Boivin, R. (1995). *Centrifuge modelling of lateral pipeline/soil interaction--Phase 2*.

Paulin, M. J., Phillips, R., Clark, J. I., Trigg, A., and Konuk, I. (1998). A full-scale investigation into pipeline/soil interaction. *Proceedings of International Pipeline Conference, ASME, Calgary, AB., pp. 779-788.* https://doi.org/10.1115/IPC1998-2091

Phillips, R., Nobahar, A., and Zhou, J. (2004, January). Trench effects on pipe-soil interaction. In *International Pipeline Conference* (Vol. 41766, pp. 321-327).

Plastics Industry Pipe Association of Australia (PIPA). (2001). *Polyolefins technical information*. Retrieved from: www.pipe.com.au (cited January 2020)

Porter, M., Ferris, G., Leir, M., Leach, M., and Haderspock, M. (2016). Updated estimates of frequencies of pipeline failures caused by geohazards. *International Pipeline Conference*, *50266*, V002T07A003.

Popescu, R., Guo, P., and Nobahar, A. (2001). 3D N analysis of pipe/soil interaction. *Final Report for Geological Survey of Canada, Chevron Corp. and Petro Canada*.

PRCI. (2017). *Guidelines for the seismic design and assessment of natural gas and liquid hydrocarbon pipelines*. Pipeline Design, Construction and Operations Technical Committee of Pipeline Research Council International, Inc, Virginia, USA.

Raheem, A. M. (2019). On the Behaviour of Lateral Pipe-Soil Interaction in Ultra-Soft Clayey Soil Using Large Scale-Laboratory Tests. *International Journal of Engineering and Technology Innovation*, *9*(2), 119.

Rajani, B. B., Robertson, P. K., and Morgenstern, N. R. (1995). Simplified design methods for pipelines subject to transverse and longitudinal soil movements. *Canadian Geotechnical Journal*, *32*(2), 309–323.

Reese, L. C., Cox, W. R., and Koop, F. D. (1975). Field testing and analysis of laterally loaded piles om stiff clay. *Offshore Technology Conference*.

Reza, A., Dhar, A. S., and Muntakim, A. H. (2019). Full-scale laboratory pullout testing of 60-mm diameter buried MDPE pipes. *Proceedings, Annual Conference - Canadian Society for Civil Engineering*, *2019-June*, 1–10.

Rowe, R. K., and Davis, E. H. (1982). The behaviour of anchor plates in sand. *Geotechnique*, *32*(1), 25–41.

Roy, K., Hawlader, B., Kenny, S., and Moore, I. (2018). Lateral resistance of pipes and strip anchors buried in dense sand. *Canadian Geotechnical Journal*, *55*(12), 1812–1823.

Saha, R. C. (2021). *Shear strength assessment of a manufactured well-graded sand*. Master's thesis, Faculty of Engineering and Applied Science, Memorial University of Newfoundland.

Sakai, T., and Tanaka, T. (2007). Experimental and numerical study of uplift behaviour of shallow circular anchor in two-layered sand. *Journal of Geotechnical and Geoenvironmental Engineering*, *133*(4), 469–477.

Sarvanis, G. C., and Karamanos, S. A. (2017). Analytical model for the strain analysis of continuous buried pipelines in geohazard areas. *Engineering structures, 152, 57-69.*

Sheil, B. B., Martin, C. M., Byrne, B. W., Plant, M., Williams, K., and Coyne, D. (2018). Full-scale laboratory testing of a buried pipeline in sand subjected to cyclic axial displacements. *Géotechnique*, *68*(8), 684–698.

Sherif, M. A., Fang, Y.-S., and Sherif, R. I. (1984). KA and K o Behind Rotating and Non-Yielding Walls. *Journal of Geotechnical Engineering*, *110*(1), 41–56.

Smith, C. C. (1998). Limit loads for an anchor/trapdoor embedded in an associative Coulomb soil. *International Journal for Numerical and Analytical Methods in Geomechanics*, *22*(11), 855–865.

Stewart, H. E., Bilgin, Ö., O'Rourke, T. D., and Keeney, T. M. J. (1999). Technical reference for improved design and construction practices to account for thermal loads in plastic gas

pipelines. *Final Rep. No. GRI-99/0192, Gas Research Institute, Chicago*.

Tagaya, K., Scott, R. F., and Aboshi, H. (1988). Pullout resistance of buried anchor in sand. *Soils and Foundations*, *28*(3), 114–130.

Tagaya, K., Tanaka, A., and Aboshi, H. (1983). Application of finite element method to pullout resistance of buried anchor. *Soils and Foundations*, *23*(3), 91–104.

Takada, S., Hassani, N., and Fukuda, K. (2001). A new proposal for simplified design of buried steel pipes crossing active faults. *Earthquake engineering and structural dynamics*, *30*(8), 1243-1257.

Talesnick, M. L., Ringel, M., and Avraham, R. (2014). Measurement of contact soil pressure in physical modelling of soil--structure interaction. *International Journal of Physical Modelling in Geotechnics*, *14*(1), 3–12. https://doi.org/10.1680/ijpmg.13.00008

Trautmann, C. H. (1983). *Behaviour of pipe in dry sand under lateral and uplift loading*. Ph.D. thesis, School of Civil and Environmental Engineering, Cornell University, Ithaca, New York.

Trautmann, C. H., and O'Rourke, T. D. (1983). *Load-displacement characteristics of a buried pipe affected by permanent earthquake ground movements* (No. CONF-830607-). School of Civil and Environmental Engineering, Cornell University, Ithaca, NY.

Trautmann, C. H., and O'Rourke, T. D. (1985). Lateral force–displacement response of buried pipe. J. Geotech. Eng., 111(9), 1077–1092.

TSB. (2019). *Marine Transportation Occurrences in 2019: Statistical Summary*. Transportation Safety Board of Canada. Retrived October 10, 2020, from

https://www.tsb.gc.ca/eng/stats/pipeline/2018/ssep-sspo-2018.html

Trifonov OV, Cherniy VP. A semi-analytical approach to a nonlinear stress–strain analysis of buried steel pipelines crossing active faults. Soil Dynam Earthquake Eng 2010;30:1298–308.

Tschebotarioff, G. P. (1973). *Soil Mechanics, Foundations, and Earth Structures* (Second Edi). McGrawHill Book Company Inc.

Vermeer, P. A., and Sutjiadi, W. (1985). The uplift resistance of shallow embedded anchors. *International Conference on Soil Mechanics and Foundation Engineering. 11*, 1635–1638.

Vesic, A. B. (1961). Beams on elastic subgrade and the Winkler's hypothesis. In *Proc. 5th Int. Conf. on SMFE (Vol. 1, pp. 845-851).*

Wang, Y., Liu, R., and Wang, L. (2018). Experimental and upper-bound analysis of lateral soil resistance for shallow-embedded pipeline in Bohai sand. *Journal of Pipeline Systems Engineering and Practice*, *9*(4), 4018014.

Weerasekara, L. (2011). *Pipe-soil interaction aspects in buried extensible pipes*. Doctoral dissertation, University of British Columbia, Canada

Weerasekara, L., and Wijewickreme, D. (2008). Mobilization of soil loads on buried, polyethylene natural gas pipelines subject to relative axial displacements. *Canadian Geotechnical Journal*, *45*(9), 1237–1249.

Weerasekara, L., and Wijewickreme, D. (2010). Response of Buried Plastic Pipelines Subject to Lateral Ground Movement. *International Pipeline Conference, 44205*, 179–186.

Wham, B.P., Argyrou, C., O'Rourke, T.D., Stewart, H.E. and Bond, T. K. (2017). PVCO pipeline performance under large ground deformation. Journal of Pressure Vessel Technology,

139(2017): 011702-1.

Wijewickreme, D., Karimian, H., and Honegger, D. (2009). Response of buried steel pipelines subjected to relative axial soil movement. *Canadian Geotechnical Journal*, *46*(7), 735–752.

Wijewickreme, D., and Sanin, M. V. (2010). Postcyclic reconsolidation strains in low-plastic Fraser River silt due to dissipation of excess pore-water pressures. *Journal of Geotechnical and Geoenvironmental Engineering*, *136*(10), 1347–1357.

Wijewickreme, D., and Weerasekara, L. (2015). Analytical modeling of field axial pullout tests performed on buried extensible pipes. *International Journal of Geomechanics*, *15*(2), 4014044.

Winkler, E. (1867). Die leher von der elastizitat und festigkeit. dominicus Prague. *Dominicus, Prague*.

Wong, D. O. (1992). LATERAL SUBGRADE MODULUS OF SANDS FOR DEEP FOUNDATIONS. *Transportation Research Record*, *1336*.

Yimsiri, S., and Soga, K. (2006). Dem analysis of soil-pipeline interaction in sand under lateral and upward movements at deep embedment. *Geotechnical Engineering*, *37*(2), 83–94.

Yimsiri, S., Soga, K., Yoshizaki, K., Dasari, G. R., and O'Rourke, T. D. (2004). Lateral and upward soil-pipeline interactions in sand for deep embedment conditions. *Journal of Geotechnical and Geoenvironmental Engineering*, *130*(8), 830–842. https://doi.org/10.1061/(ASCE)1090-0241(2004)130:8(830)

Yoshizaki, K., O'Rourke, T. D., Bond, T., Mason, J., and Hamada, M. (2001). Large scale experiments of permanent ground deformation effects on steel pipelines. *The 3th Annual*

Research Progress and Accomplishments Report of MCEER, 21–28.

Youd, T. L., and Perkins, D. M. (1987). Mapping of liquefaction severity index. *Journal of Geotechnical Engineering*, *113*(11), 1374–1392.

Zheng, J. Y., Zhang, B. J., Liu, P. F., and Wu, L. L. (2012). Failure analysis and safety evaluation of buried pipeline due to deflection of landslide process. *Engineering Failure Analysis*, *25*, 156–168.